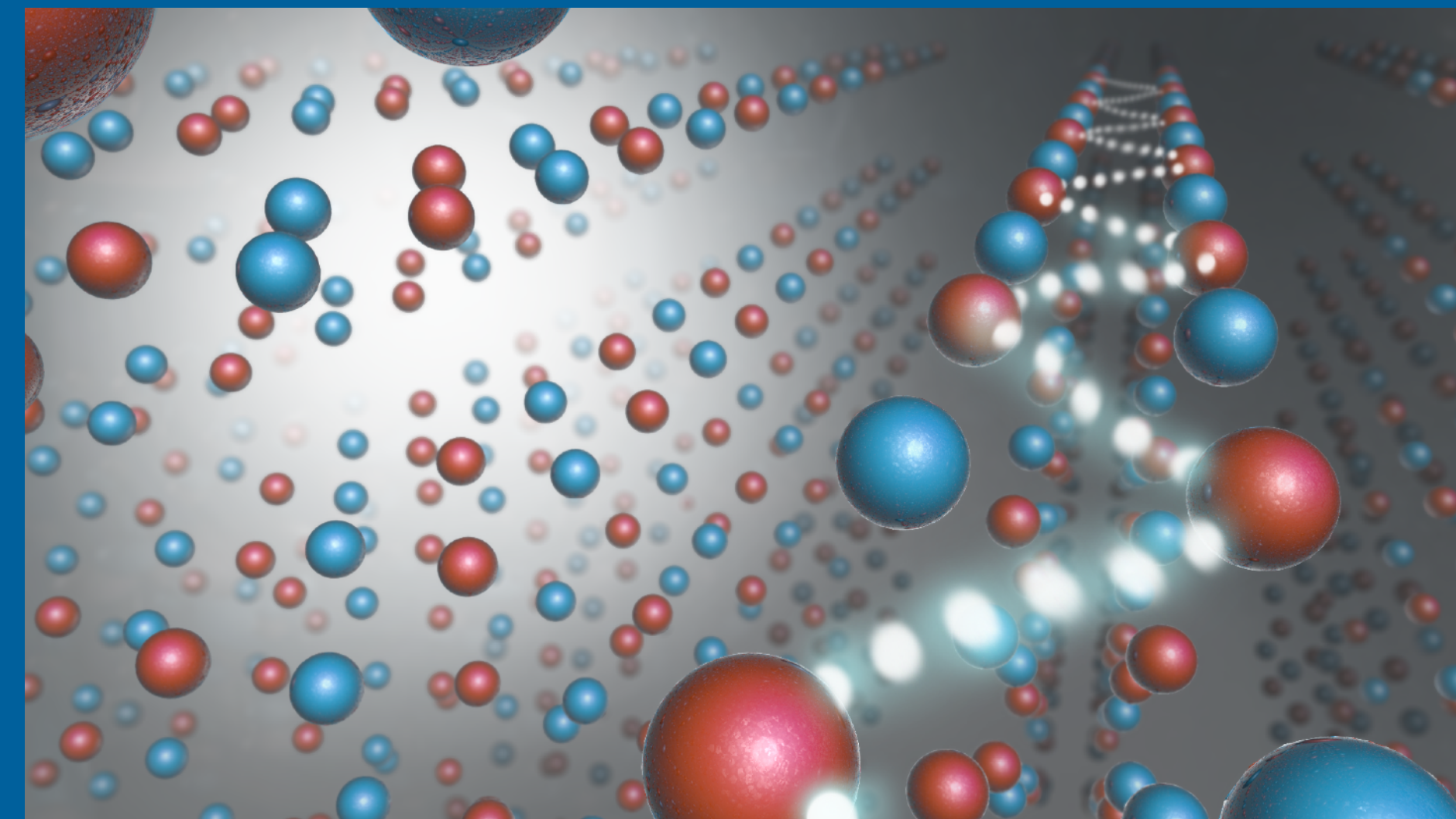


SINGLE CRYSTAL DIFFUSE SCATTERING

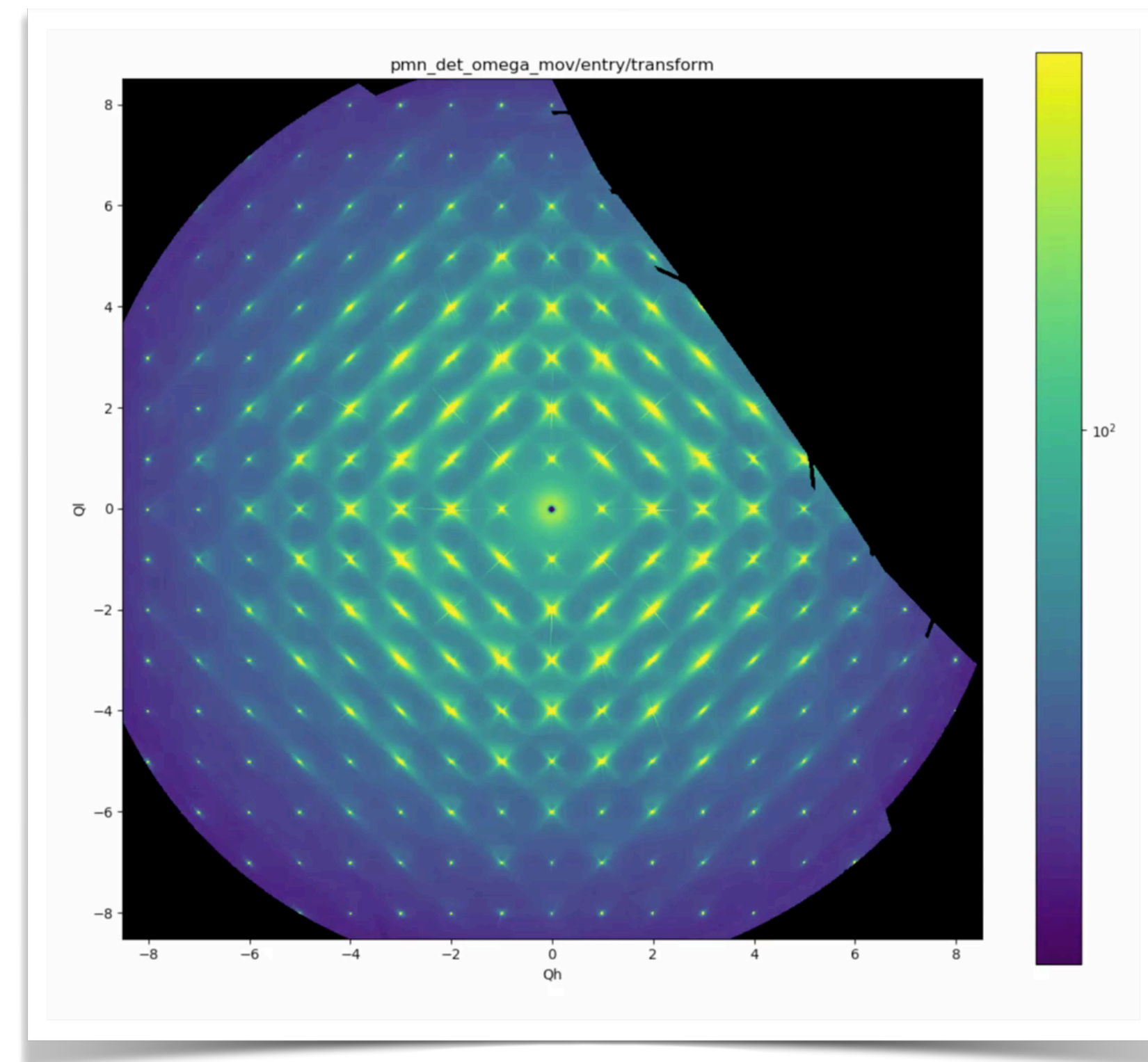


RAYMOND OSBORN
Neutron & X-ray Scattering Group
Materials Science Division

Acknowledgements: Stephan Rosenkranz and Matthew Krogstad

OUTLINE

- What is diffuse scattering?
 - What causes it?
- What is it good for?
 - A random walk through disordered materials
- How do I model it?
 - A few equations
- How do I measure it?
- Case Study 1: Diffuse scattering from vacancies in mullite
- Case Study 2: 3D- Δ PDF in sodium-intercalated V_2O_5
- How do I look at static disorder?
 - Diffuse scattering with elastic discrimination



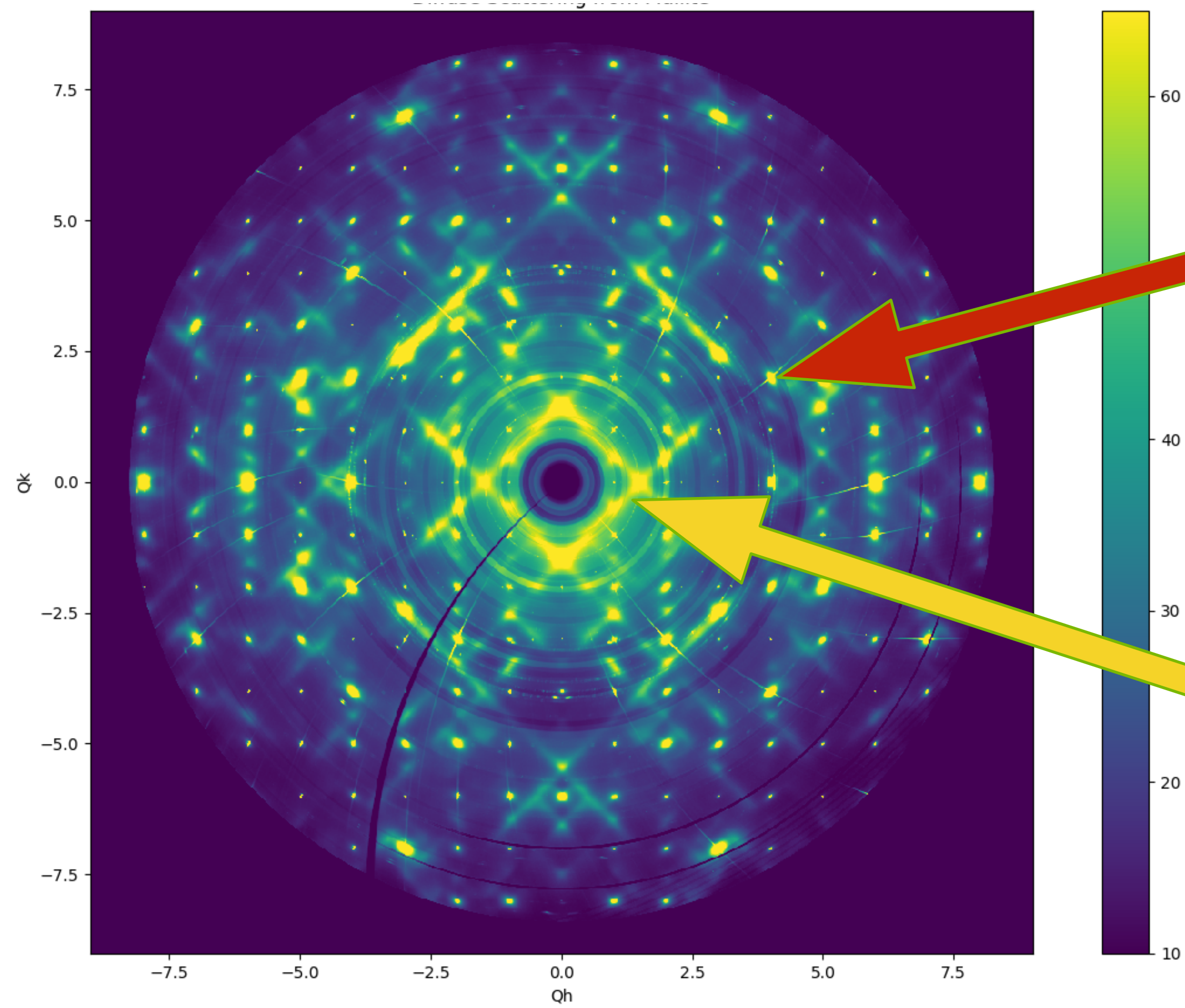


WHAT IS DIFFUSE SCATTERING?



Argonne National Laboratory is a U.S. Department of Energy laboratory managed by UChicago Argonne, LLC.





Bragg Scattering
Average Structure

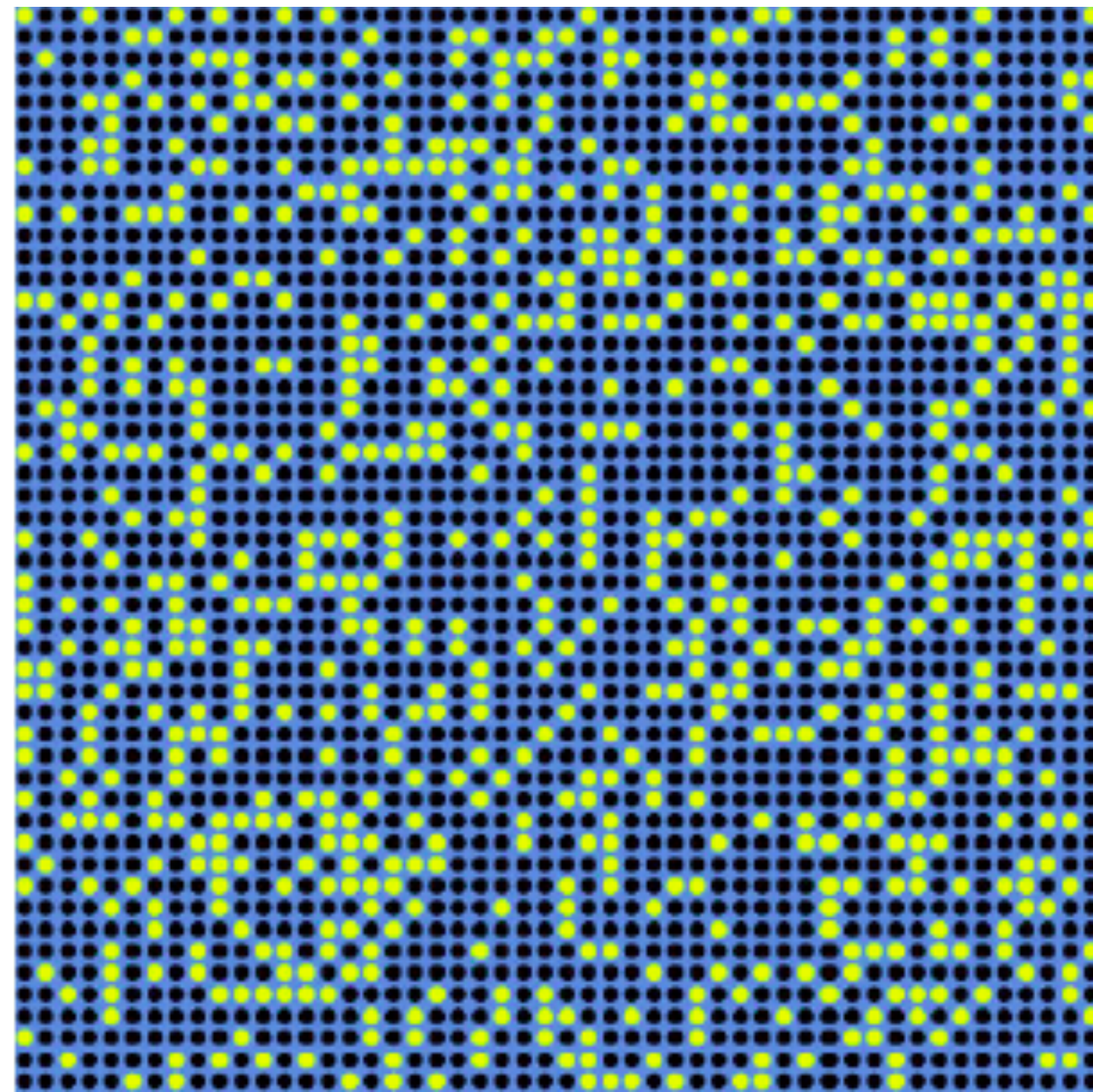
Diffuse Scattering
Deviations from the Average Structure

DIFFUSE SCATTERING

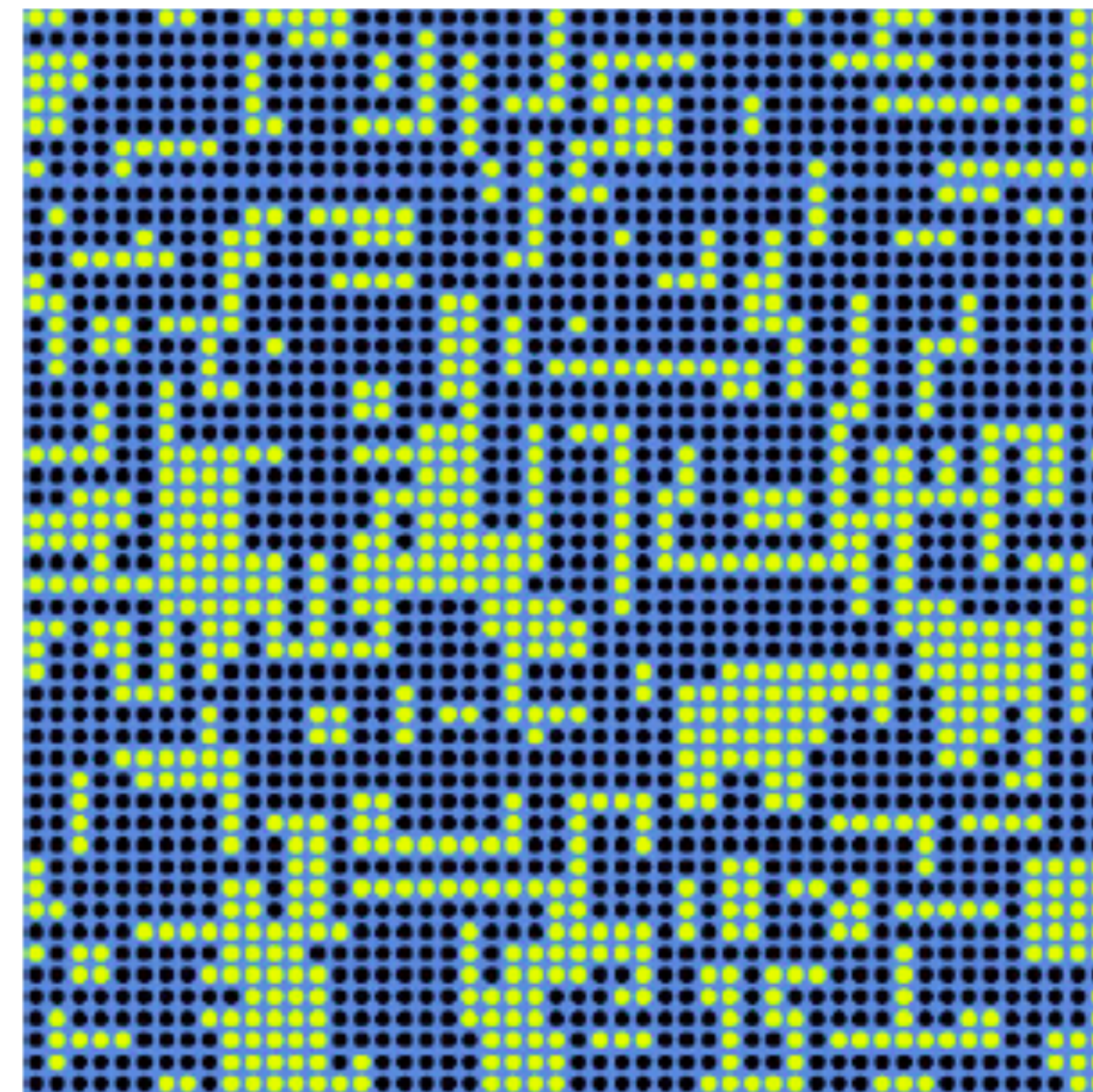
SIMPLE EXAMPLE OF DISORDER

Replace 30% of atoms (blue dots) by vacancies (green dots)

Random Vacancies



Vacancy Clusters

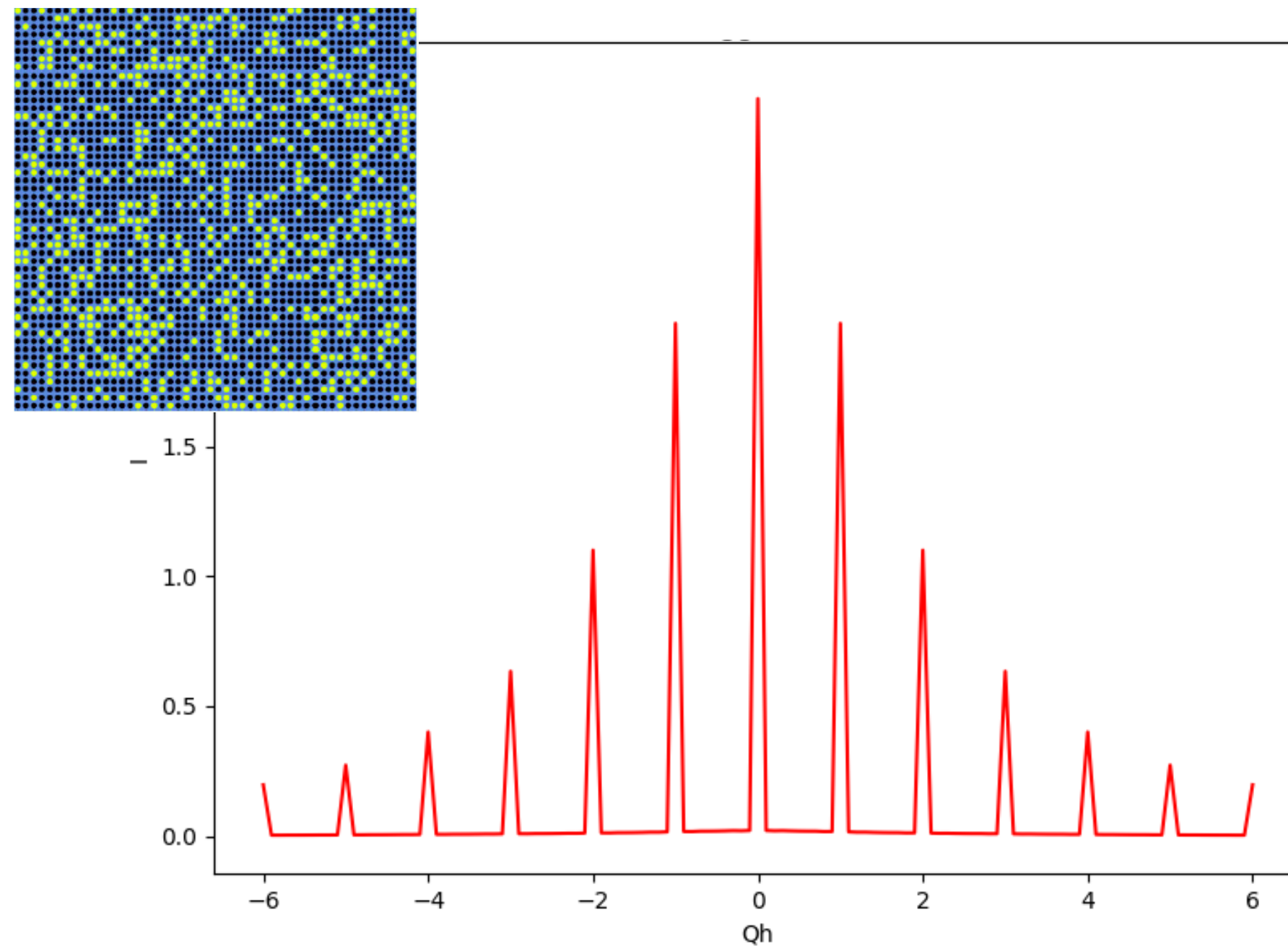


Model due to Thomas Proffen

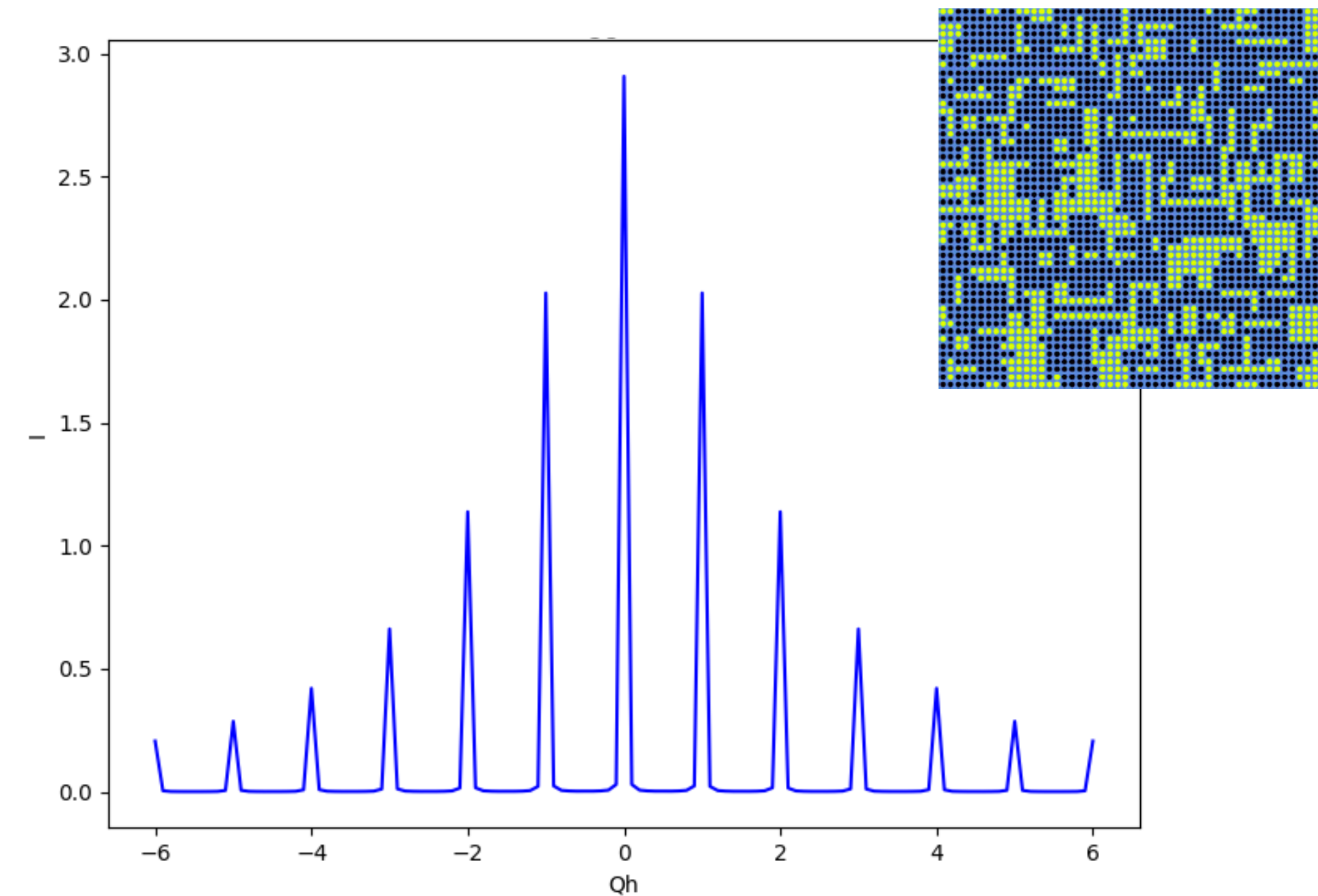
BRAGG SCATTERING

The average occupancy is unchanged \rightarrow Bragg peaks are identical

Random Vacancies



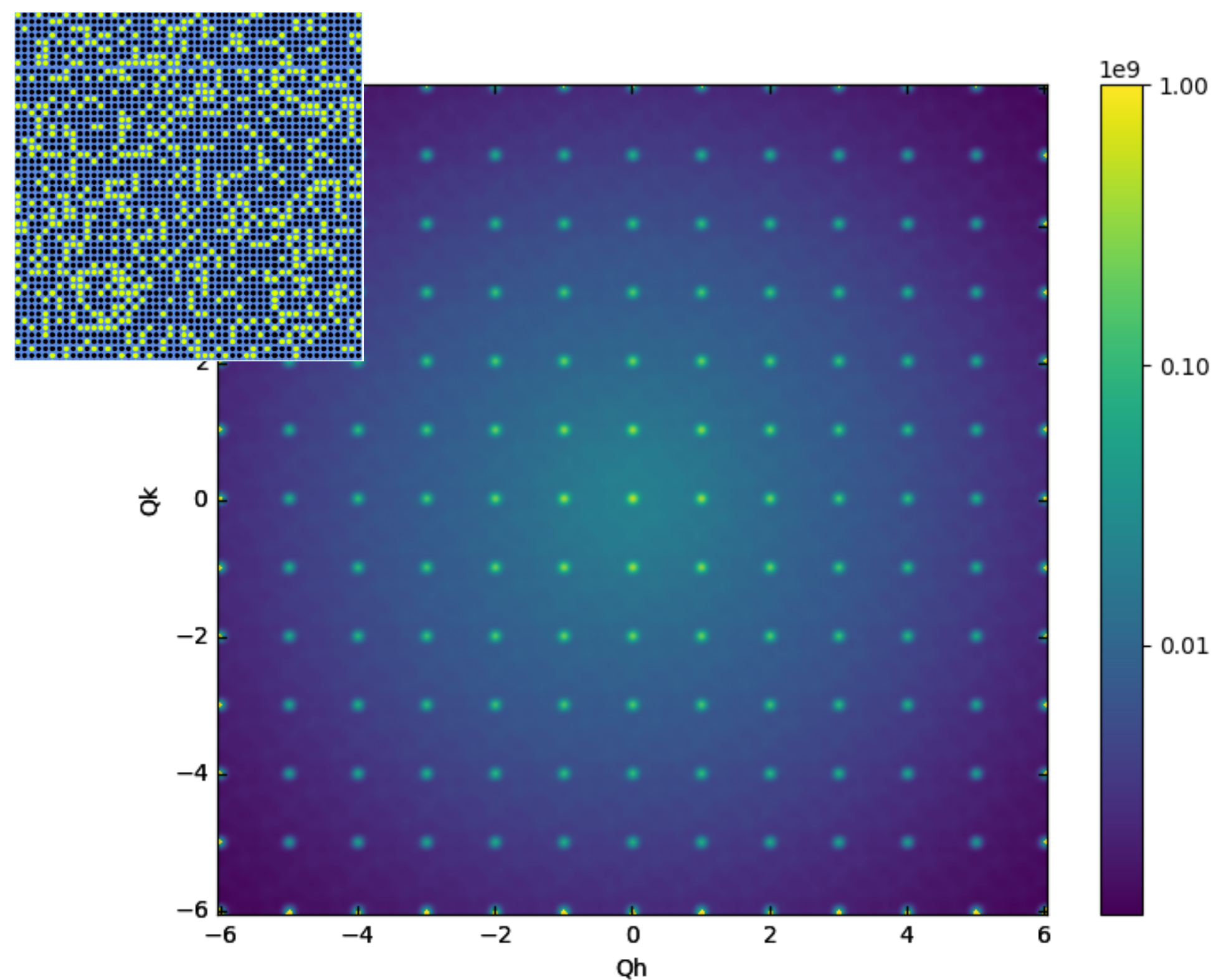
Vacancy Clusters



DIFFUSE SCATTERING

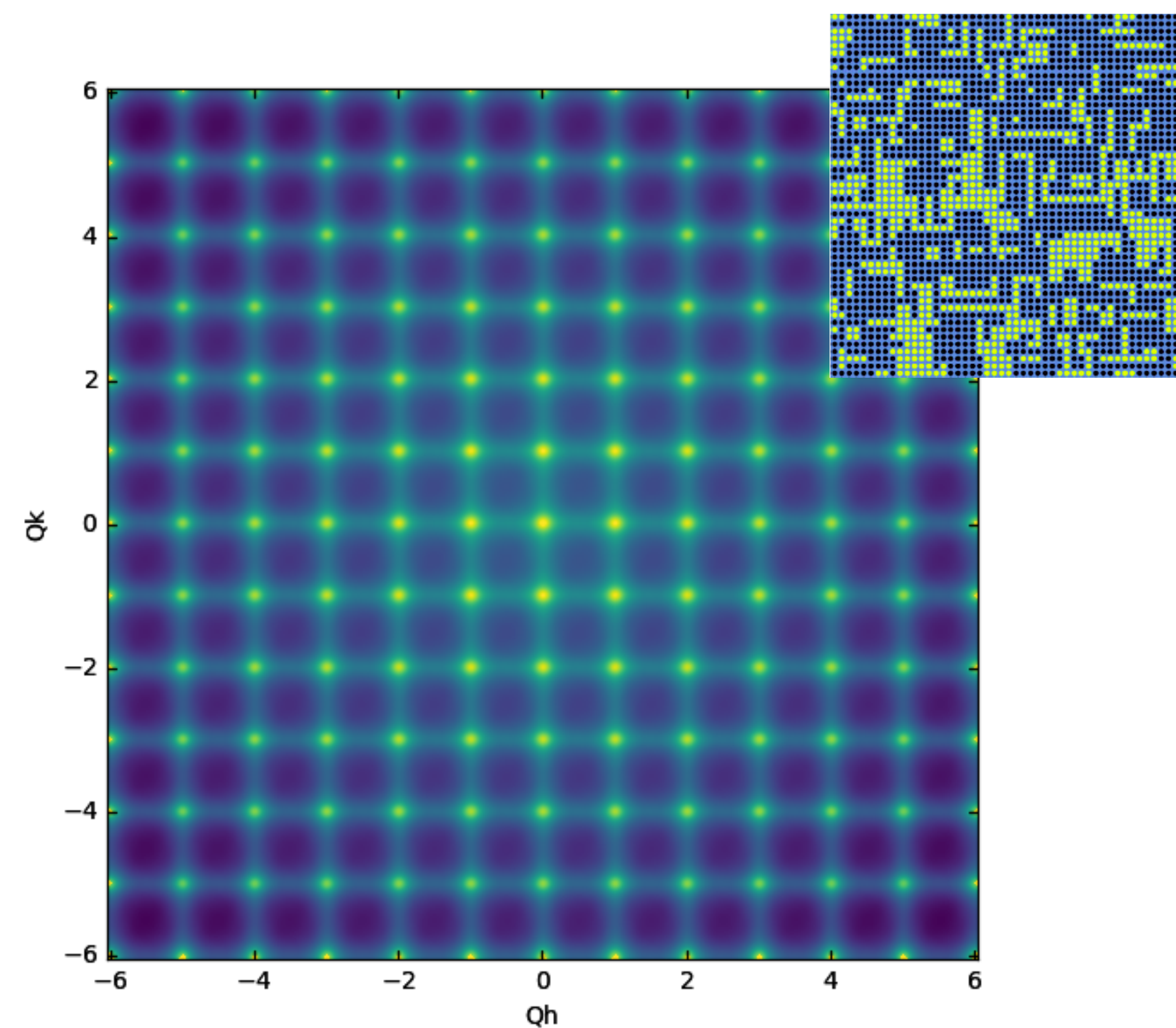
The diffuse scattering is quite different.

Random Vacancies



Laue Monotonic Scattering

Vacancy Clusters



Substitutional Diffuse Scattering

WHAT IS IT GOOD FOR?



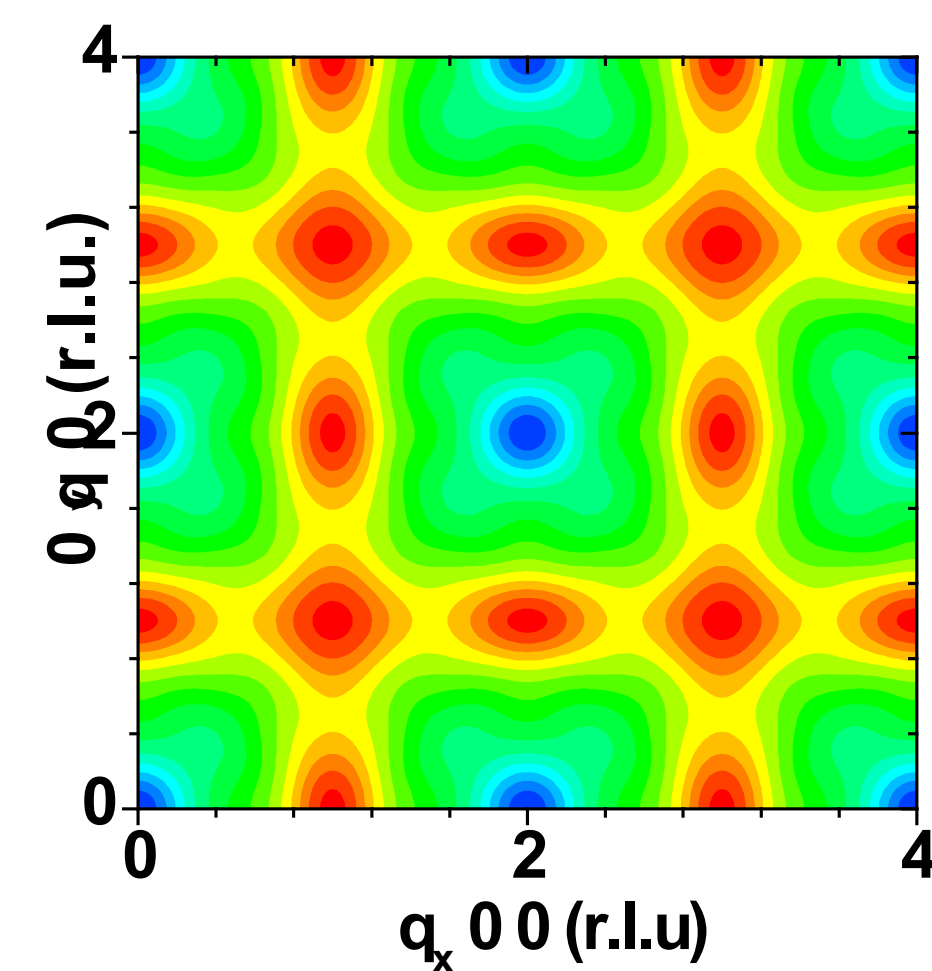
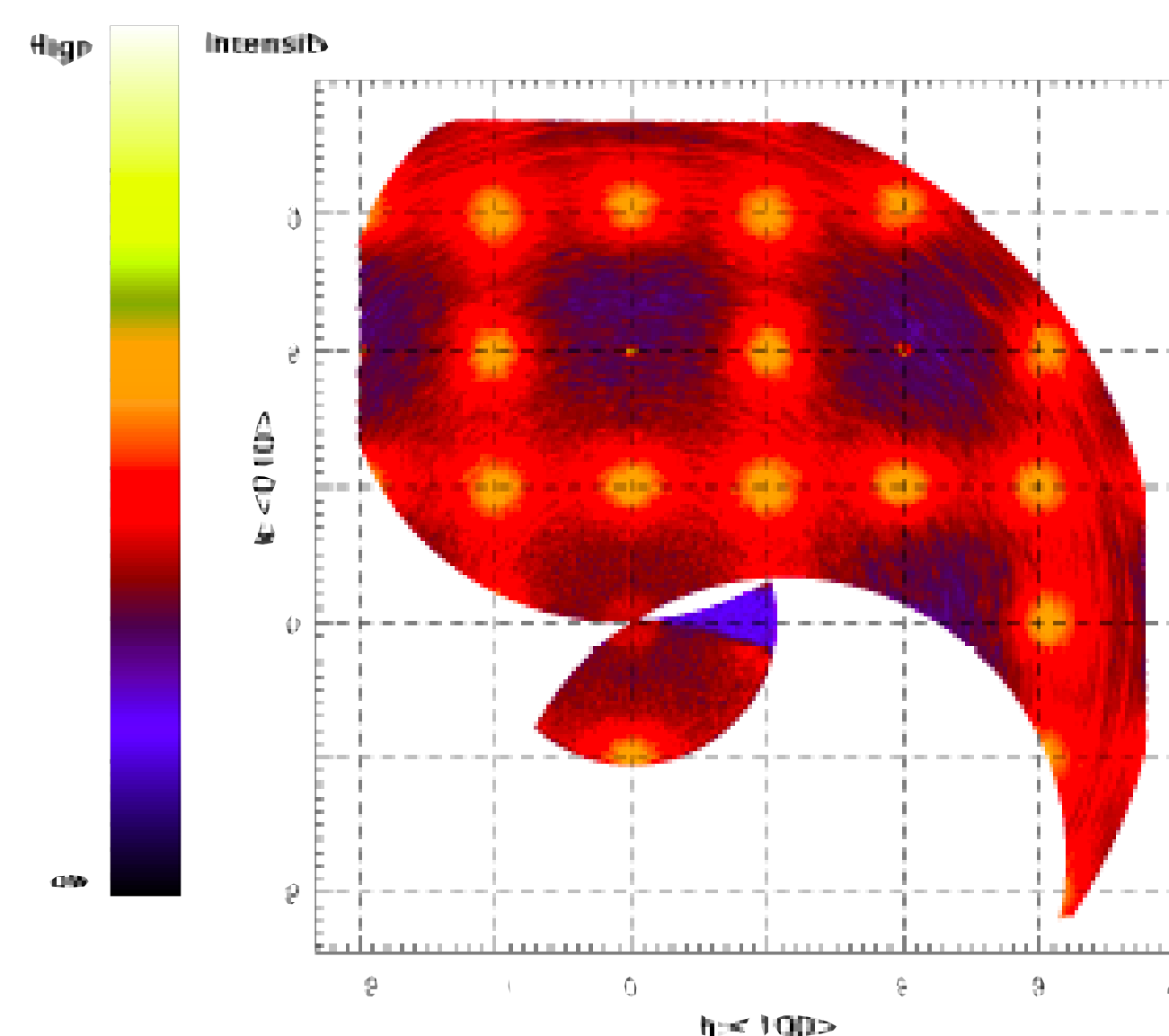
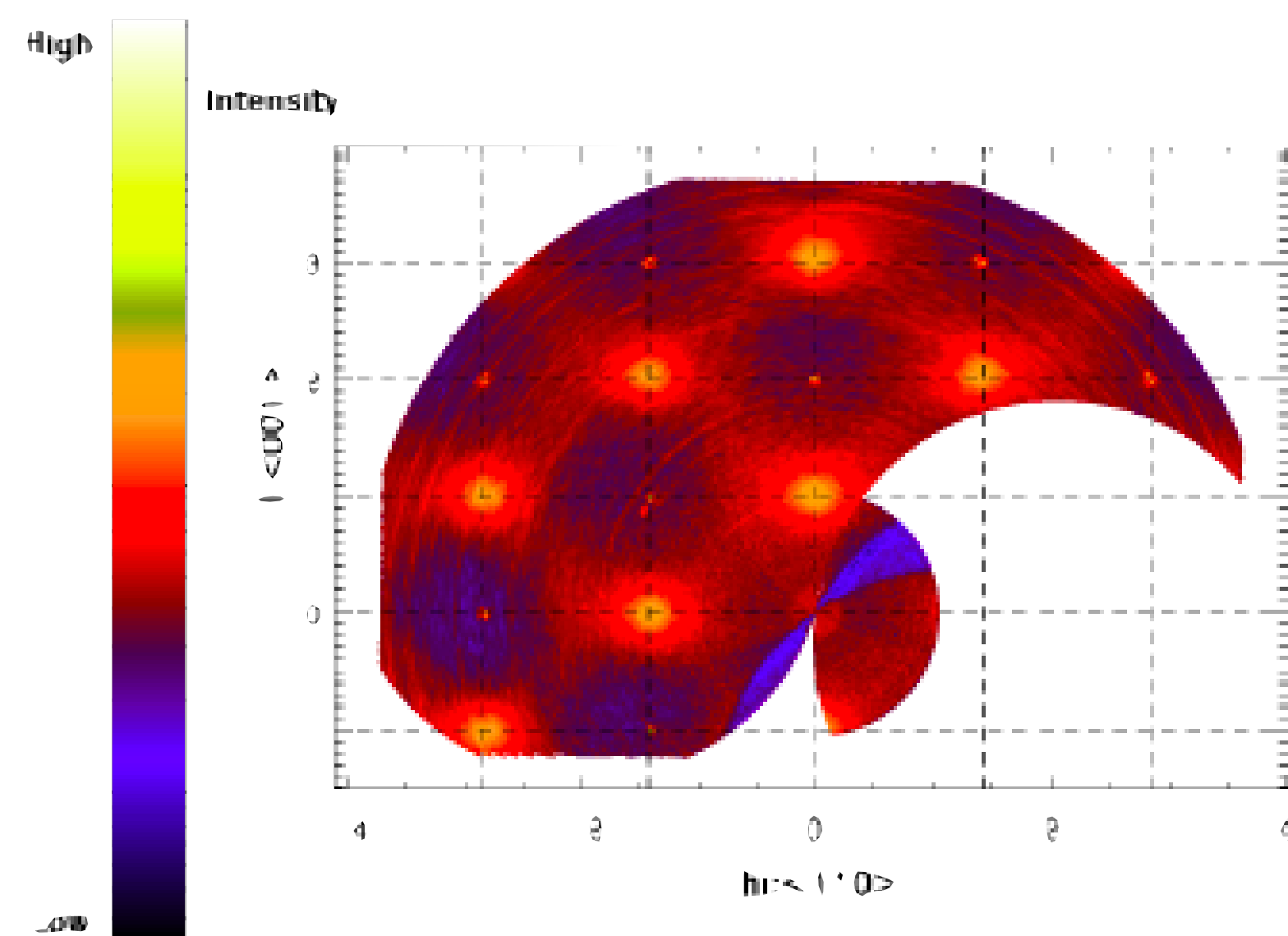
U.S. DEPARTMENT OF
ENERGY

Argonne National Laboratory is a
U.S. Department of Energy laboratory
managed by UChicago Argonne, LLC.



DIFFUSE SCATTERING FROM METALLIC ALLOYS

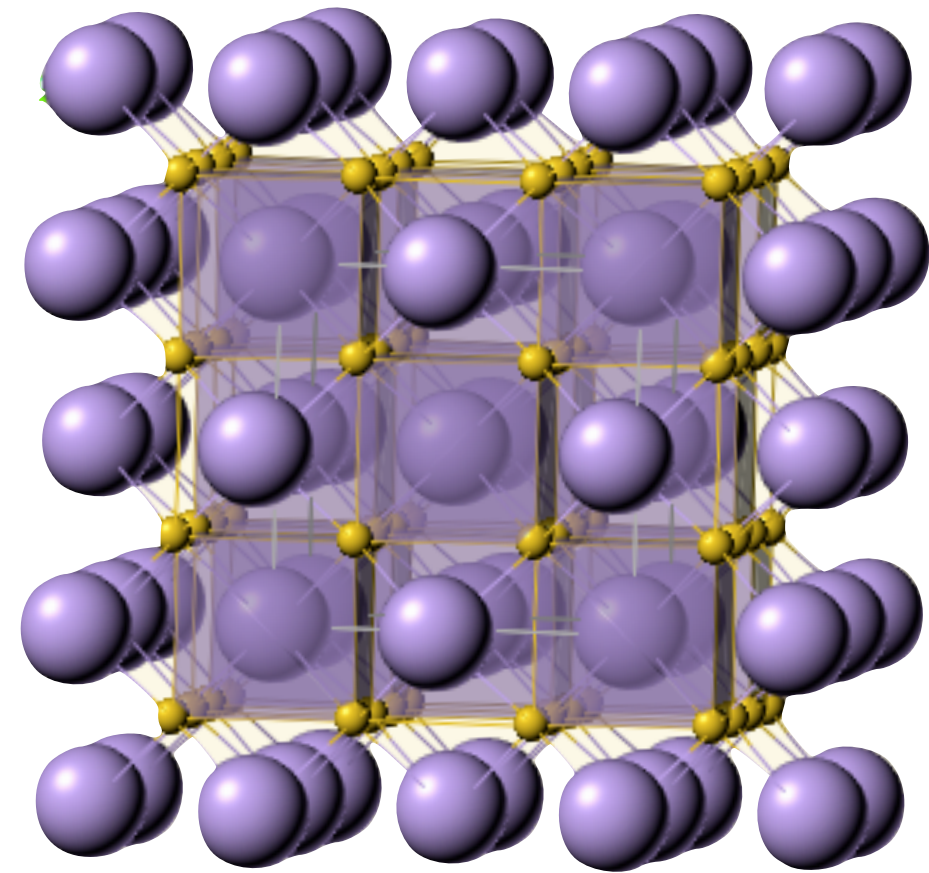
Short-range Order in Null Matrix $^{62}\text{Ni}_{0.52}\text{Pt}_{0.52}$



J. A. Rodriguez, *et al.*, Phys. Rev. B **74**, 104115

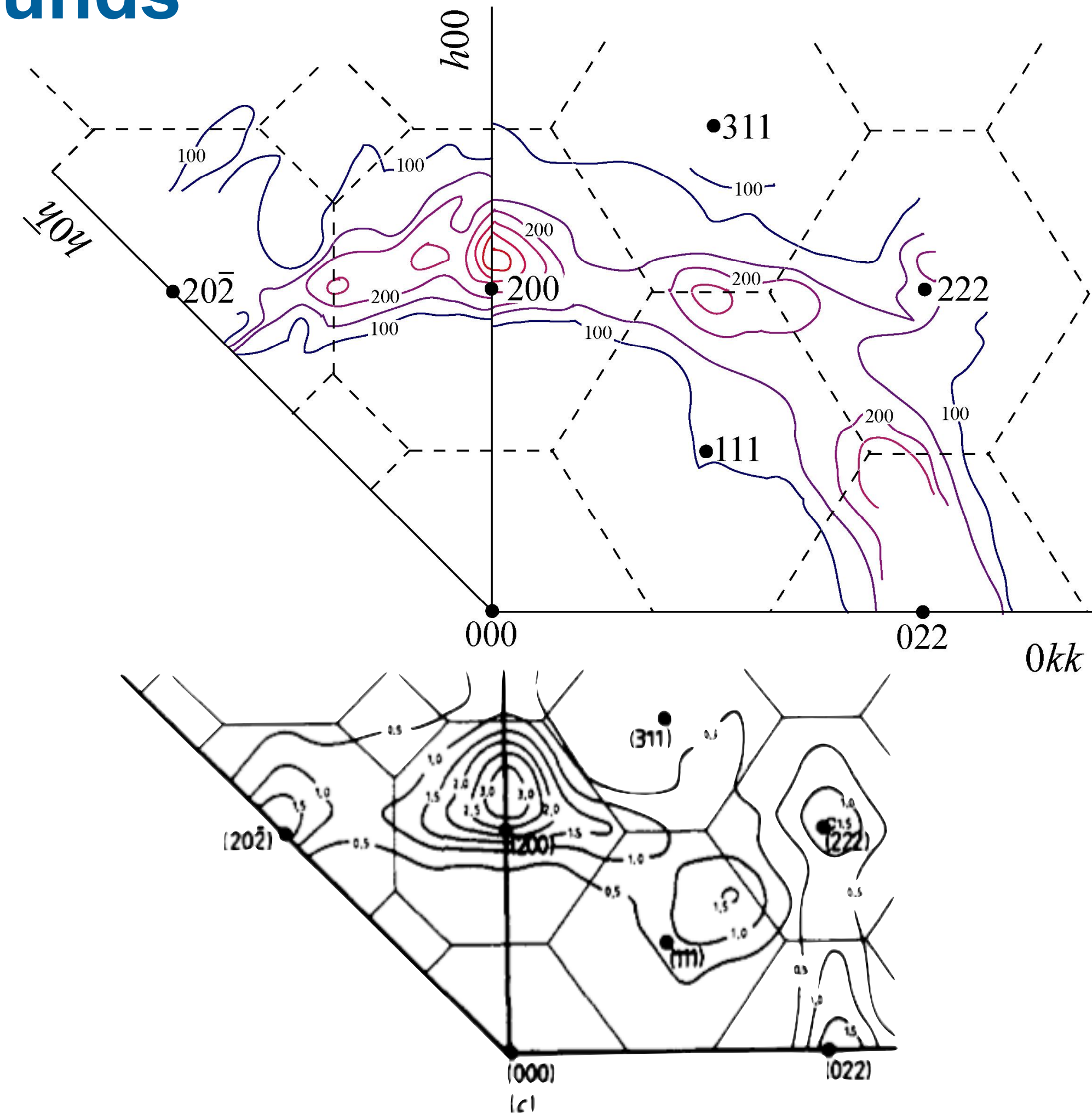
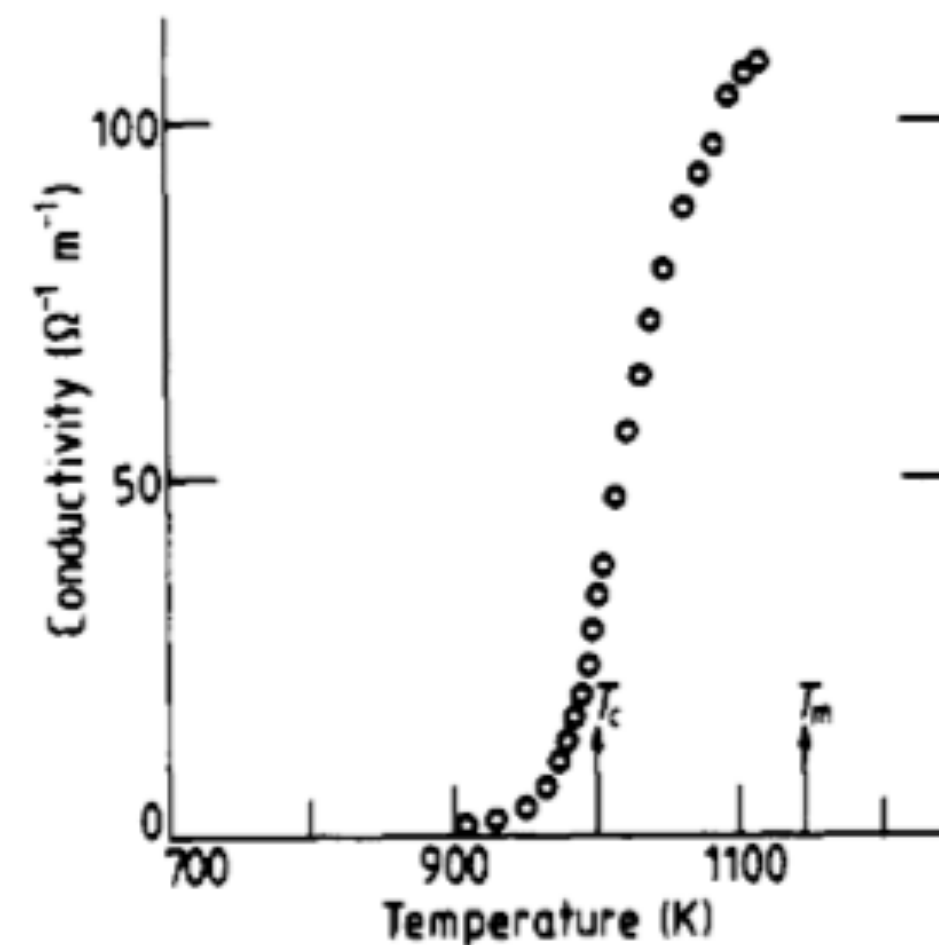
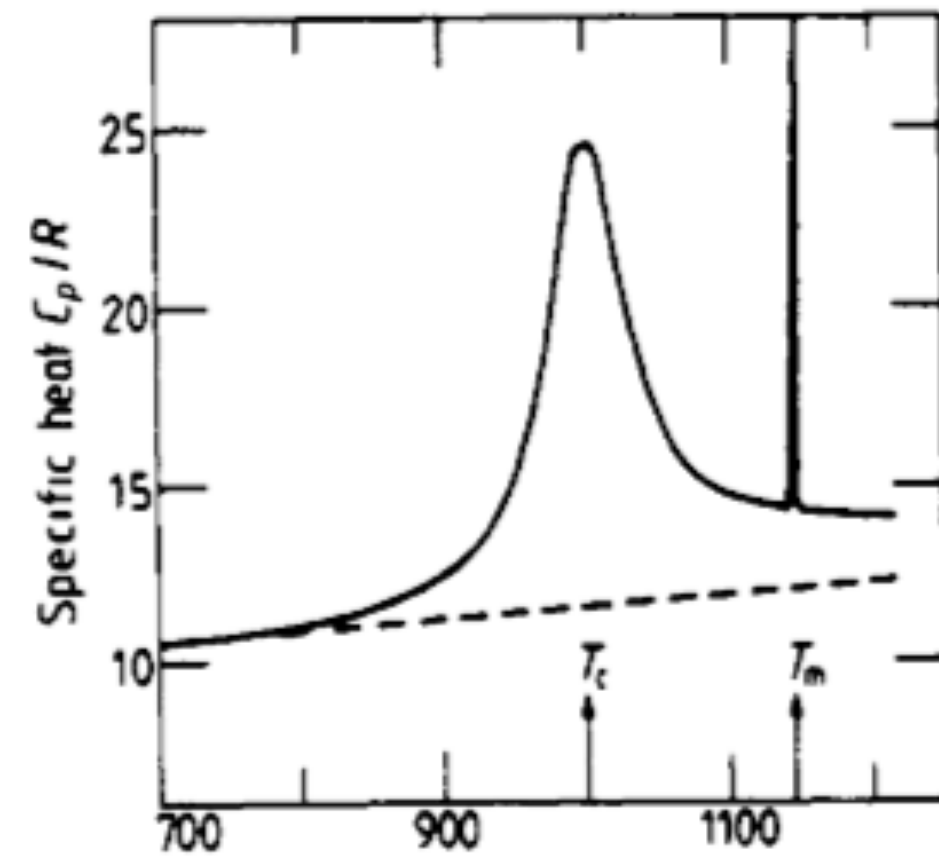
DIFFUSE SCATTERING FROM A FAST-ION CONDUCTOR

Sublattice Melting in Fluorite Compounds



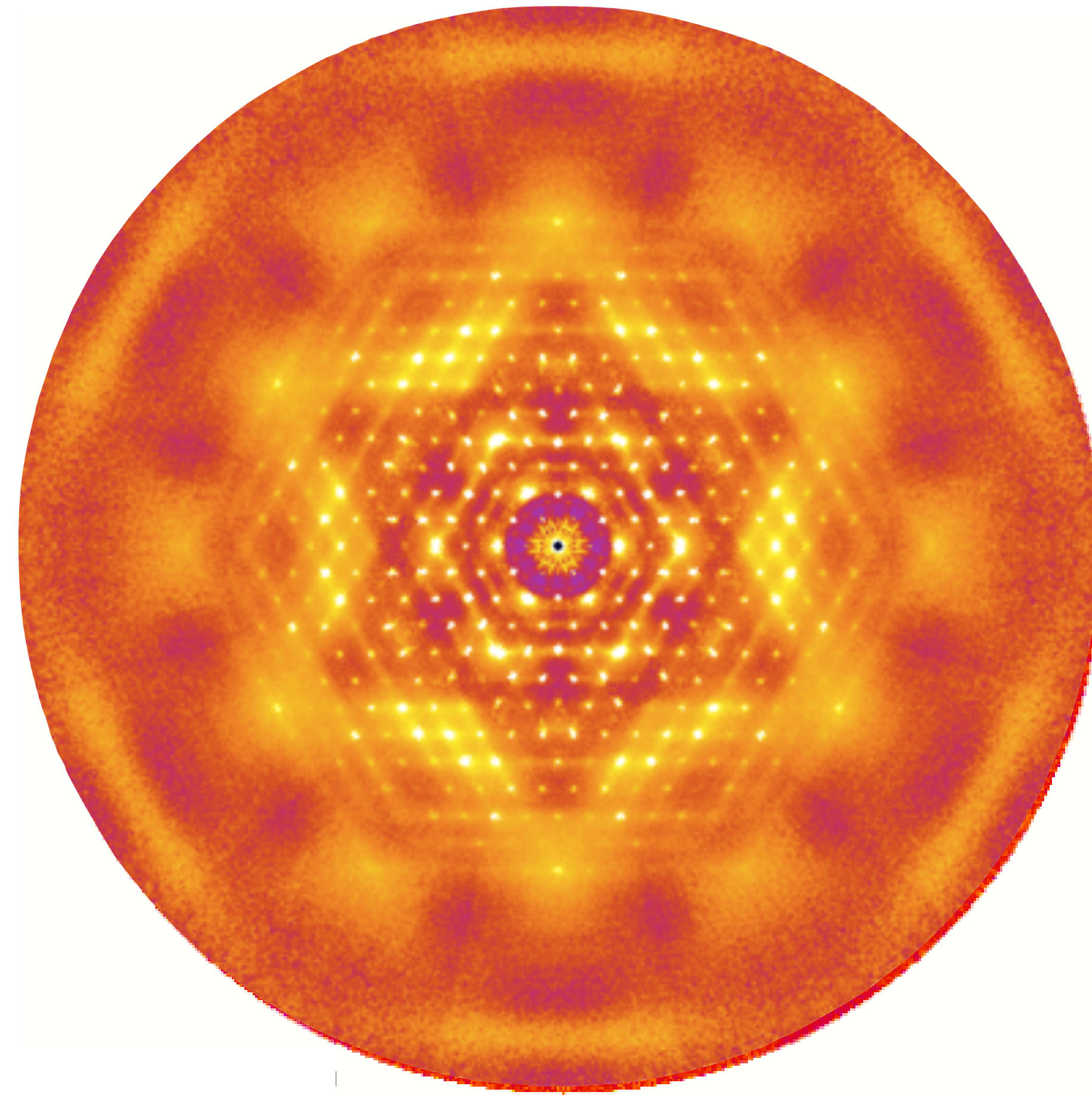
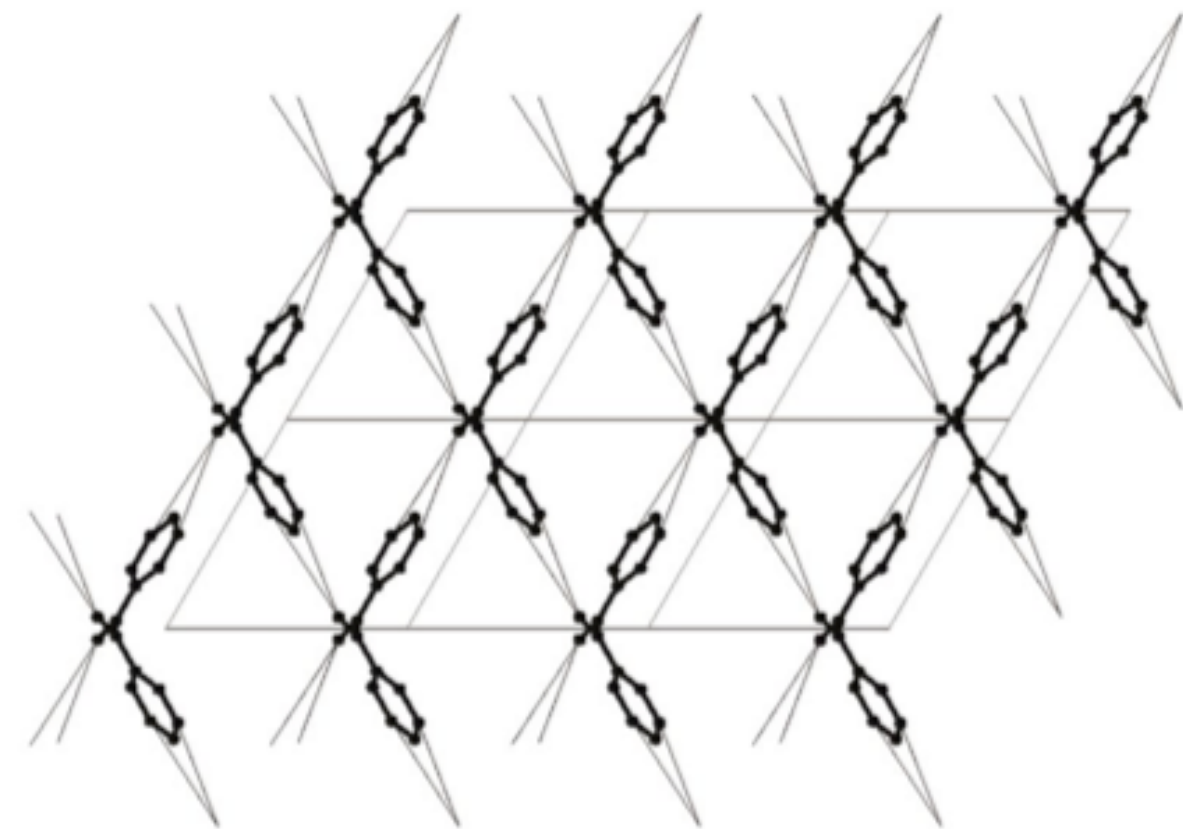
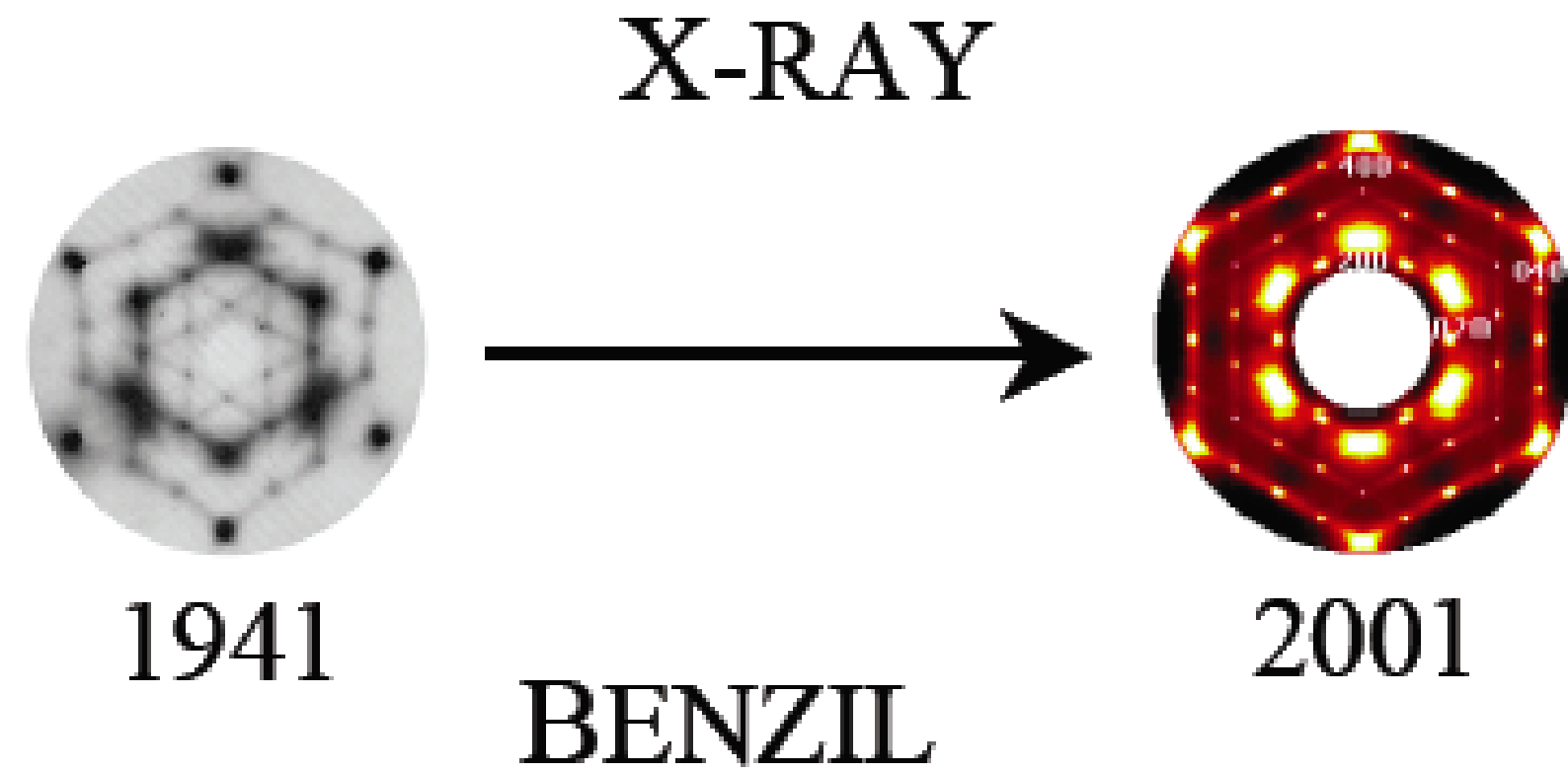
CaF₂

M. T. Hutchings *et al*
 J. Phys. C **17**, 3903 (1984)



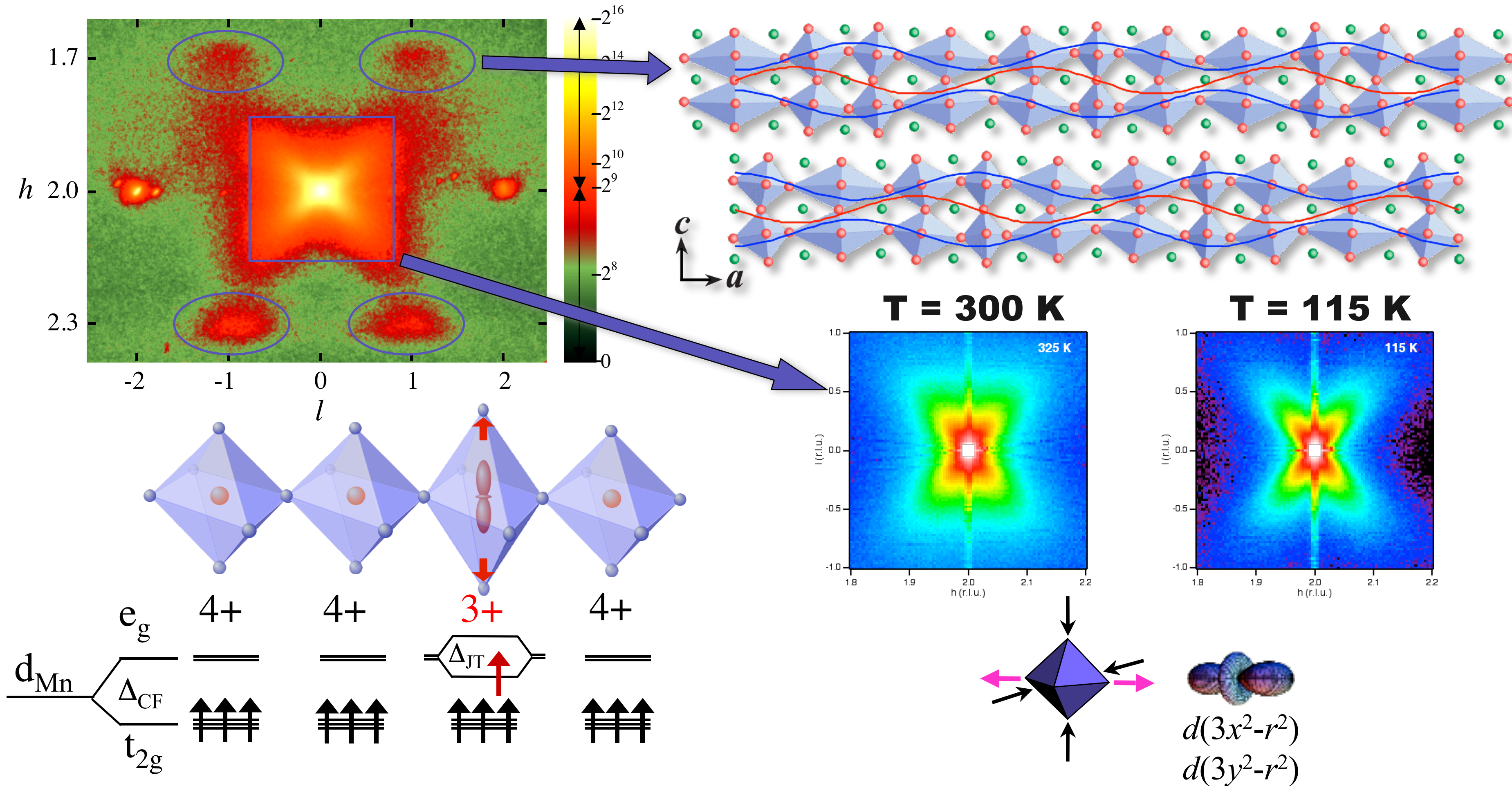
DIFFUSE SCATTERING FROM MOLECULAR SOLIDS

Molecular Flexibility in Benzil



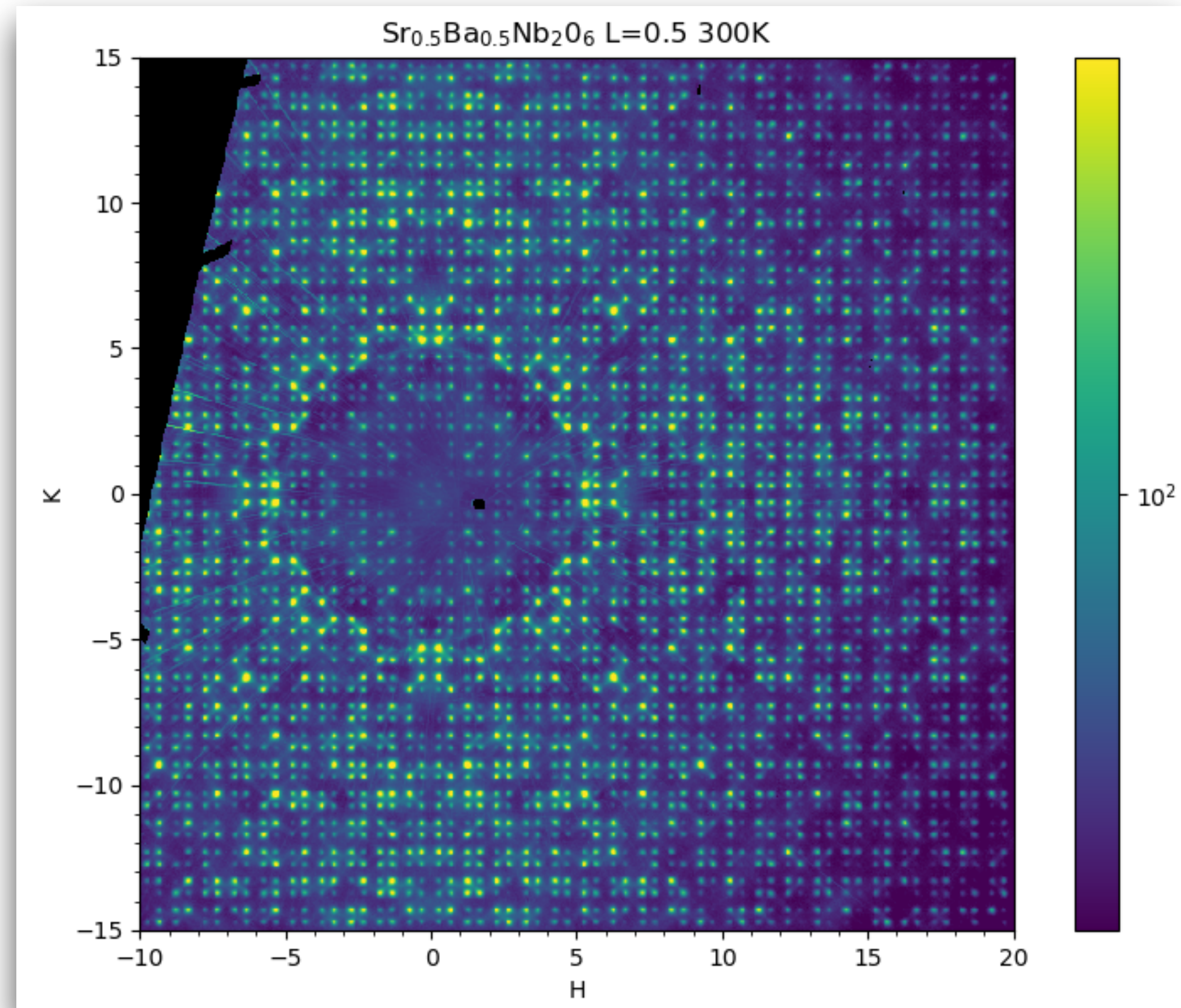
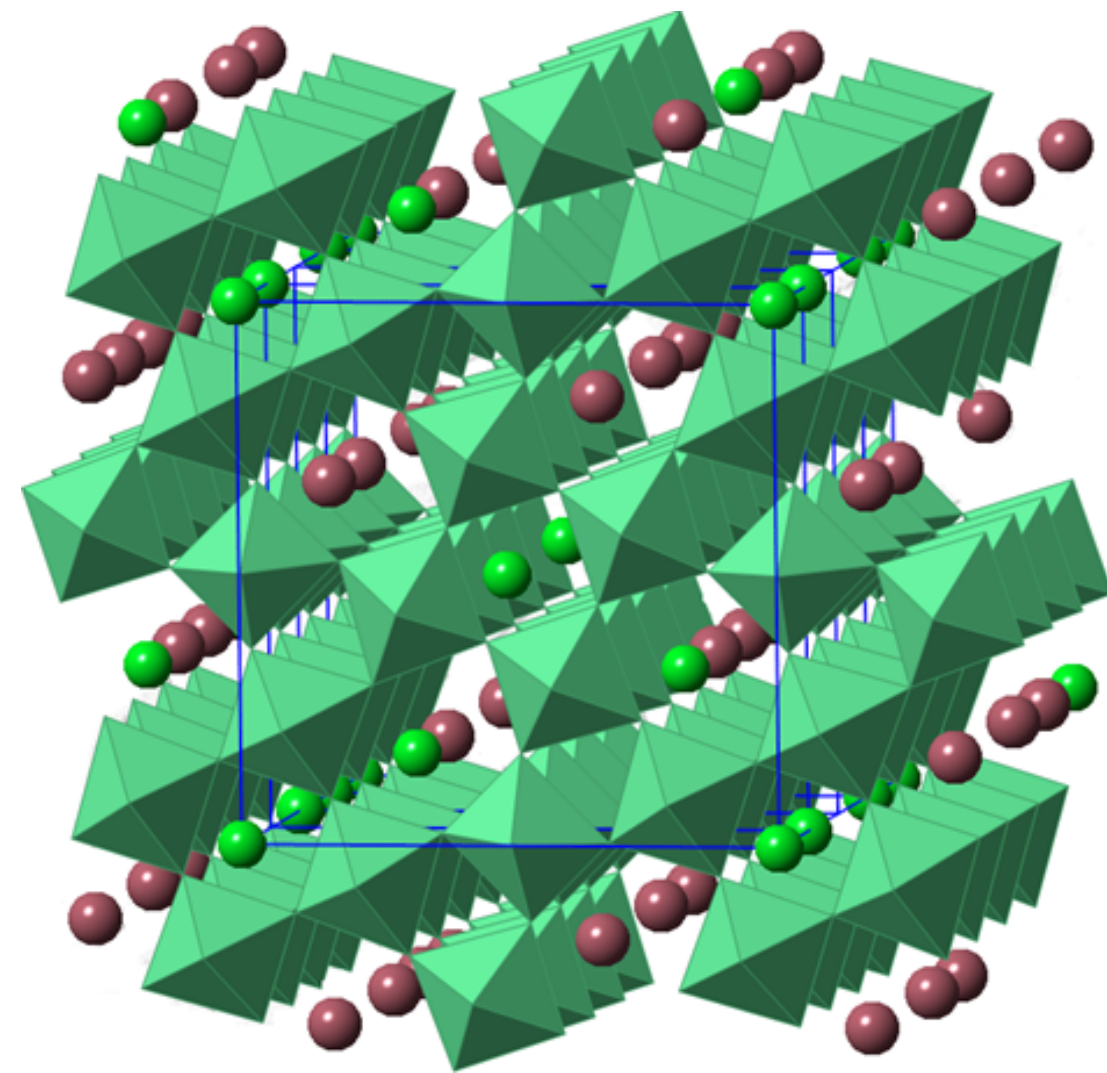
T. R. Welberry *et al* J. Appl. Cryst. **36**, 1400 (2003)

DIFFUSE SCATTERING FROM JAHN-TELLER POLARONS



B. J. Campbell, *et al.*, Phys Rev B **65**, 014427 (2002).

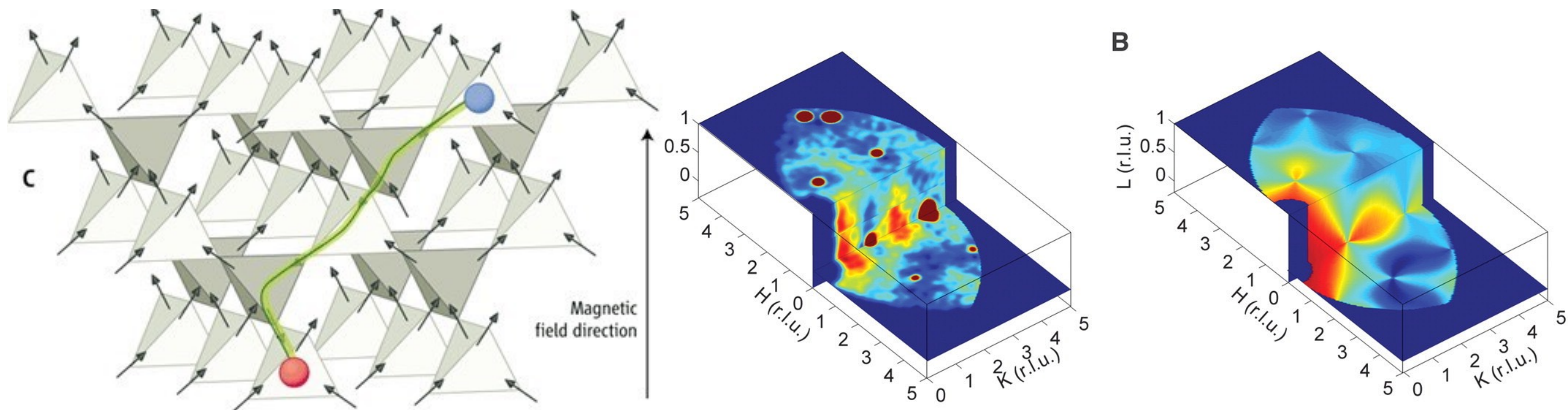
INCOMMENSURATE MODULATIONS IN $\text{Sr}_{0.5}\text{Ba}_{0.5}\text{NbO}_6$



Acknowledgements:
Bixia Wang and Daniel Phelan

MAGNETIC MONOPOLES IN SPIN ICE

Diffuse Magnetic Scattering in $\text{Dy}_2\text{Ti}_2\text{O}_7$



D. J. P. Morris, *et al.*, *Science* **326**, 411 (2009).

HOW DO I MODEL IT?



U.S. DEPARTMENT OF
ENERGY

Argonne National Laboratory is a
U.S. Department of Energy laboratory
managed by UChicago Argonne, LLC.

Argonne 
NATIONAL LABORATORY

DIFFUSE SCATTERING THEORY

A Few Equations $I = \sum_i \sum_j b_i b_j \exp(i\mathbf{Q} \cdot \mathbf{r}_{ij})$

- **Laue Monotonic Diffuse Scattering**

$$I = \bar{b}^2 \sum_{ij} \exp(i\mathbf{Q} \cdot \mathbf{r}_{ij}) + N(\bar{b}^2 - \bar{b}^2); \quad \bar{b}^2 = (c_A b_A + c_B b_B)^2; \quad \bar{b}^2 = c_A c_B (b_B - b_A)^2$$

- **Cowley Short-Range Order**

$$I_{diffuse} = N c_A c_B (b_B - b_A)^2 + \sum_{ij} \alpha_{ij} c_B c_A (b_B - b_A)^2 \exp(i\mathbf{Q} \cdot \mathbf{r}_{ij}); \quad \alpha_{ij} = \left(1 - \frac{P_{ij}}{c_j}\right)$$

- **Warren Size Effect**

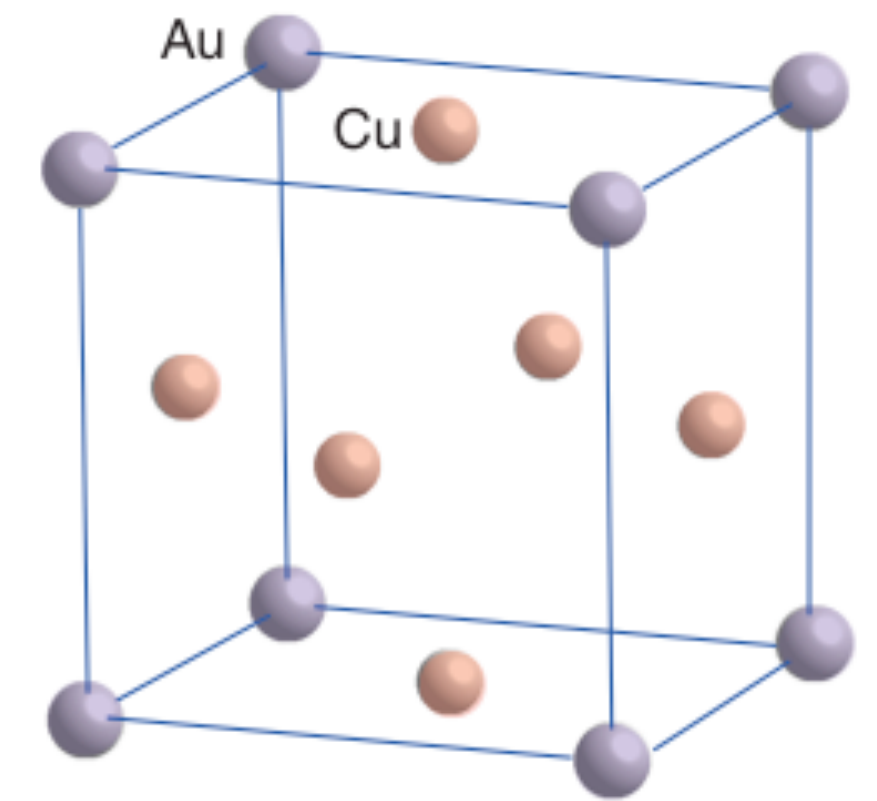
$$I_{diffuse} = N c_A c_B (b_B - b_A)^2 \left(1 + \sum_{ij} \alpha_{ij} \exp(i\mathbf{Q} \cdot \mathbf{r}_{ij}) + \beta_{ij} \exp(i\mathbf{Q} \cdot \mathbf{r}_{ij})\right); \quad \beta_{ij} = f(\epsilon_{AA}^{ij}, \epsilon_{BB}^{ij})$$

- **Borie and Sparks Correlations**

$$I = \sum_i \sum_j b_i b_j \exp(i\mathbf{Q} \cdot (\mathbf{R}_i - \mathbf{R}_j)) \left[1 + i\mathbf{Q} \cdot (\mathbf{u}_i - \mathbf{u}_j) - \frac{1}{2} (\mathbf{Q} \cdot (\mathbf{u}_i - \mathbf{u}_j))^2 + \dots\right]$$

V. M. Nield and D. A. Keen *Diffuse Neutron Scattering From Crystalline Materials* (2001)

T. R. Welberry *Diffuse X-ray Scattering and Models of Disorder* (2022)



J. M. Cowley, J. Appl. Phys. 21, 24 (1950)

SOME RULES OF THUMB

Acknowledgment: Hans Beat Bürgi

Reciprocal space

- Sharp Bragg reflections
 - no defects
- Sharp diffuse rods
 - no defects
- Sharp diffuse planes
 - no defects
- Diffuse clouds
 - no defects



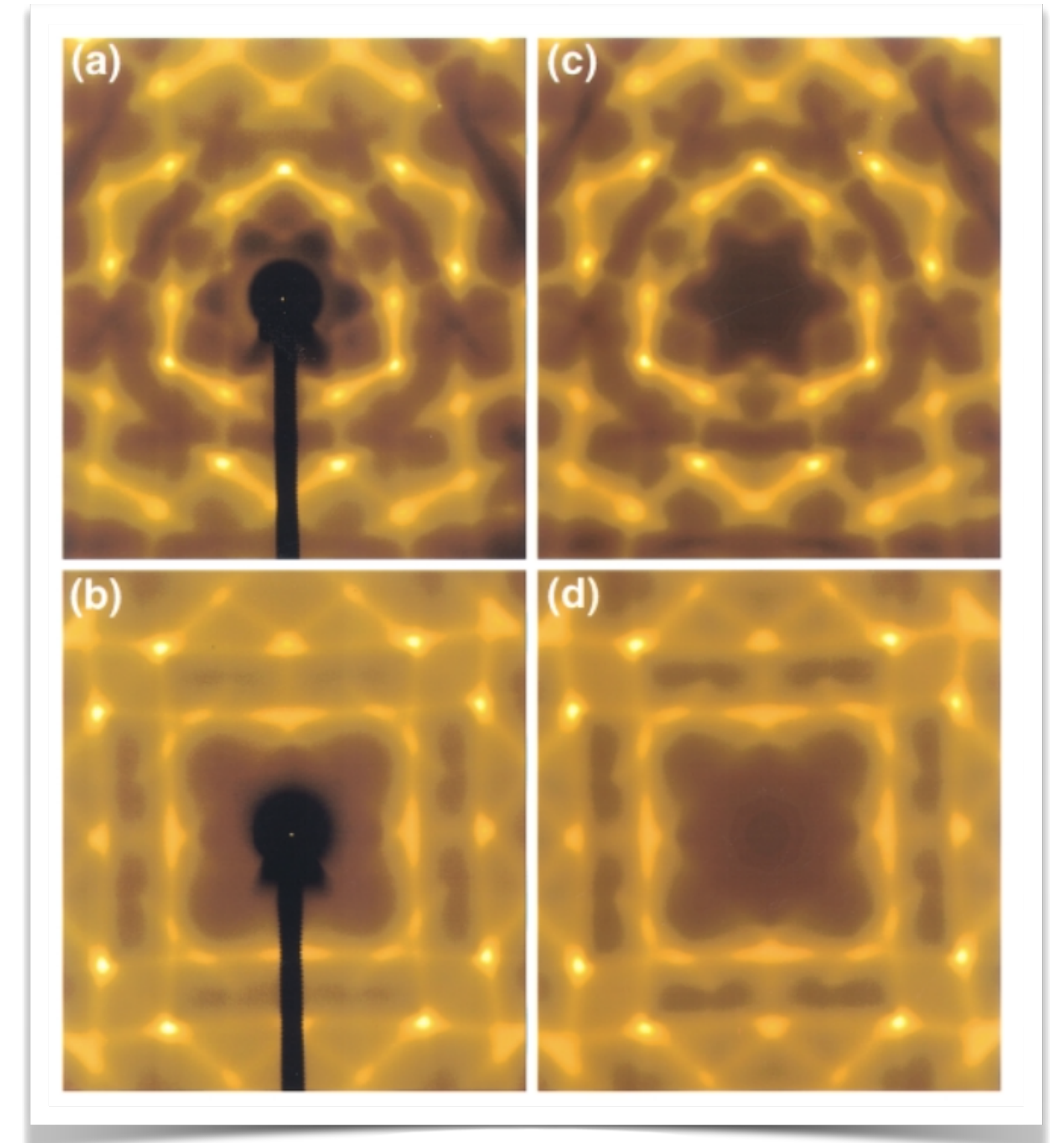
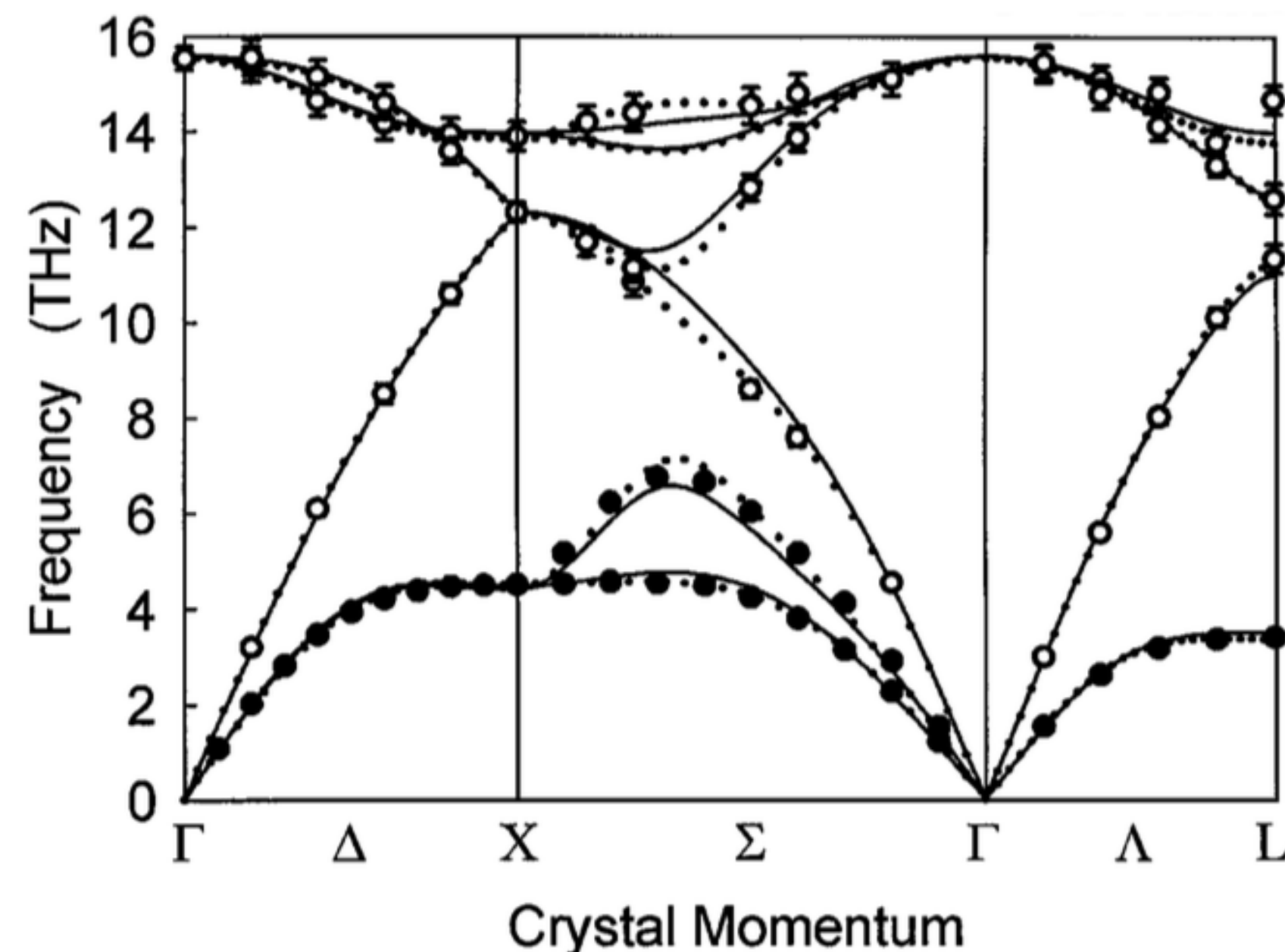
Direct space

- 3D-periodic structure
 - no defects
- 2D-periodic structure
 - perpendicular to the streaks
 - disordered in streak directions
- 1D-periodic structure
 - perpendicular to the planes
 - disordered within the plane
- 0D-periodic structure
 - no fully ordered direction

THERMAL DIFFUSE SCATTERING

M. Holt, *et al*, Phys Rev Lett **83**, 3317 (1999).

- Lattice vibrations produce deviations from the average structure even in perfect crystals
- X-ray scattering intensity is given by the integral over all the phonon branches at each Q



$$I_0 \propto f^2 e^{-2M} \sum_{j=1}^6 \frac{|\mathbf{q} \cdot \hat{\mathbf{e}}_j|^2}{\omega_j} \coth\left(\frac{\hbar\omega_j}{2k_B T}\right).$$

HOW DO I MEASURE IT?



U.S. DEPARTMENT OF
ENERGY

Argonne National Laboratory is a
U.S. Department of Energy laboratory
managed by UChicago Argonne, LLC.



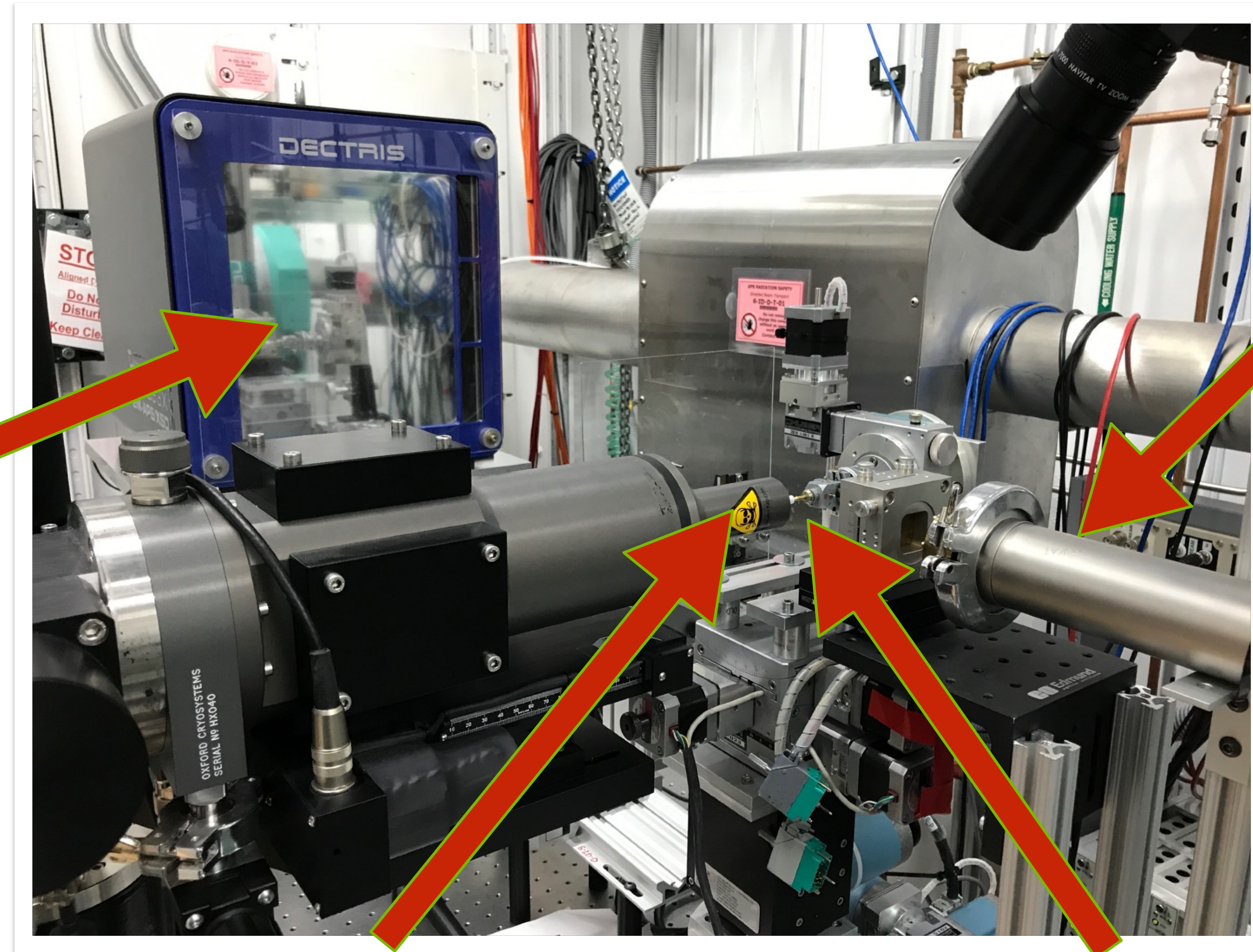
MEASURING X-RAY DIFFUSE SCATTERING

Continuous Rotation Method

Sector 6 - APS

Detector

Incident Beam



Cryocooler

Sample

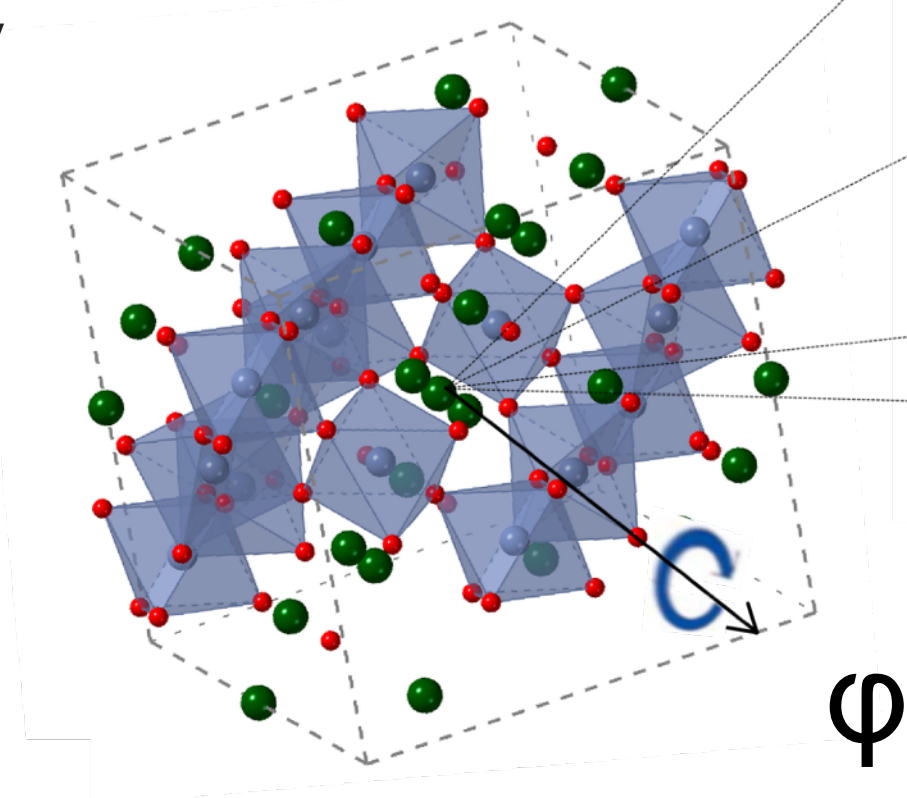
X-RAY SCATTERING GEOMETRY

Continuous Rotation Method

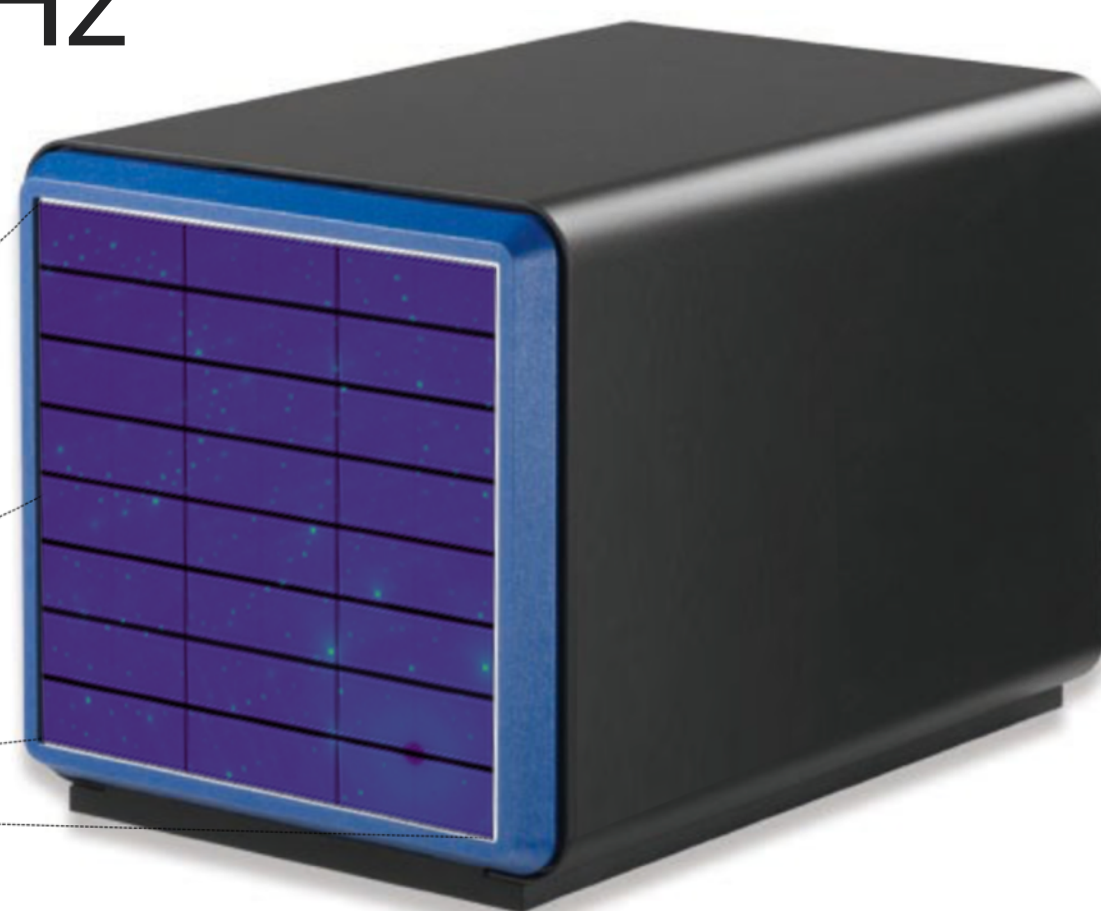
- The sample is continuously rotated at 1°s^{-1}
- Frames are collected at 10Hz
 - 3600 x 8MB frames
 - 30GB every 6 minutes
 - 3TB per day



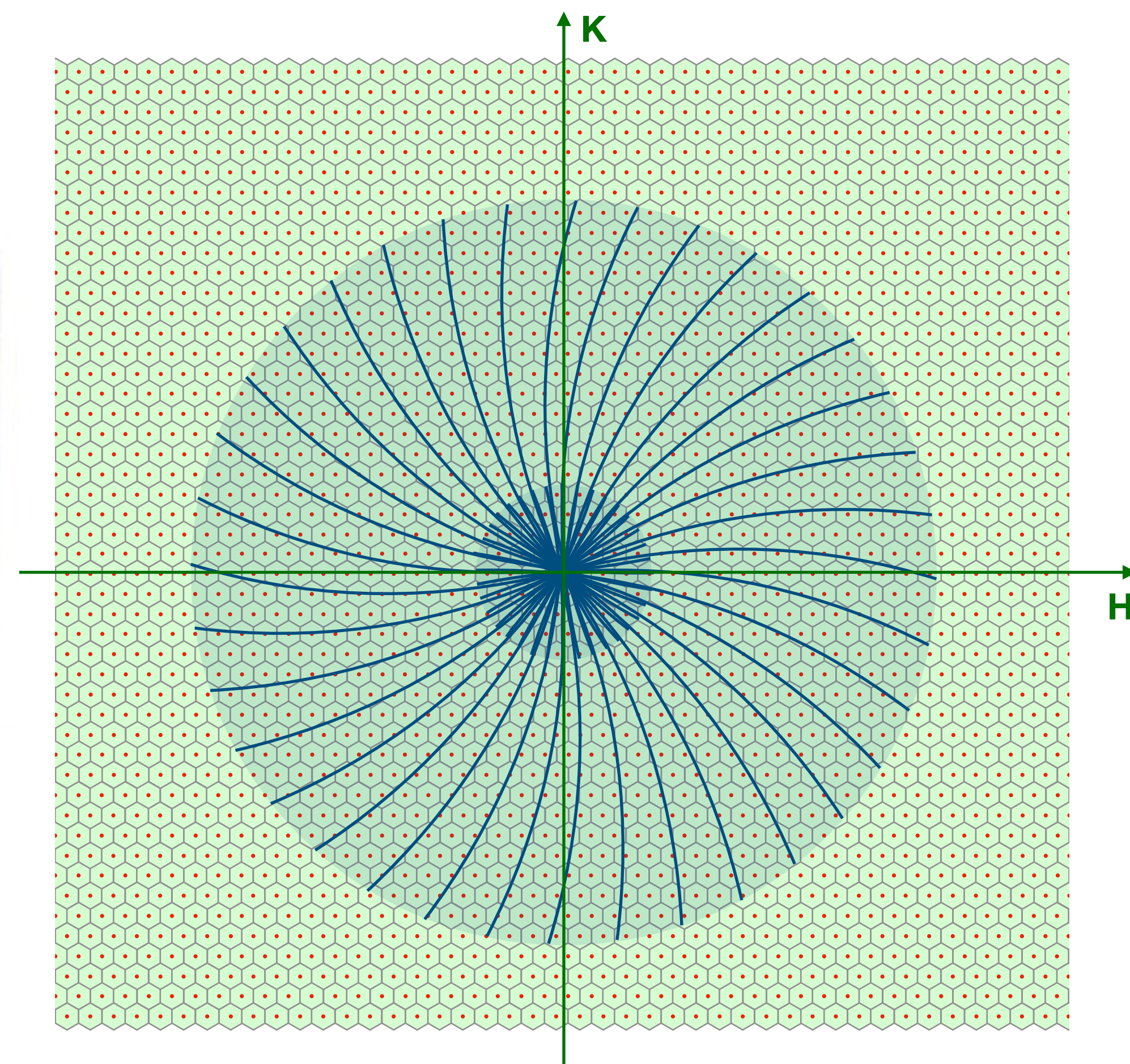
Incident
Beam



Sample



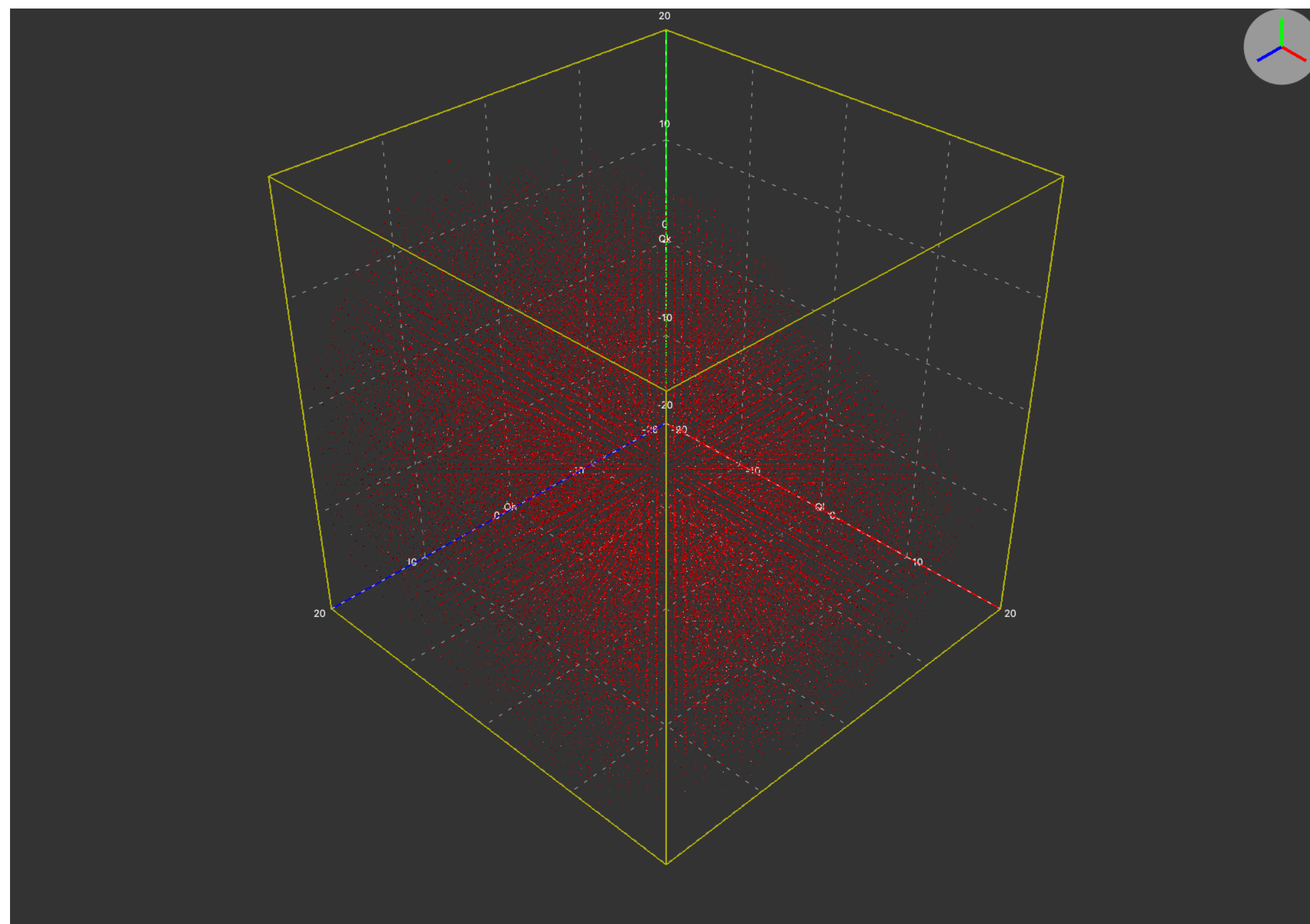
Pilatus 2M CdTe
Detector



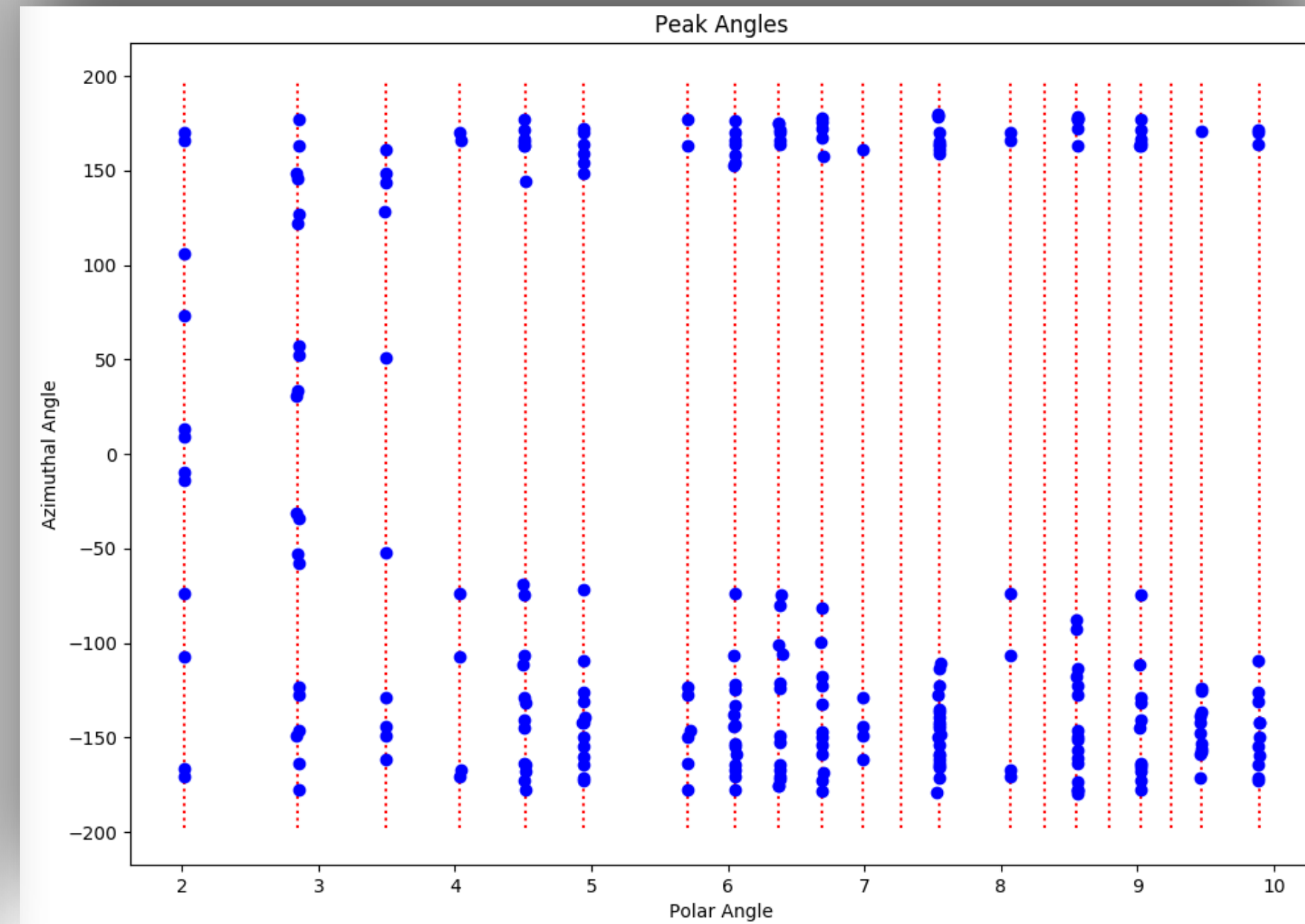
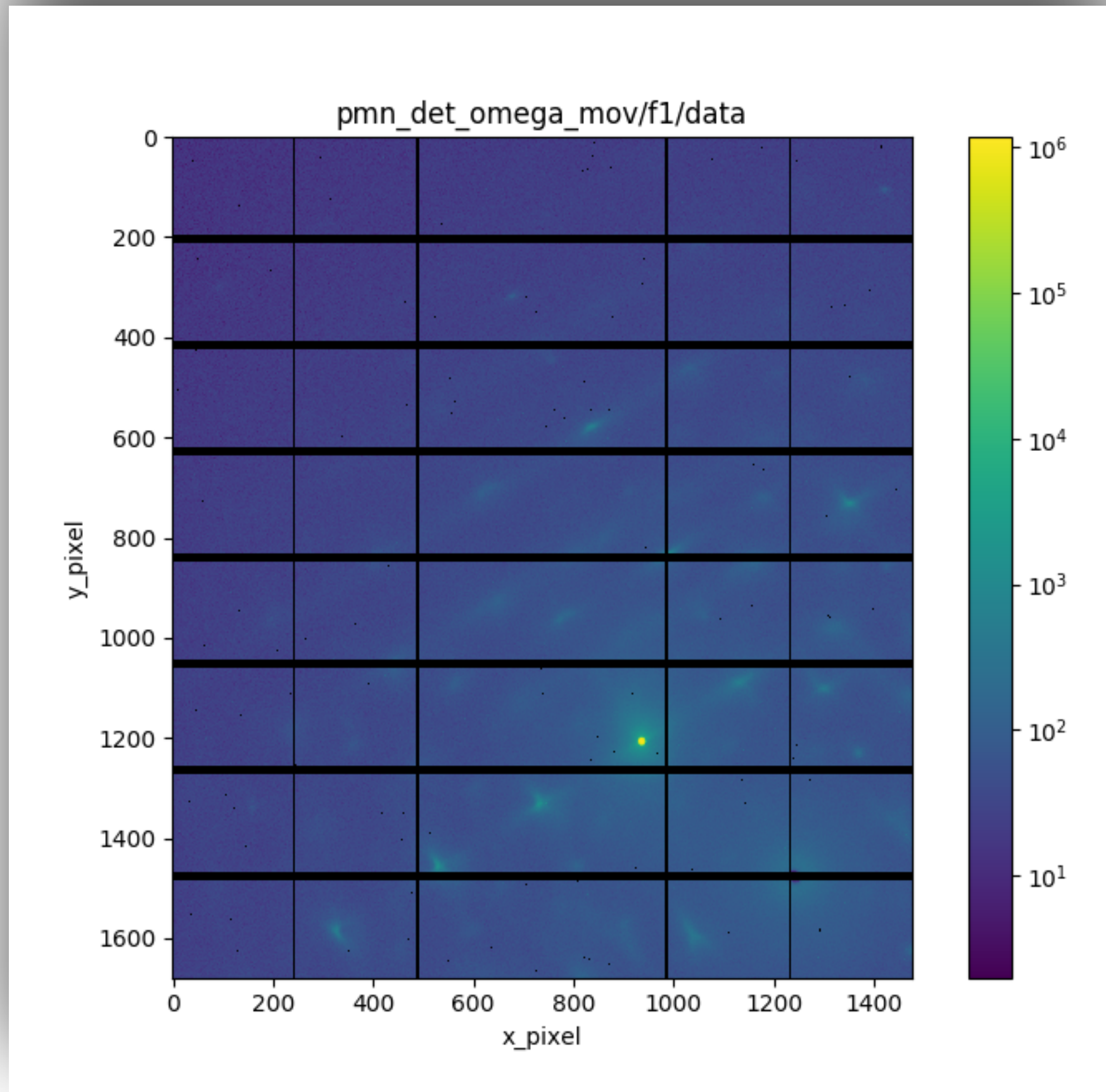
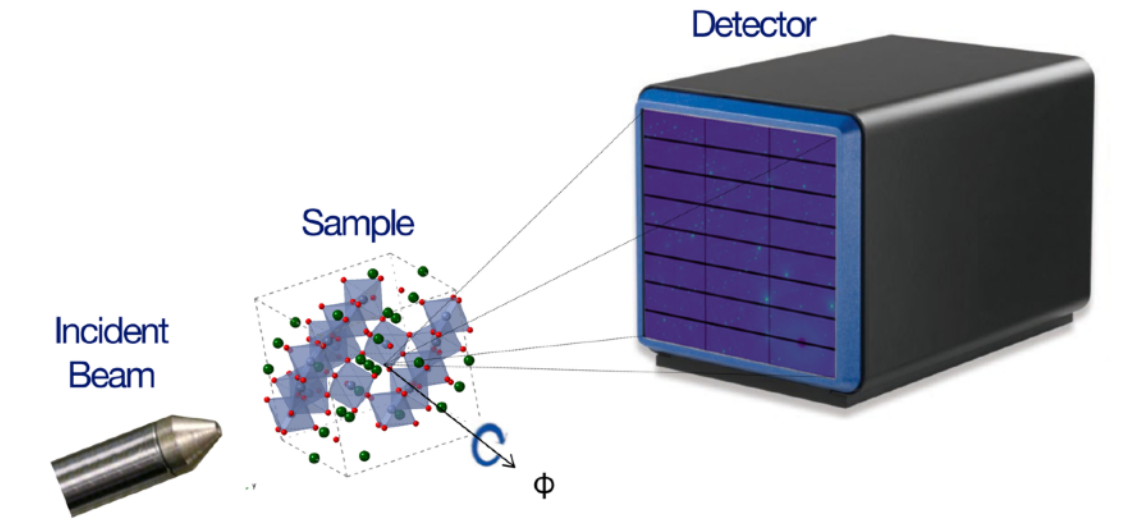
Reciprocal Space

Q-RANGE IN ROTATION METHOD ON SECTOR 6

- With the following parameters, we cover $-15\text{\AA}^{-1} < \mathbf{Q} < 15\text{\AA}^{-1}$
 - $E_i \sim 87 \text{ keV}$
 - $\lambda \sim 0.14 \text{ \AA}$
 - Detector distance $\sim 650 \text{ mm}$
 - Pilatus 2M CdTe: 1679×1475 pixels
 - Pixel size $\sim 170 \text{ }\mu\text{m}$
- This Q-range includes thousands of Brillouin zones.
 - *e.g.*, for $a \sim 10 \text{ \AA}$, $\sim 60,000$ Bragg peaks



EXPERIMENT WORKFLOW



pmn_det_omega_mov_mask/f1 Peak Table

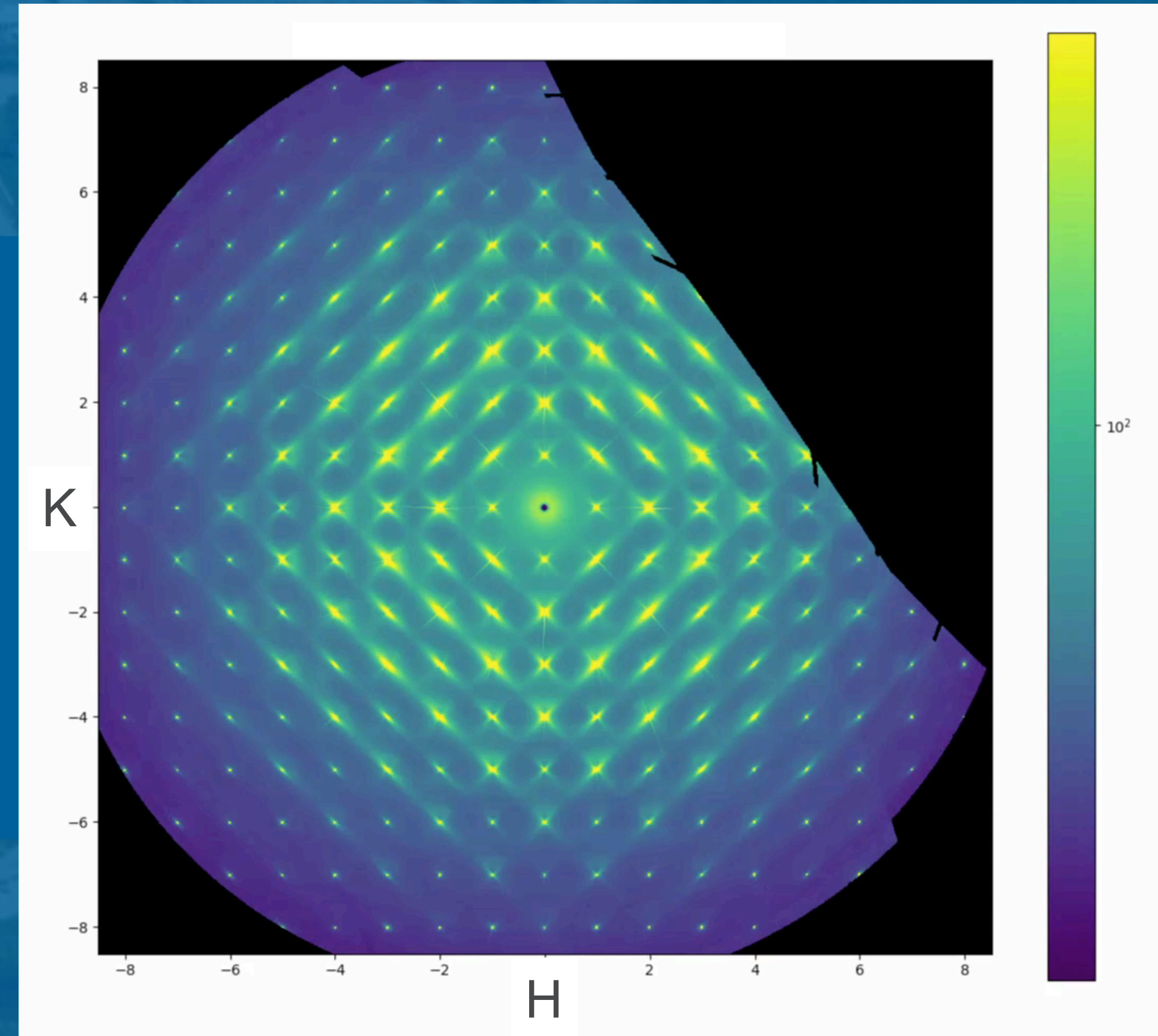
Primary Secondary

| i | x | y | z | olz | Δ | Azi | Intensity | H | K | L | Diff |
|-----|------|------|------|------|---------|----------|-----------|-------|-------|-------|------|
| 195 | 1214 | 1638 | 1574 | 2.01 | -10.00 | 2.44e+07 | -0.00 | 0.00 | -1.00 | 0.000 | |
| 291 | 1280 | 1637 | 2447 | 2.01 | 13.15 | 1.8e+07 | 1.00 | -0.00 | 0.00 | 0.000 | |
| 403 | 1269 | 1639 | 3371 | 2.01 | 9.14 | 2.12e+07 | -0.00 | 0.00 | 1.00 | 0.001 | |
| 76 | 1203 | 1636 | 652 | 2.01 | -13.70 | 3.89e+06 | -1.00 | -0.00 | -0.00 | 0.001 | |
| 336 | 1083 | 1522 | 2824 | 2.01 | -73.81 | 2.35e+08 | 0.00 | 1.00 | 0.00 | 0.001 | |
| 116 | 1401 | 1523 | 960 | 2.01 | 73.36 | 1.99e+08 | -0.00 | -1.00 | 0.00 | 0.000 | |
| 342 | 1402 | 1428 | 2894 | 2.01 | 106.43 | 2.37e+08 | -0.00 | -1.00 | 0.00 | 0.000 | |
| 126 | 1083 | 1426 | 1030 | 2.02 | -107.25 | 2.36e+08 | 0.00 | 1.00 | 0.00 | 0.000 | |
| 78 | 1282 | 1313 | 672 | 2.02 | 166.43 | 1.95e+07 | 1.00 | 0.00 | -0.00 | 0.001 | |
| 406 | 1215 | 1311 | 3391 | 2.02 | -170.57 | 2.74e+07 | -0.00 | 0.00 | -1.00 | 0.001 | |
| 196 | 1271 | 1311 | 1595 | 2.02 | 170.31 | 1.49e+07 | -0.00 | 0.00 | 1.00 | 0.001 | |
| 296 | 1204 | 1313 | 2468 | 2.03 | -166.77 | 1.99e+07 | -1.00 | 0.00 | -0.00 | 0.001 | |
| 84 | 1362 | 1676 | 718 | 2.83 | 30.83 | 3.35e+07 | -0.99 | -1.00 | 0.00 | 0.003 | |
| 302 | 1120 | 1675 | 2530 | 2.83 | -31.44 | 3.53e+07 | 0.99 | 1.00 | -0.00 | 0.002 | |
| 306 | 1364 | 1275 | 2563 | 2.84 | 148.77 | 4.44e+07 | -0.99 | -1.00 | 0.00 | 0.002 | |
| 90 | 1122 | 1274 | 751 | 2.84 | -149.17 | 2.49e+07 | 0.99 | 1.00 | -0.00 | 0.003 | |
| 181 | 1373 | 1670 | 1443 | 2.84 | 33.83 | 8.12e+07 | 0.00 | -1.00 | -1.00 | 0.000 | |
| 215 | 1055 | 1616 | 1732 | 2.84 | -53.13 | 1.23e+08 | 0.00 | 1.00 | -1.00 | 0.001 | |
| 274 | 1440 | 1602 | 2288 | 2.85 | 57.29 | 1.25e+08 | 1.00 | -1.00 | 0.00 | 0.001 | |
| 421 | 1429 | 1618 | 3506 | 2.85 | 52.51 | 1.32e+08 | 0.00 | -1.00 | 1.00 | 0.001 | |
| 391 | 1109 | 1669 | 3256 | 2.85 | -34.45 | 6.54e+07 | -0.00 | 1.00 | 1.00 | 0.000 | |
| 58 | 1043 | 1601 | 518 | 2.85 | -57.74 | 1.13e+08 | -1.00 | 1.00 | 0.00 | 0.001 | |
| 64 | 1441 | 1349 | 571 | 2.85 | 122.40 | 1.08e+08 | 1.00 | -1.00 | 0.00 | 0.000 | |
| 394 | 1375 | 1281 | 3290 | 2.85 | 145.75 | 8.31e+07 | -0.00 | -1.00 | -1.00 | 0.000 | |
| 220 | 1430 | 1333 | 1779 | 2.86 | 127.17 | 1.31e+08 | -0.00 | -1.00 | 1.00 | 0.001 | |
| 427 | 1056 | 1331 | 3553 | 2.86 | -127.69 | 9.27e+07 | -0.00 | 1.00 | -1.00 | 0.001 | |
| 186 | 1112 | 1279 | 1477 | 2.86 | -146.36 | 8.88e+07 | 0.00 | 1.00 | 1.00 | 0.000 | |
| 23 | 1254 | 1240 | 232 | 2.86 | 177.08 | 2.57e+07 | 1.00 | 0.00 | -1.00 | 0.000 | |
| 280 | 1045 | 1346 | 2341 | 2.86 | -123.16 | 1.37e+08 | -1.00 | 1.00 | 0.00 | 0.001 | |

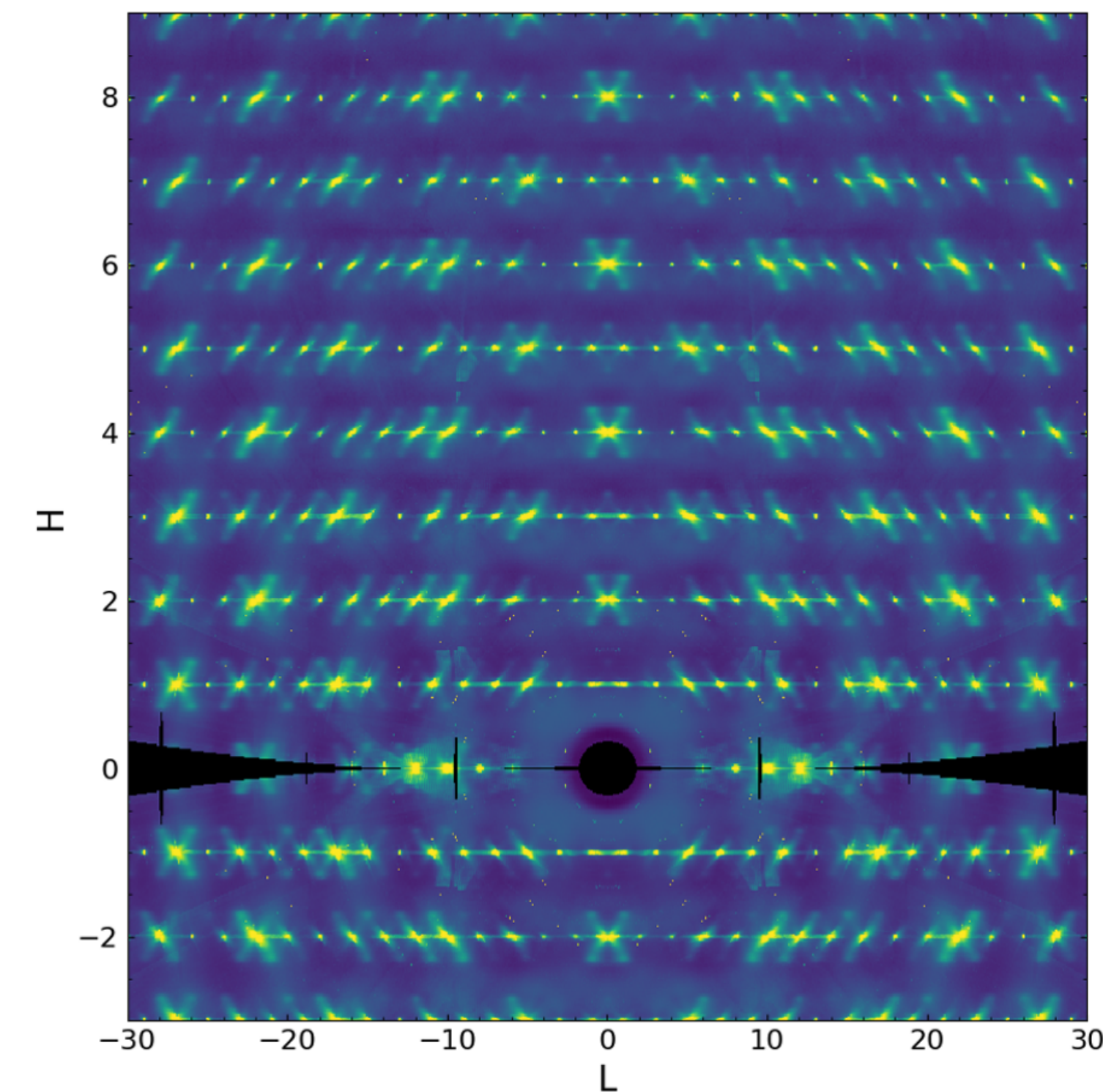
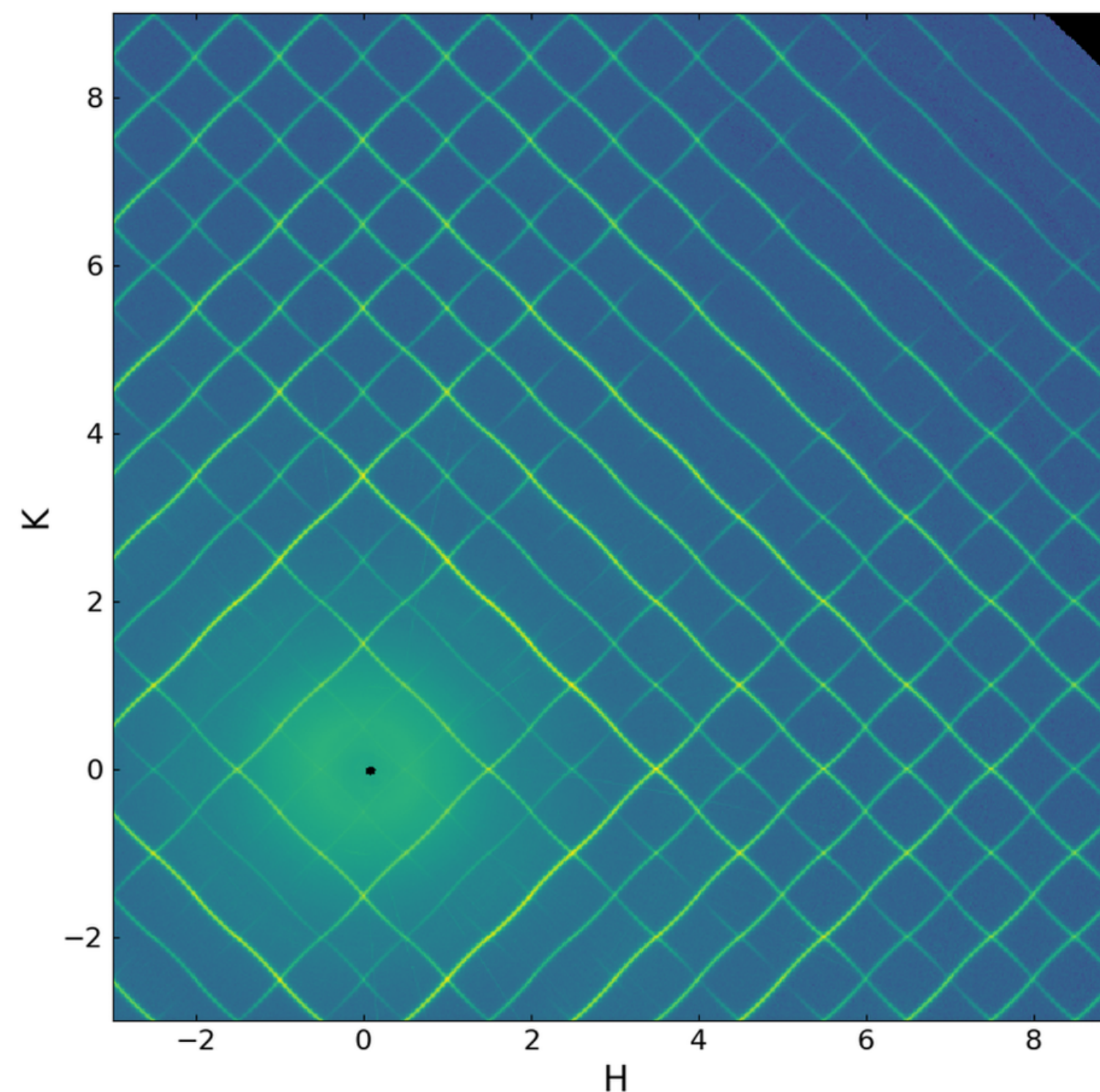
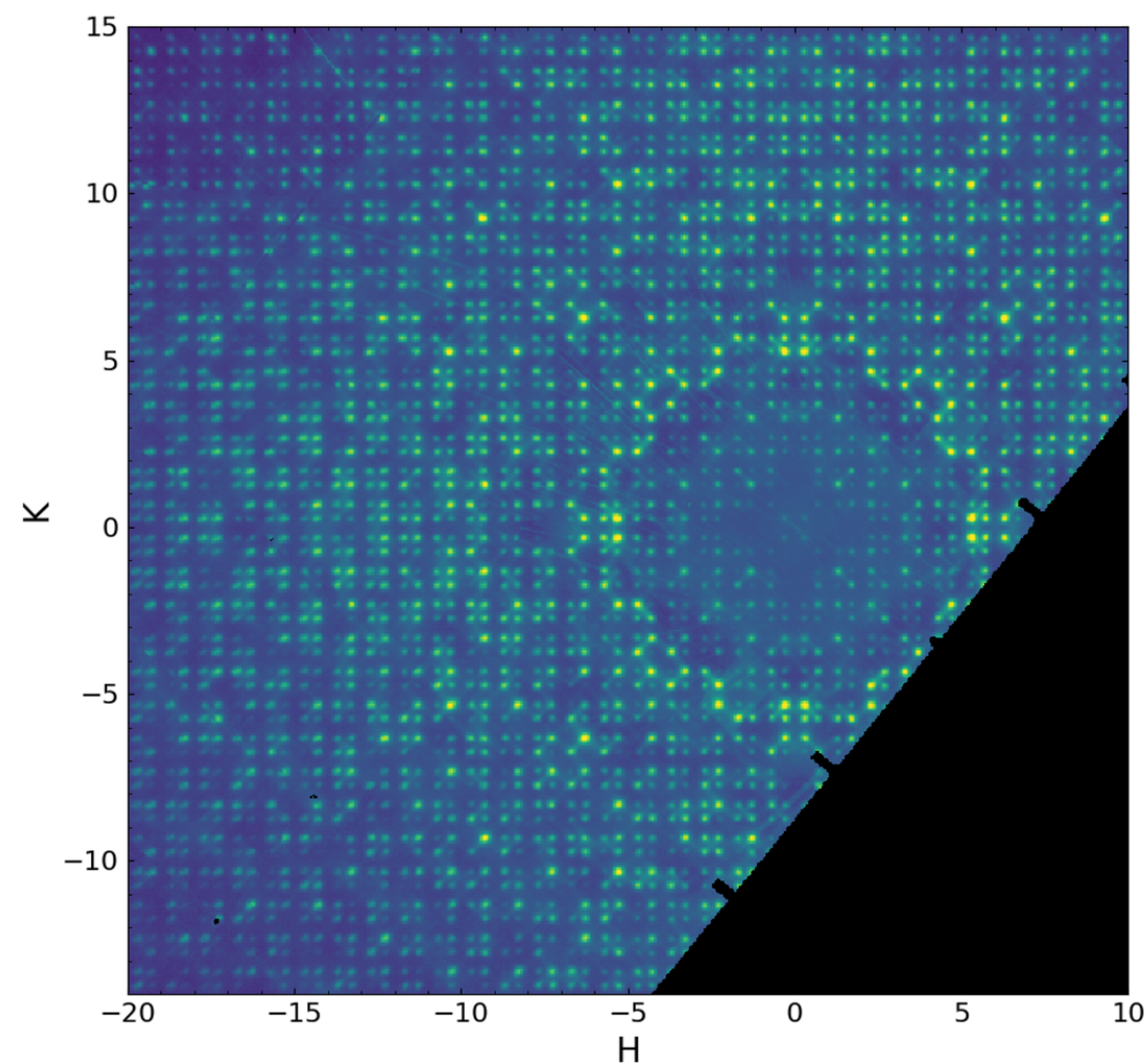
Score: 0.0007 Threshold

DIFFUSE SCATTERING IN 3D THE RELAXOR $\text{PbMg}_{1/3}\text{Nb}_{2/3}\text{O}_3$

M. J. Krogstad, *et al*, Nature Materials 48, 1 (2018).



DIFFUSE GALLERY



CASE STUDY 1: MULLITE



U.S. DEPARTMENT OF
ENERGY

Argonne National Laboratory is a
U.S. Department of Energy laboratory
managed by UChicago Argonne, LLC.

Argonne 
NATIONAL LABORATORY

MULLITE - A CASE STUDY

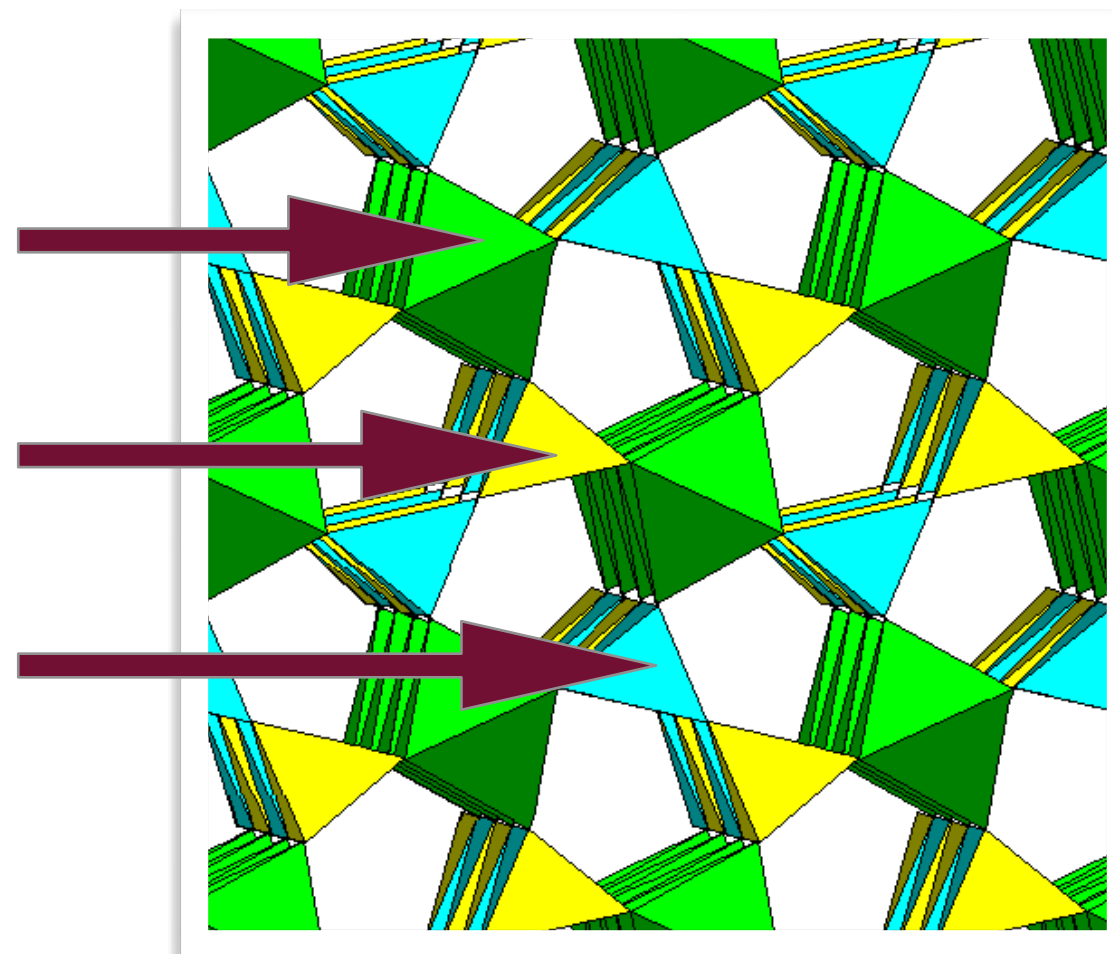
B. D. Butler, T. R. Welberry, & R. L. Withers, *Phys Chem Minerals* **20**, 323 (1993)

- Mullite is a ceramic that is formed by adding O^{2+} vacancies to Sillimanite
 - Sillimanite has alternating AlO_4 and SiO_4 tetrahedra
 - Mullite has excess Al^{3+} occupying Si^{2+} sites for charge balance
- This results in strong vacancy-vacancy correlations

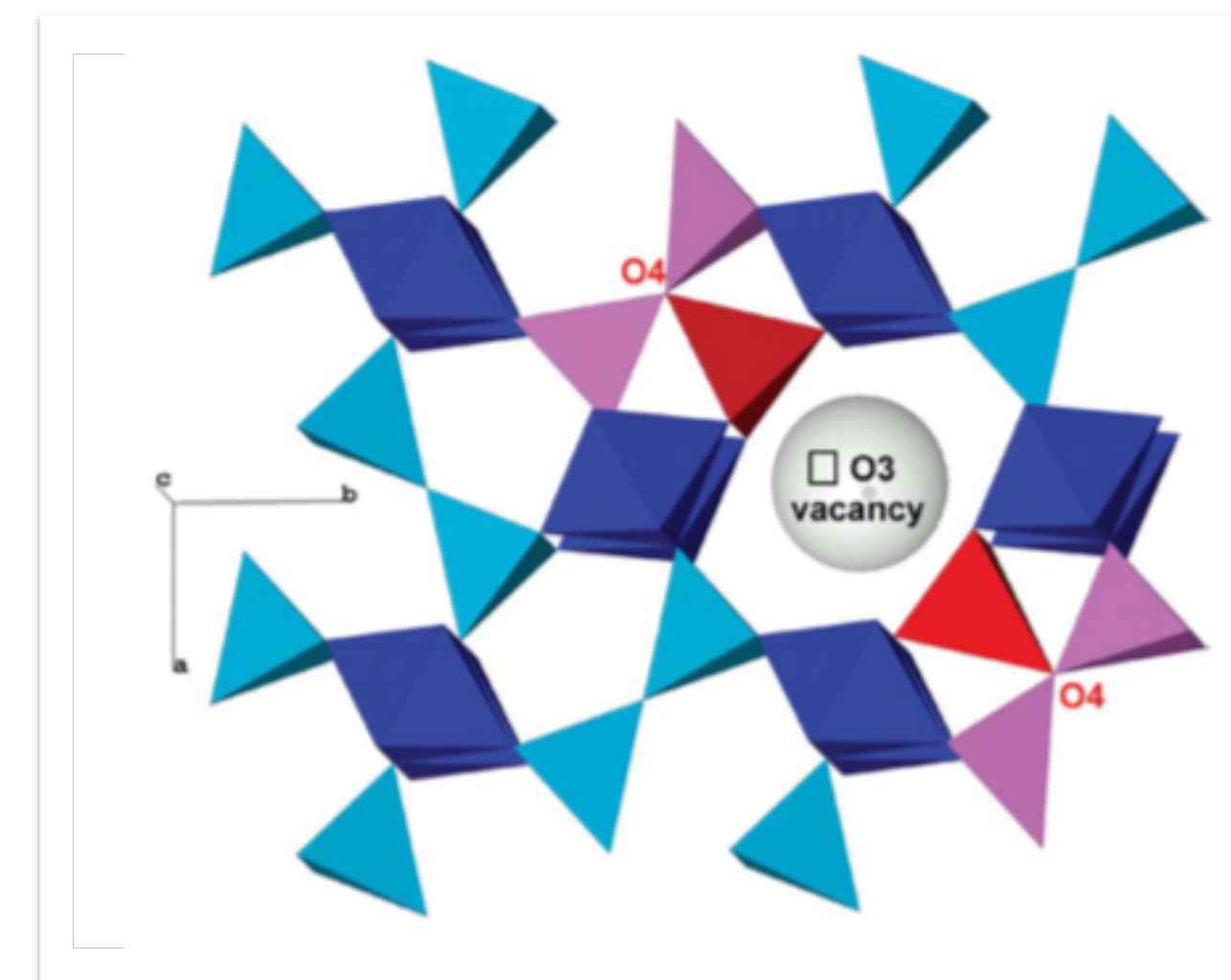
AlO_6 Octahedra

SiO_4 Tetrahedra

AlO_4 Tetrahedra



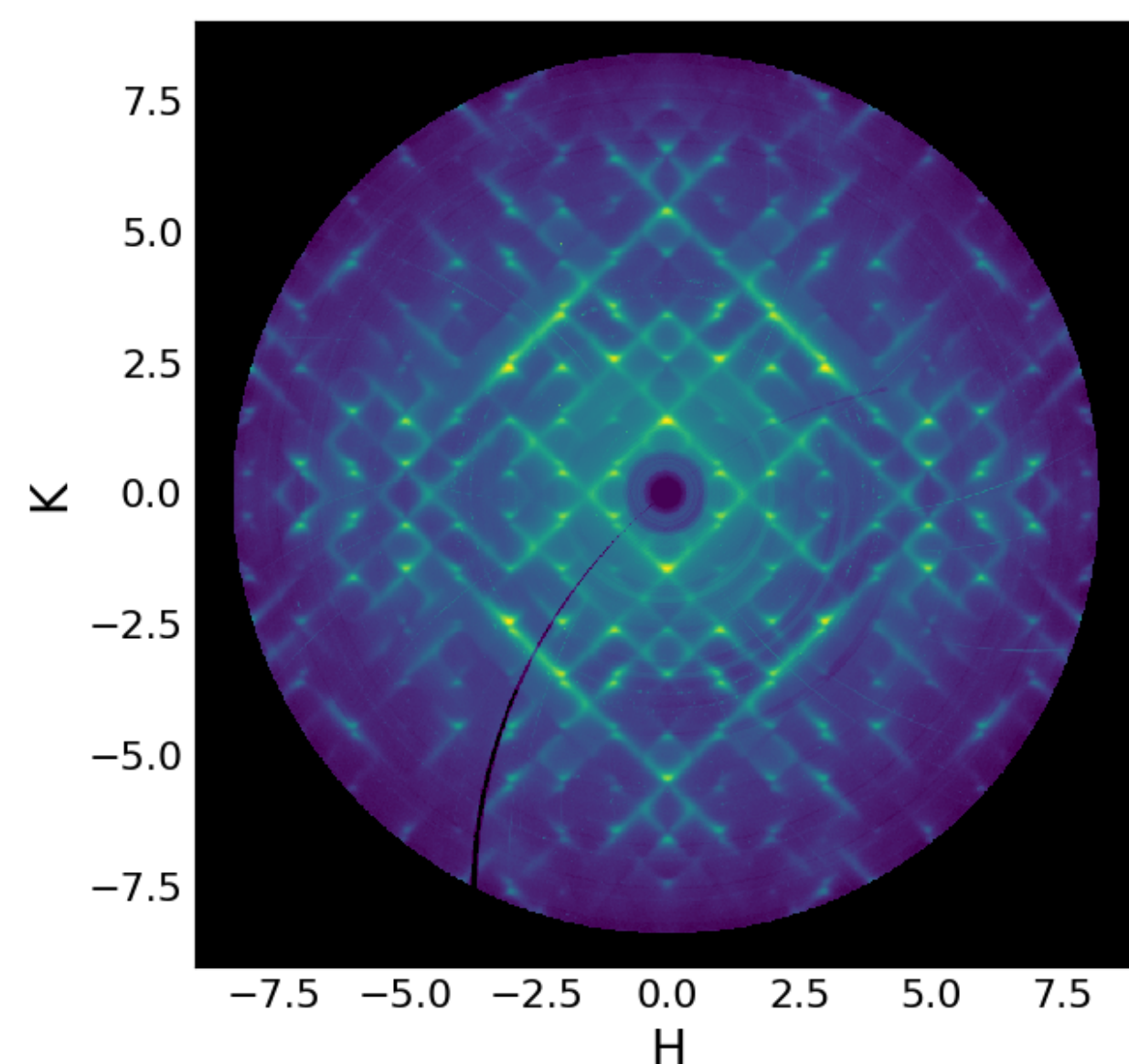
Sillimanite: Al_2SiO_5



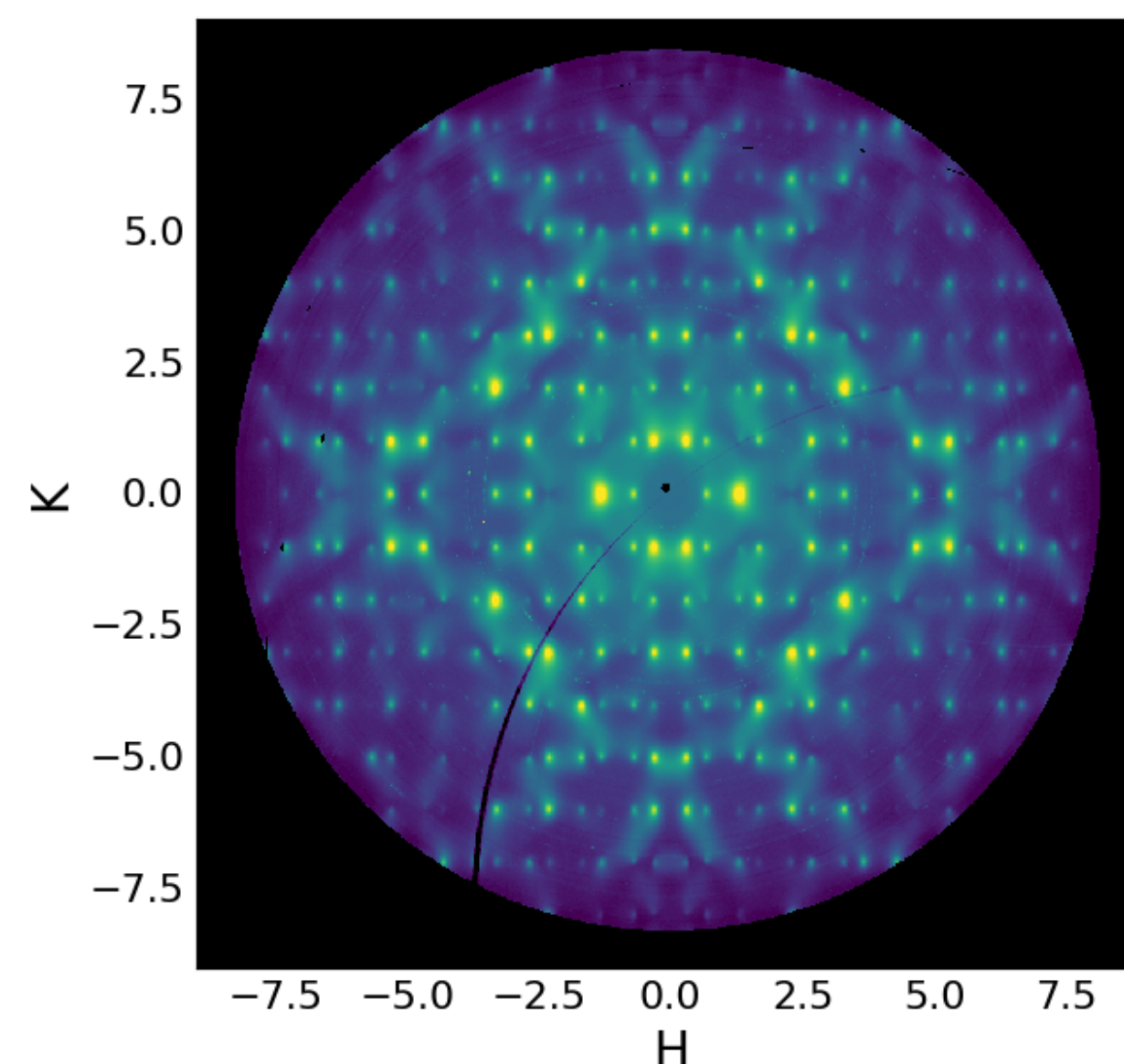
Mullite: $Al_2(Al_{2+2x}Si_{2-2x})O_{10-x}$

3D DIFFUSE SCATTERING IN MULLITE

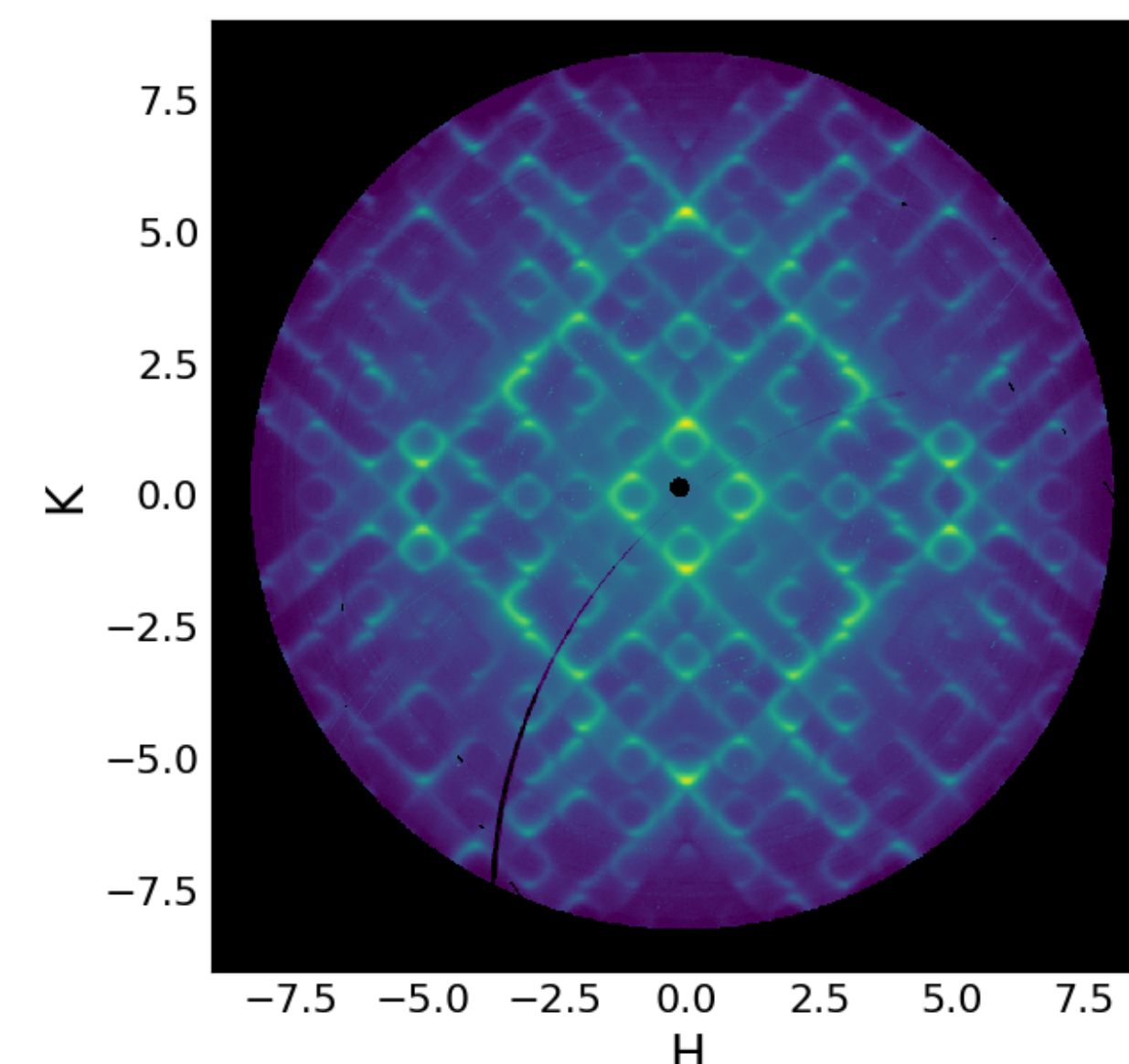
- There is strong diffuse scattering throughout reciprocal space
- The shape of the diffuse scattering is strongly dependent on the value of L



$L=0.16$



$L=0.5$

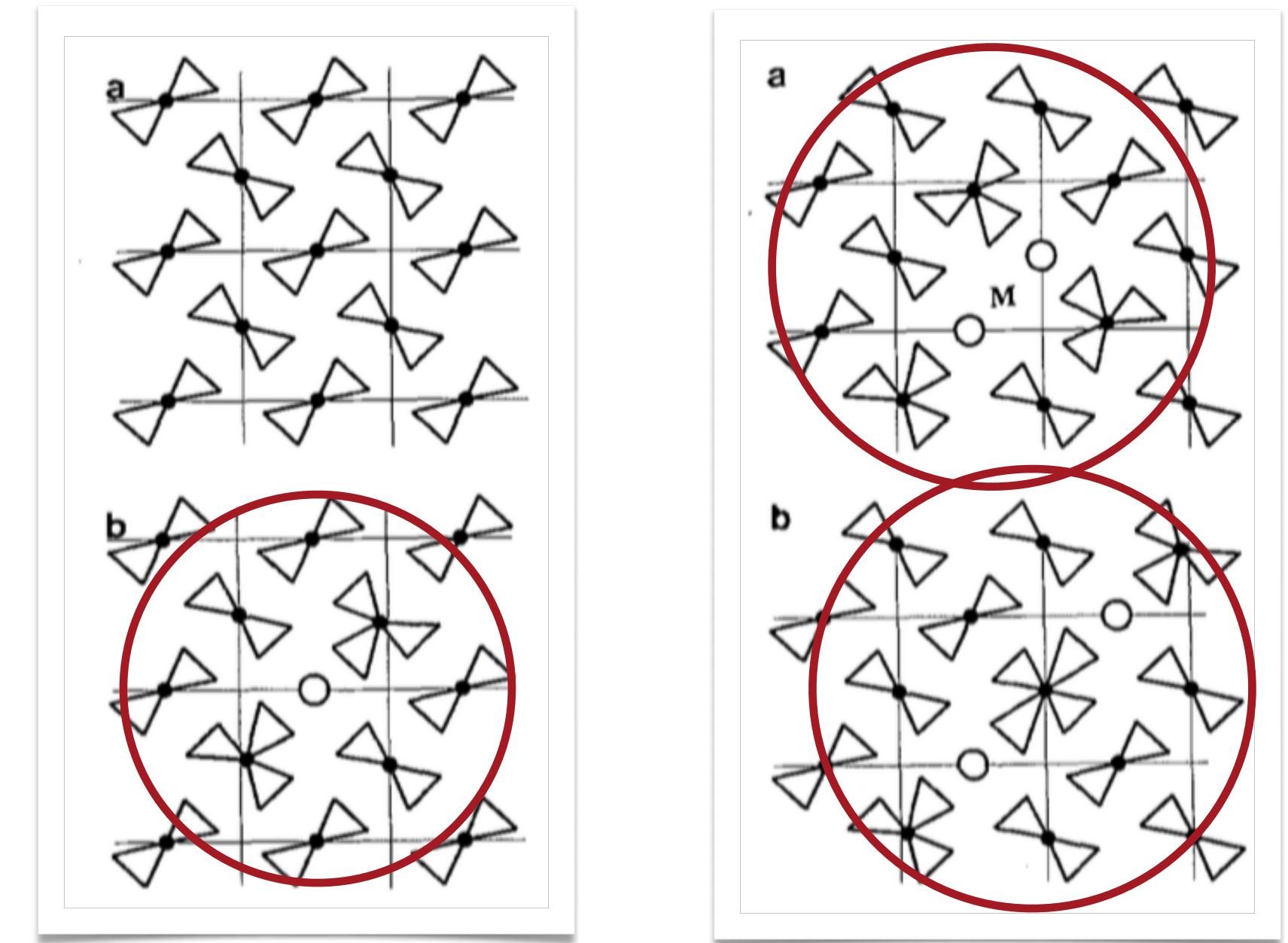


$L=0.75$

MONTE CARLO ANALYSIS

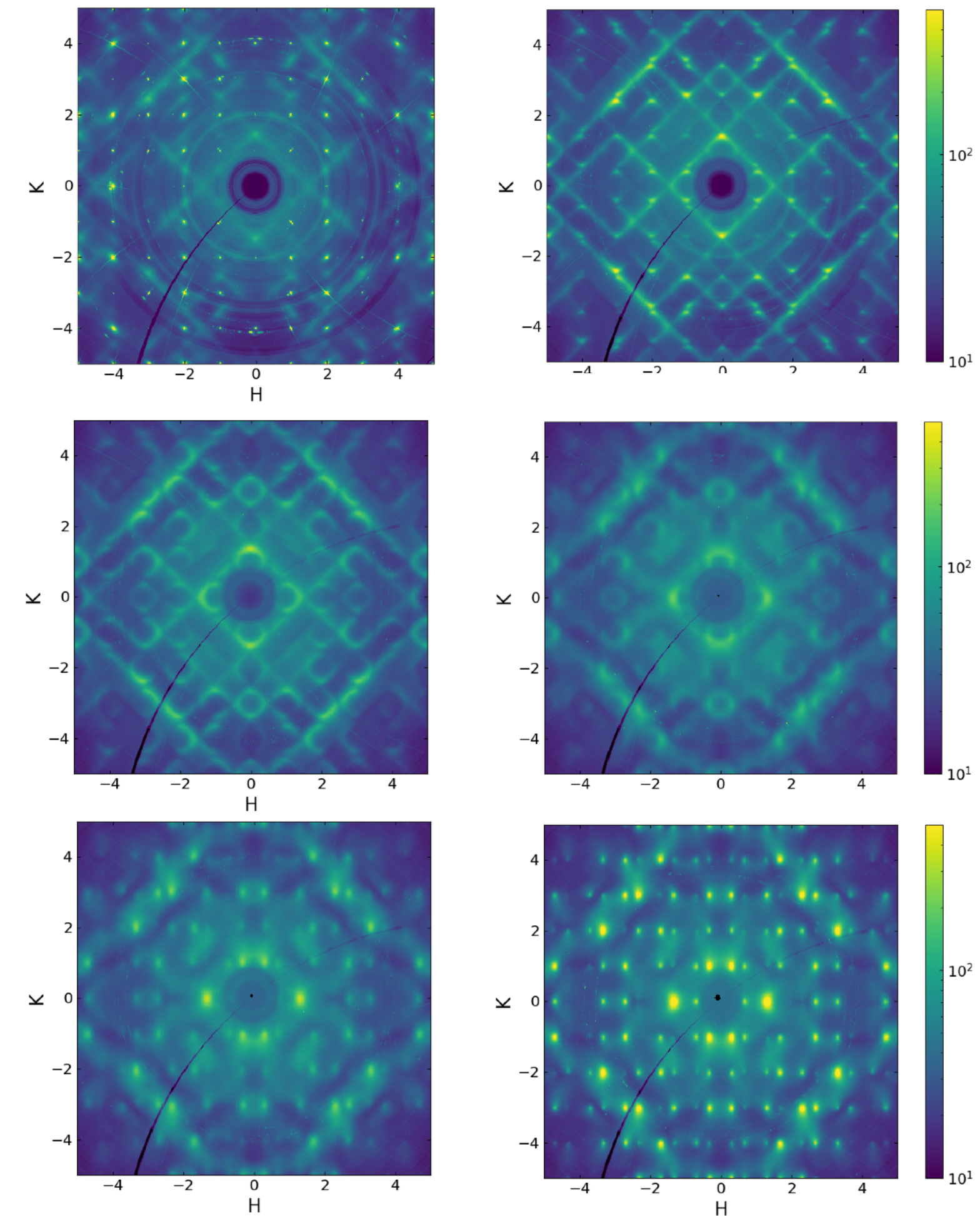
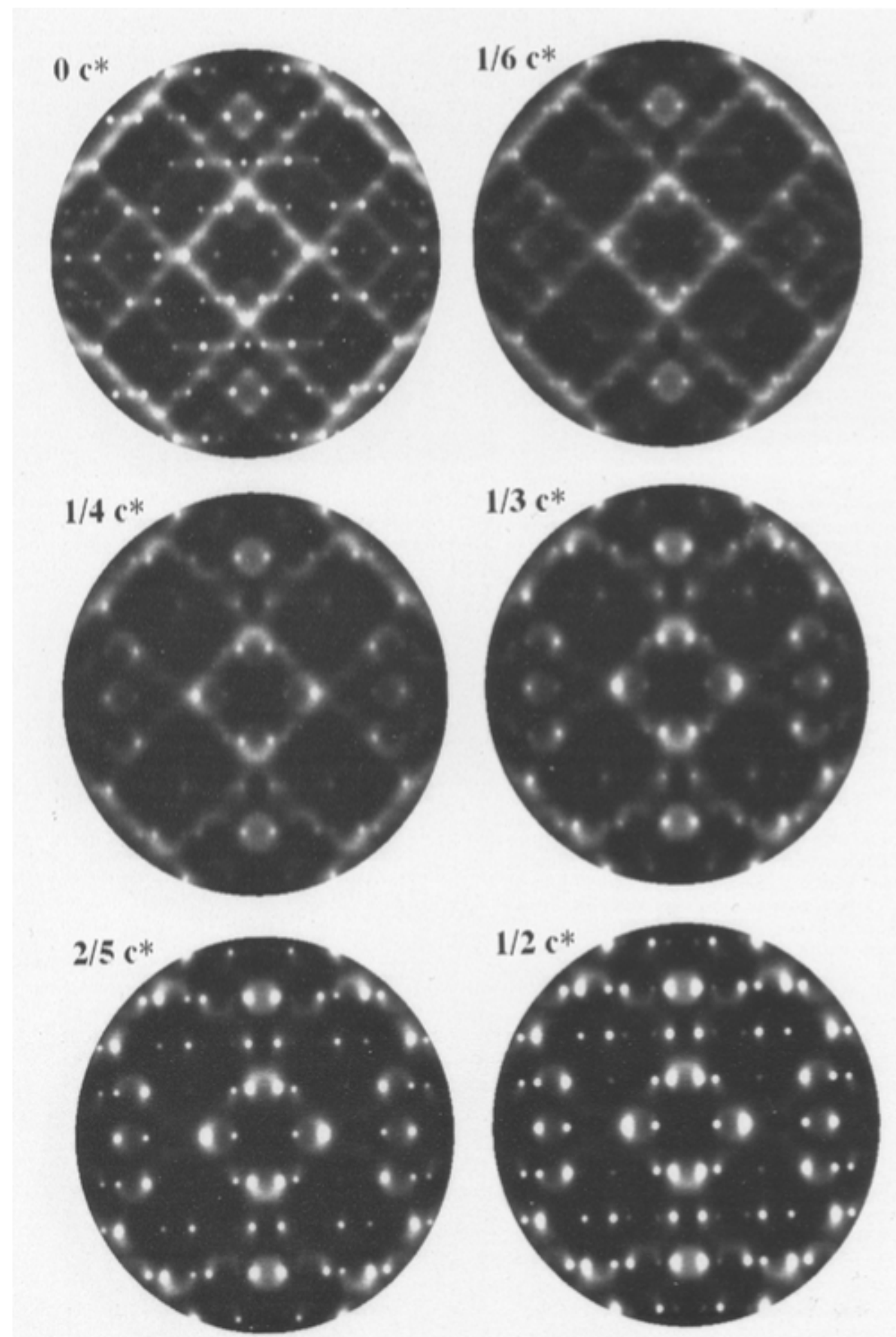
B. D. Butler, T. R. Welberry, & R. L. Withers,
Phys Chem Minerals **20**, 323 (1993)

- In a classic analysis, Richard Welberry and colleagues developed a set of interaction energies to model mullite disorder
- Interaction energies were initialized:
 - insights from chemical intuition
 - insights from the measured diffuse scattering
- The diffuse scattering was calculated using a Monte Carlo algorithm to generate vacancy distributions first in 2D slices and then in 3D

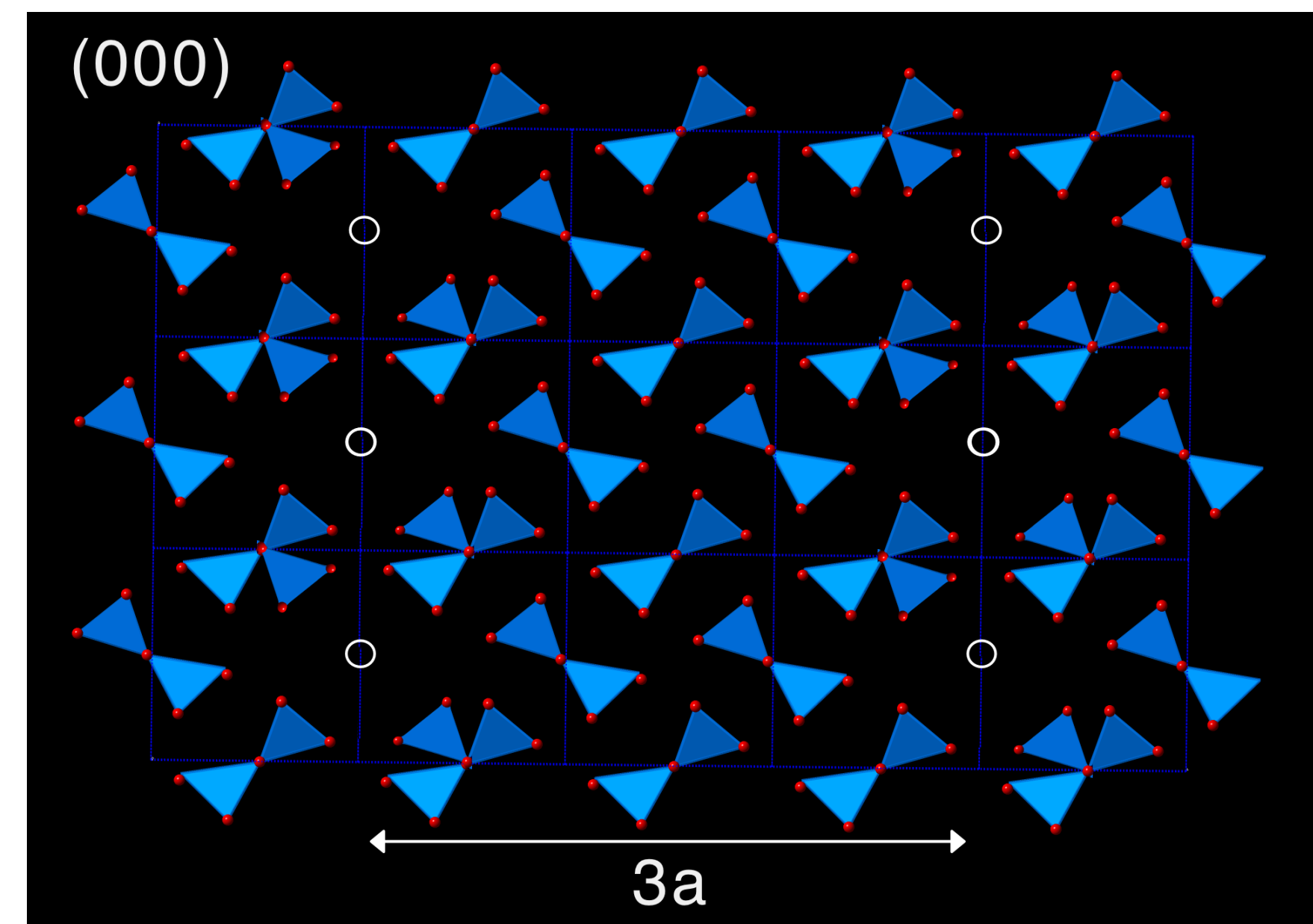
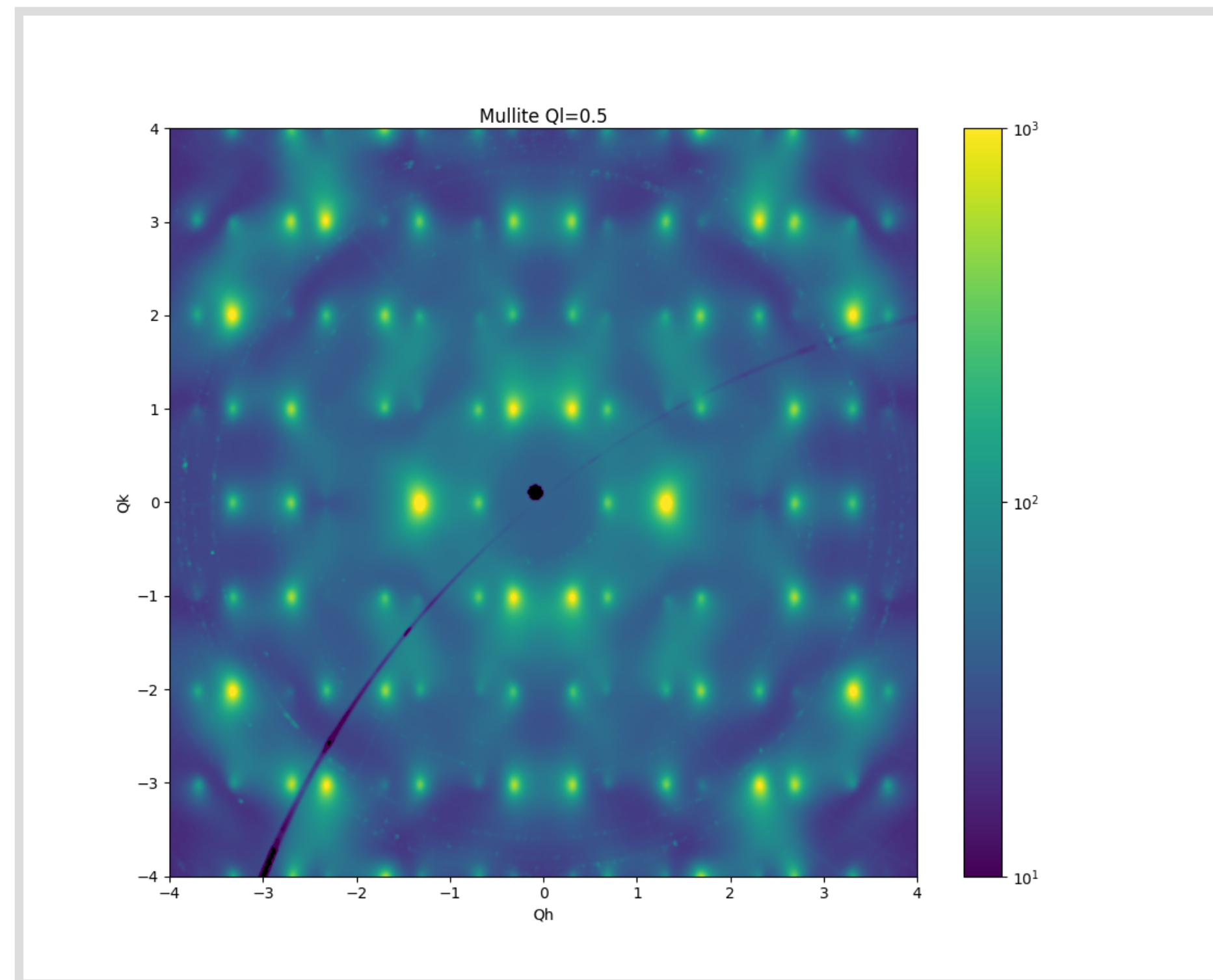


| Interatomic vector | α_{lmn} | Interatomic vector | α_{lmn} |
|--------------------------------------|----------------|--------------------------------------|----------------|
| $\frac{1}{2}\langle 1\ 1\ 0 \rangle$ | -0.24 | $\langle 0\ 2\ 0 \rangle$ | +0.13 |
| $[1\ 1\ 0]$ | -0.23 | $\frac{1}{2}\langle 3\ 1\ 0 \rangle$ | +0.22 |
| $[1\ -1\ 0]$ | -0.05 | $\frac{1}{2}\langle 1\ 3\ 0 \rangle$ | -0.01 |
| $\langle 1\ 0\ 0 \rangle$ | -0.06 | $\langle 1\ 0\ 1 \rangle$ | +0.07 |
| $\langle 0\ 1\ 0 \rangle$ | +0.22 | $\langle 0\ 1\ 1 \rangle$ | -0.12 |
| $\langle 0\ 0\ 1 \rangle$ | -0.03 | $\frac{1}{2}\langle 3\ 3\ 0 \rangle$ | +0.17 |
| $\frac{1}{2}[1\ -1\ 2]$ | +0.12 | $\langle 1\ 1\ 1 \rangle$ | -0.01 |
| $\frac{1}{2}[1\ 1\ 2]$ | +0.12 | $\frac{1}{2}\langle 3\ 1\ 2 \rangle$ | -0.11 |
| $\langle 2\ 0\ 0 \rangle$ | -0.12 | $\frac{1}{2}\langle 3\ 3\ 2 \rangle$ | -0.07 |

MONTE CARLO ANALYSIS RESULTS



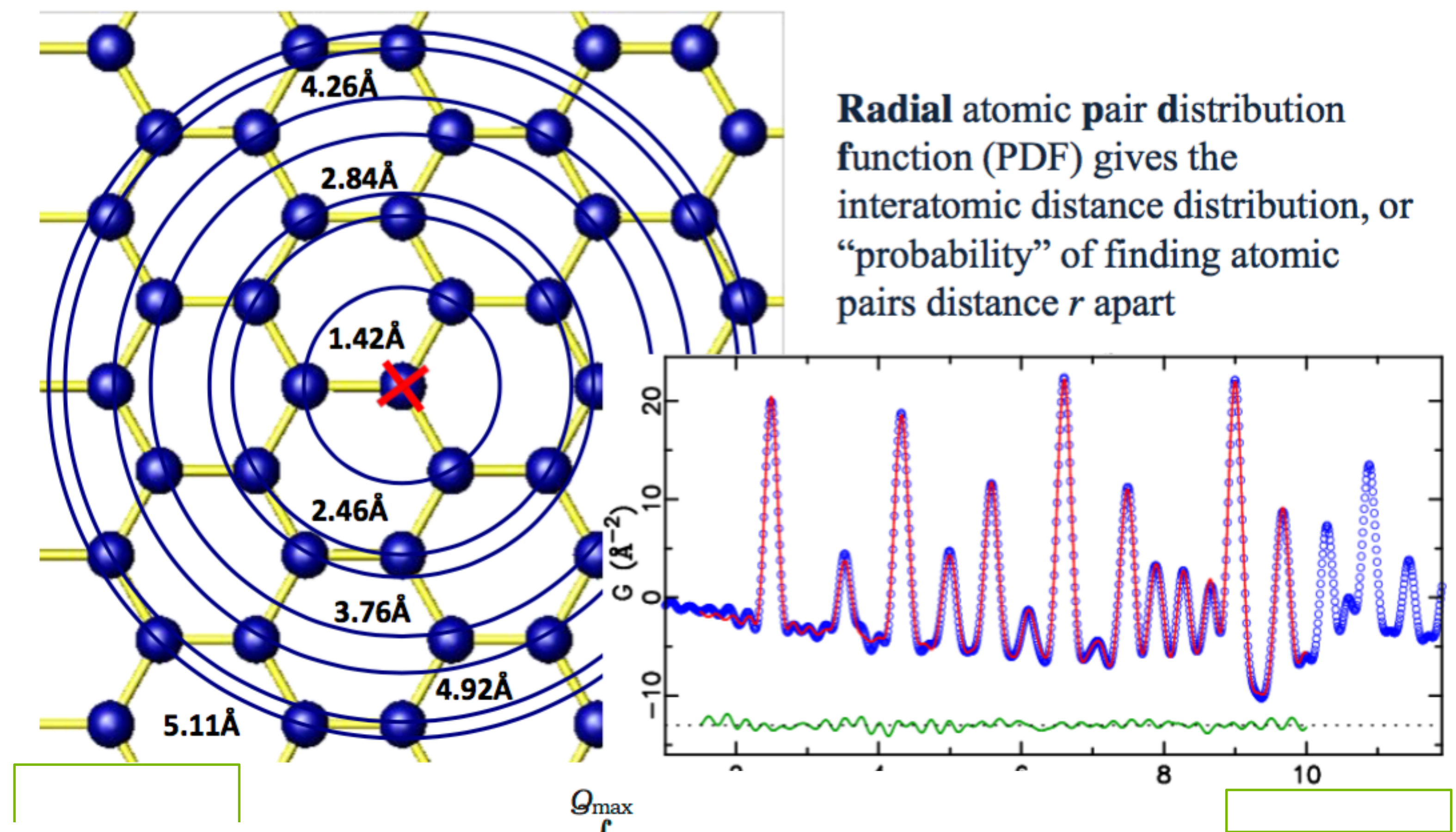
VACANCY ORDERING IN MULLITE



$$\mathbf{q} = \pm \frac{1}{2} \mathbf{c}^* \pm \frac{1}{3} \mathbf{a}^*$$

CASE STUDY 2: SODIUM-INTERCALATED V_2O_5 3D- Δ PDF

PAIR DISTRIBUTION FUNCTION ANALYSIS



$$G(r) = 4\pi r[\rho(r) - \rho_0] = (2/\pi) \int_{Q=Q_{\min}}^{Q_{\max}} Q[S(Q) - 1] \sin(Qr) dQ$$

Emil Bozin (ADD 2013)

THREE-DIMENSIONAL PAIR DISTRIBUTION FUNCTIONS

238

Z. Kristallogr. 2012, 227, 238–247 / DOI 10.1524/zkri.2012.1504

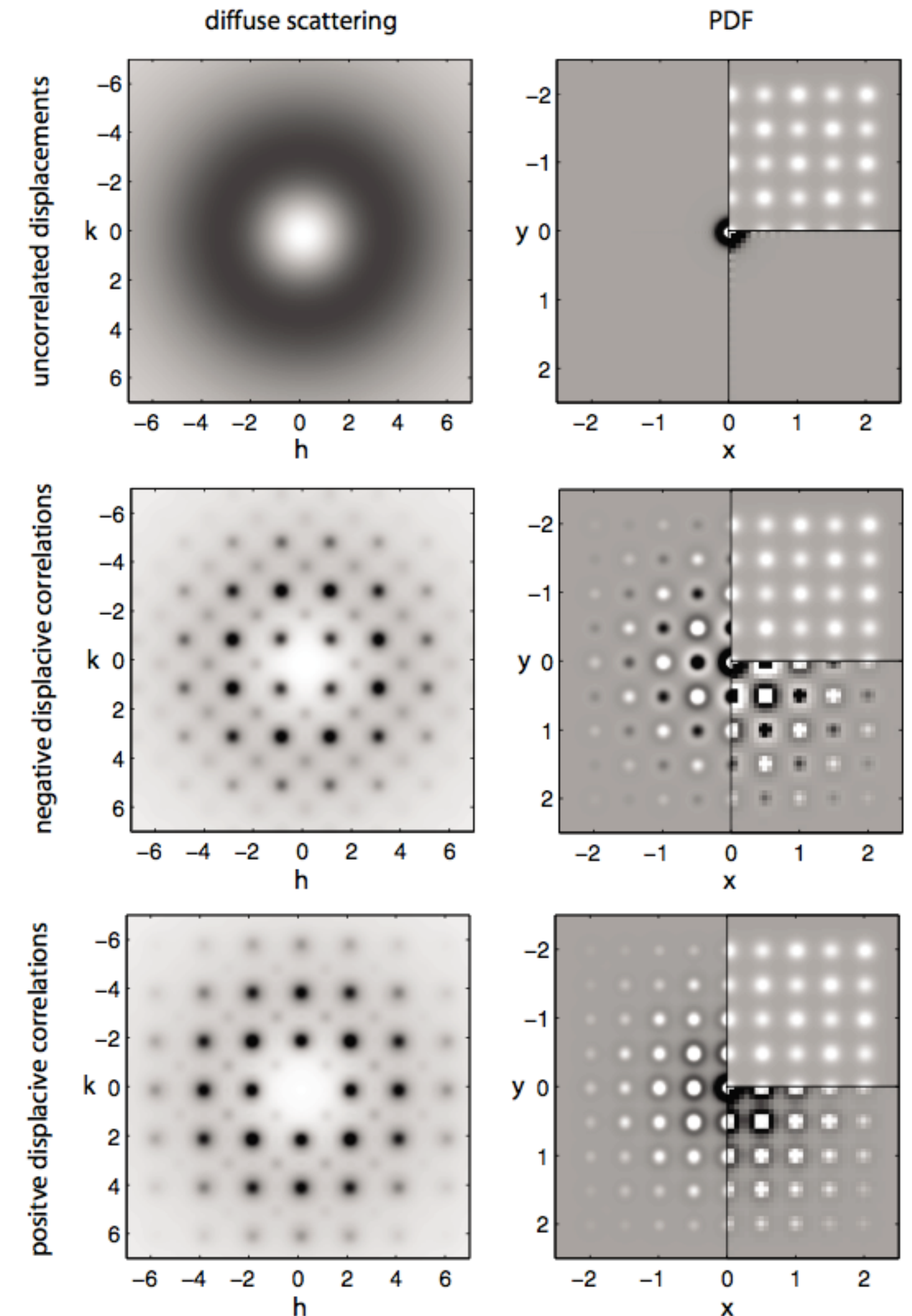
© by Oldenbourg Wissenschaftsverlag, München

The three-dimensional pair distribution function analysis of disordered single crystals: basic concepts

Thomas Weber* and Arkadiy Simonov

Laboratory of Crystallography, ETH Zurich Wolfgang-Pauli-Str. 10, 8093 Zurich, Switzerland

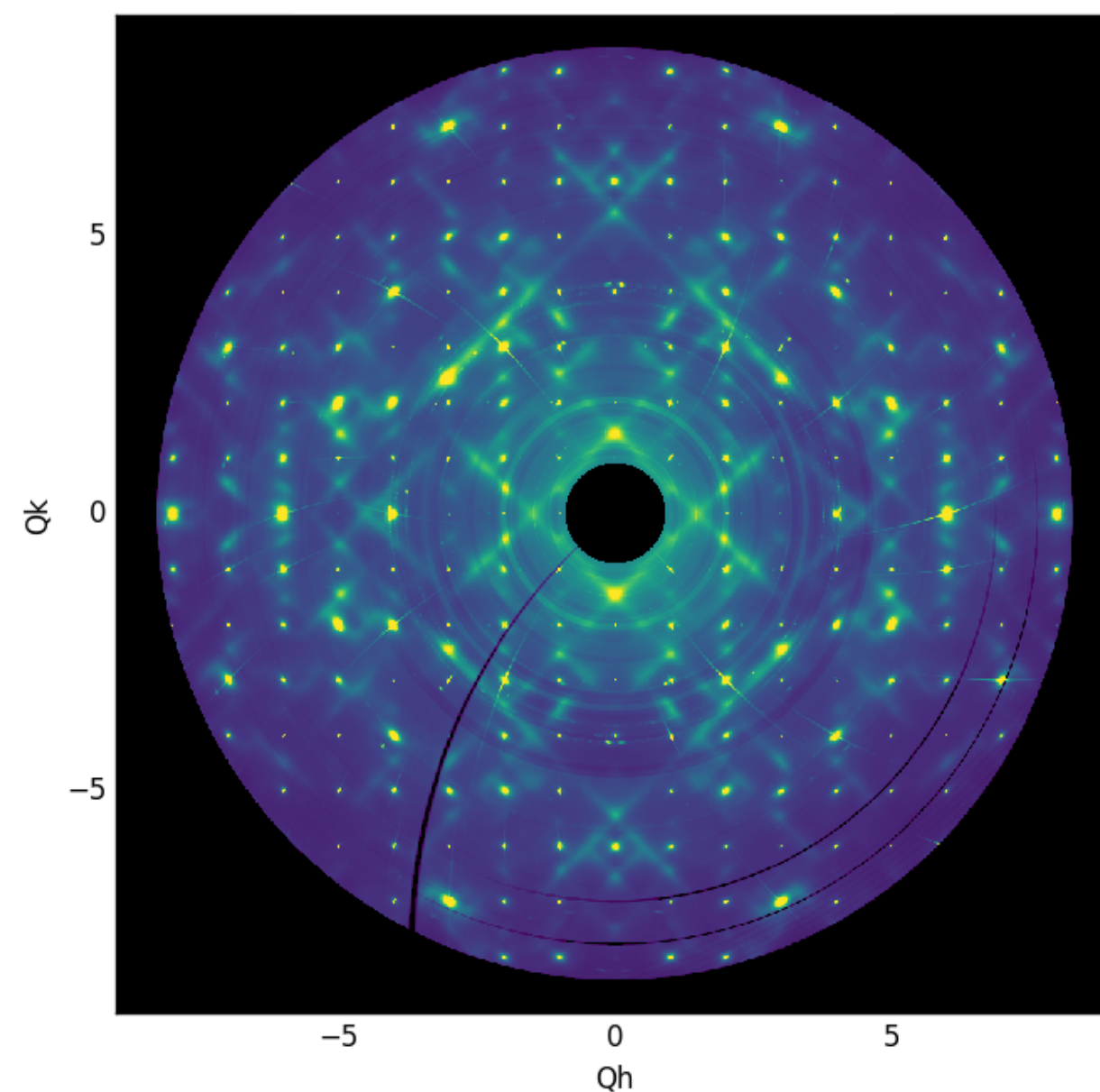
- The 3D PDF technique was pioneered by Thomas Weber and colleagues at ETH
 - Philippe Schaub, Walter Steurer, Arkadiy Simonov
 - See Yell - A. Simonov, *et al*, J Appl Cryst **47**, 1146 (2014).
- The ability to measure three-dimensional $S(\mathbf{Q})$ over a large volume of reciprocal space provides the 3D analog of PDF measurements.
 - Total PDFs if Bragg peaks and diffuse scattering can be measured simultaneously
 - Δ PDFs if the Bragg peaks are eliminated
- This allows a model-independent view of the measurements in real space.



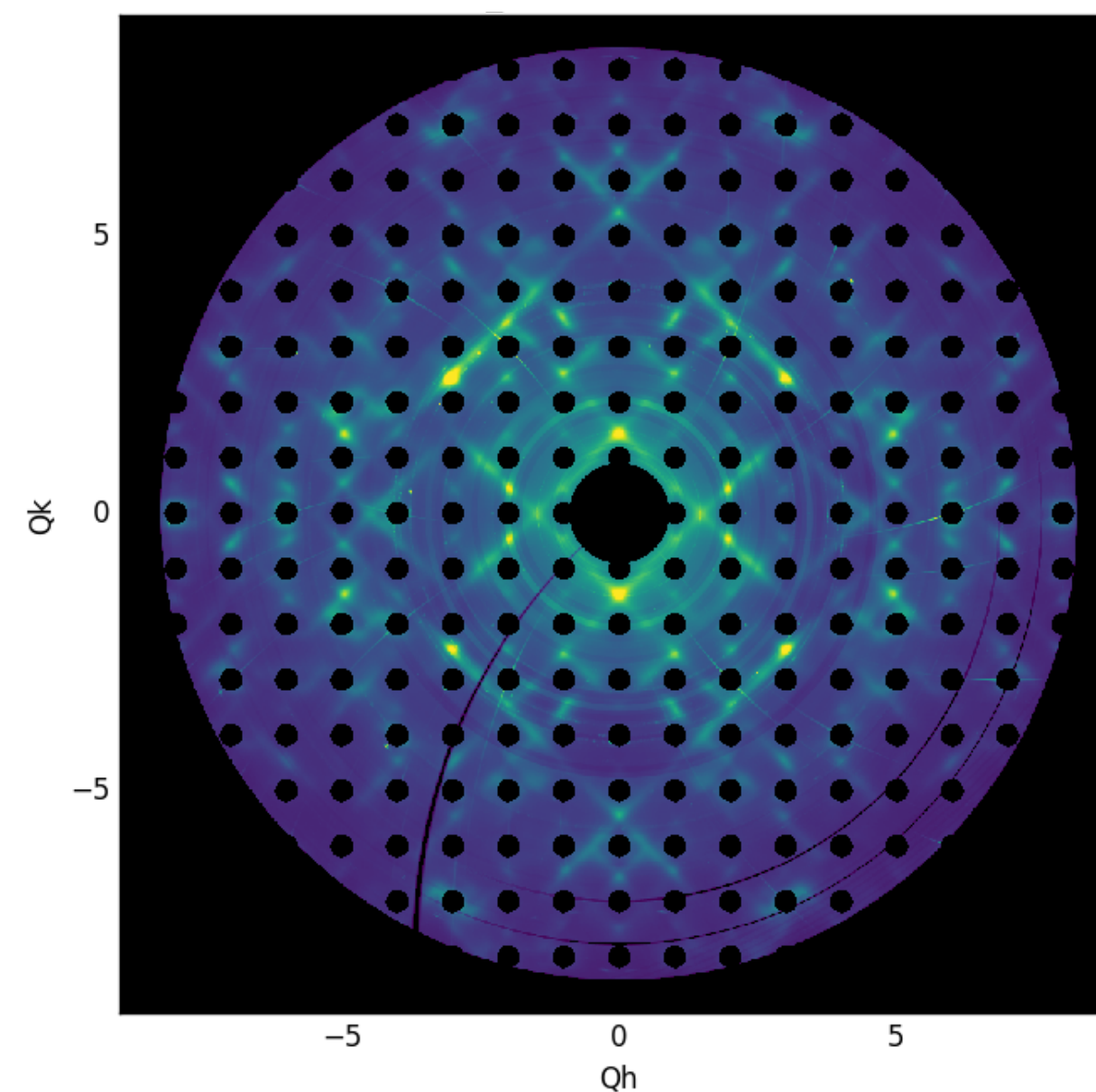
“PUNCH AND FILL”

$$I = \sum_i \sum_j b_i b_j \exp(i\mathbf{Q} \cdot \mathbf{r}_{ij})$$

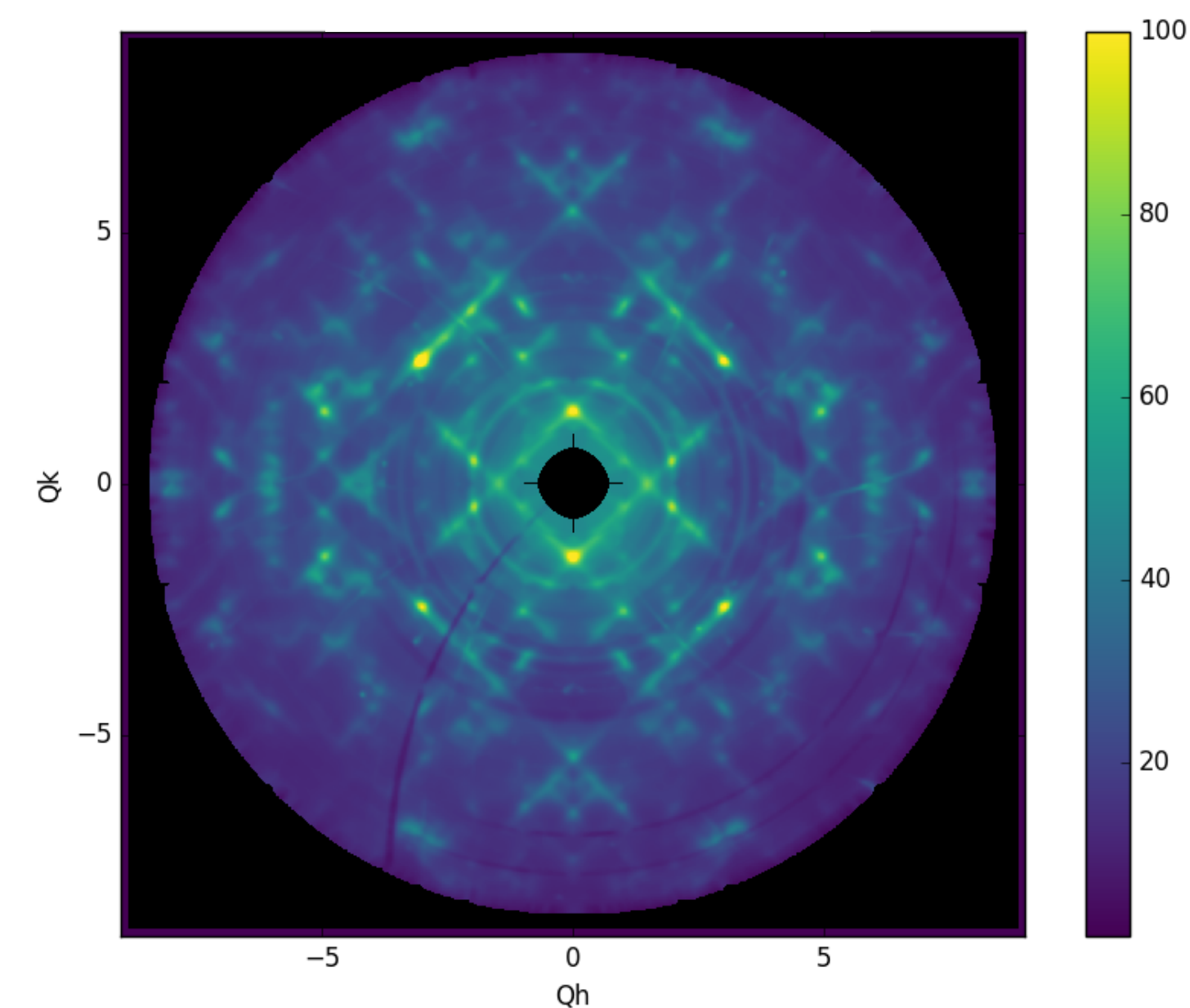
$$P_{tot}(\mathbf{r}) = FT [I(\mathbf{Q})] = FT [|\bar{F}(\mathbf{Q})|^2] + FT [|\Delta F(\mathbf{Q})|^2] = P_{hkl}(\mathbf{r}) + \Delta P(\mathbf{r})$$



Symmetrize



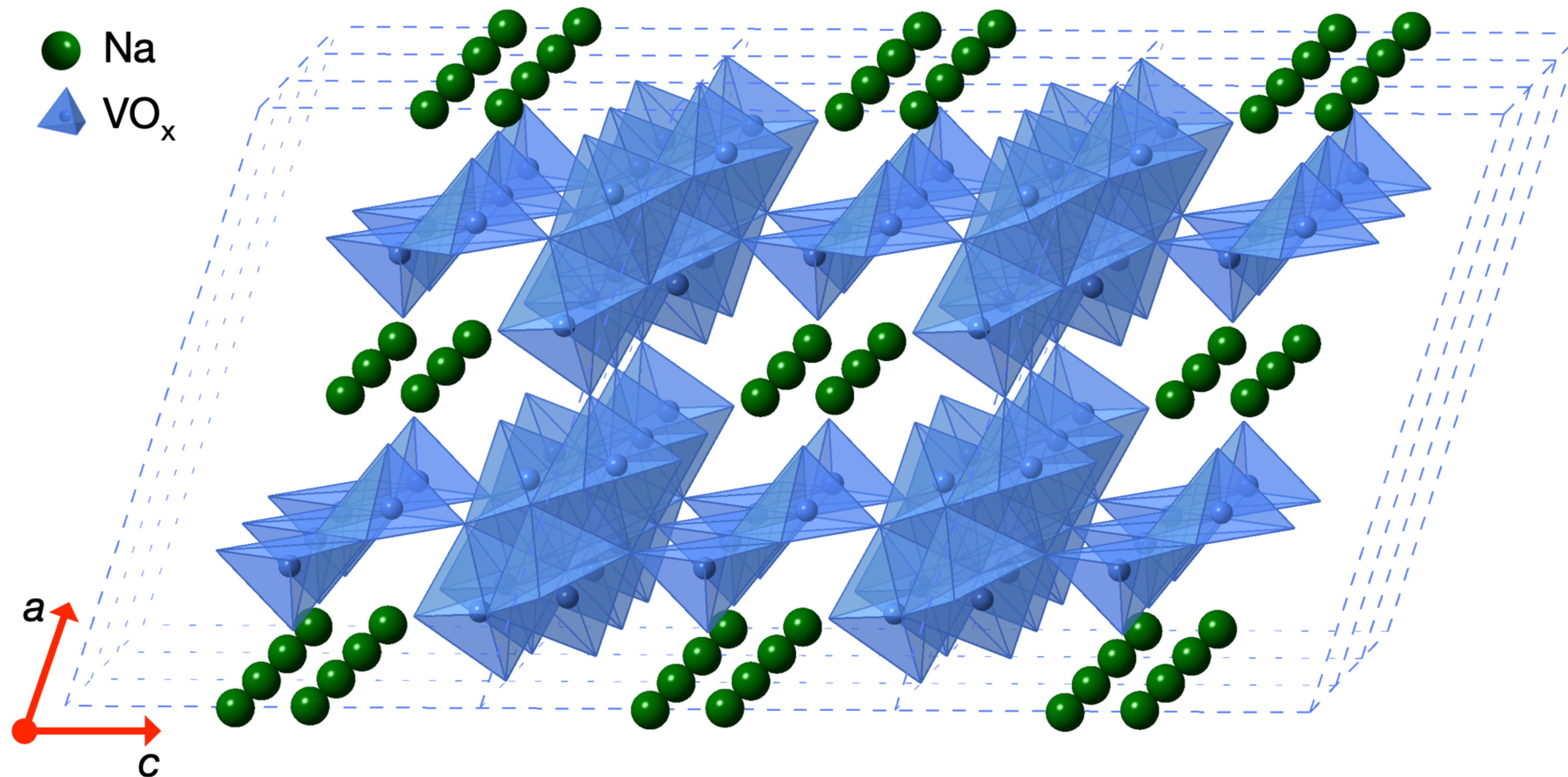
Punch



Fill

A. Simonov, T. Weber, and W. Steurer, Journal of Applied Crystallography **47**, 1146 (2014).

SODIUM-INTERCALATED V_2O_5

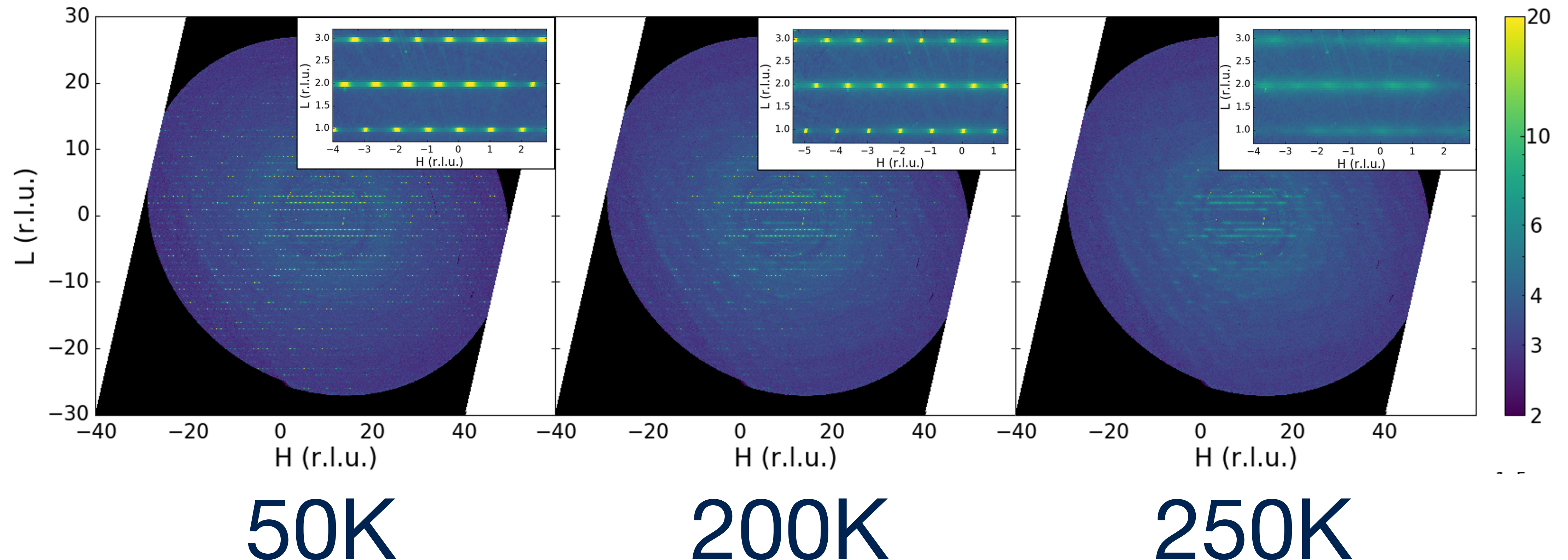


M. J. Krogstad, S. Rosenkranz, J. M. Wozniak, G. Jennings, J. P. C. Ruff, J. T. Vaughey, and R. Osborn
Nature Materials **19**, 63 (2020).

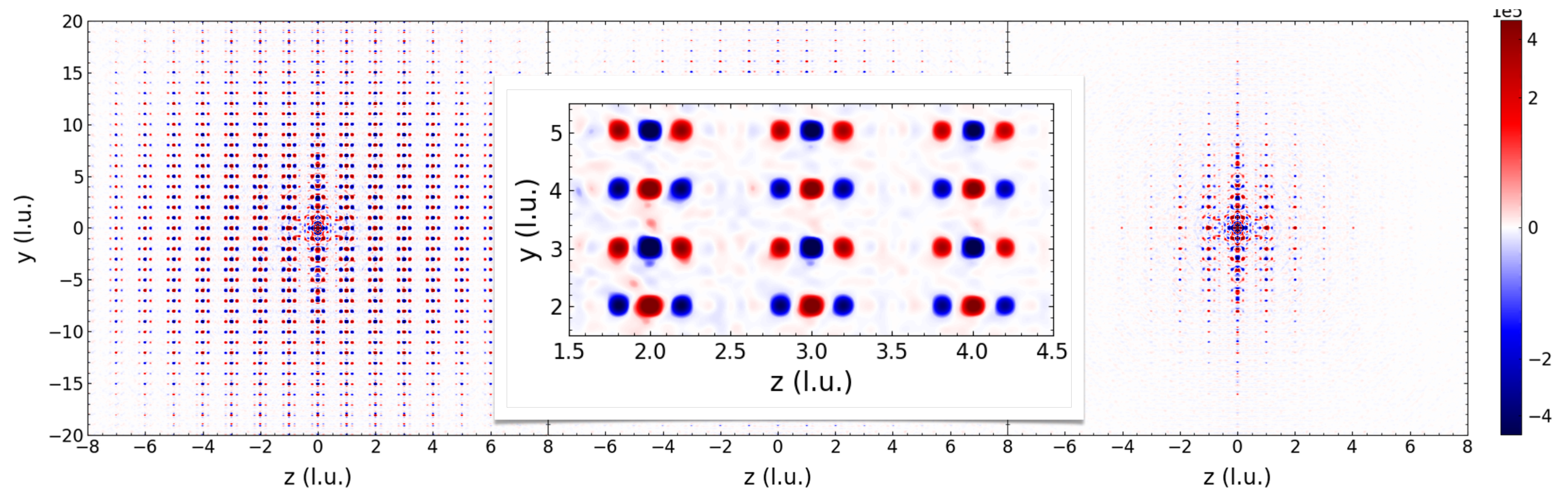
SUBLATTICE MELTING IN $\text{Na}_{0.45}\text{V}_2\text{O}_5$

Order-Disorder Transition in the Half-Filled Sodium Sublattice

$K=0.5$



3D- Δ PDF ANALYSIS OF $\text{Na}_{0.45}\text{V}_2\text{O}_5$

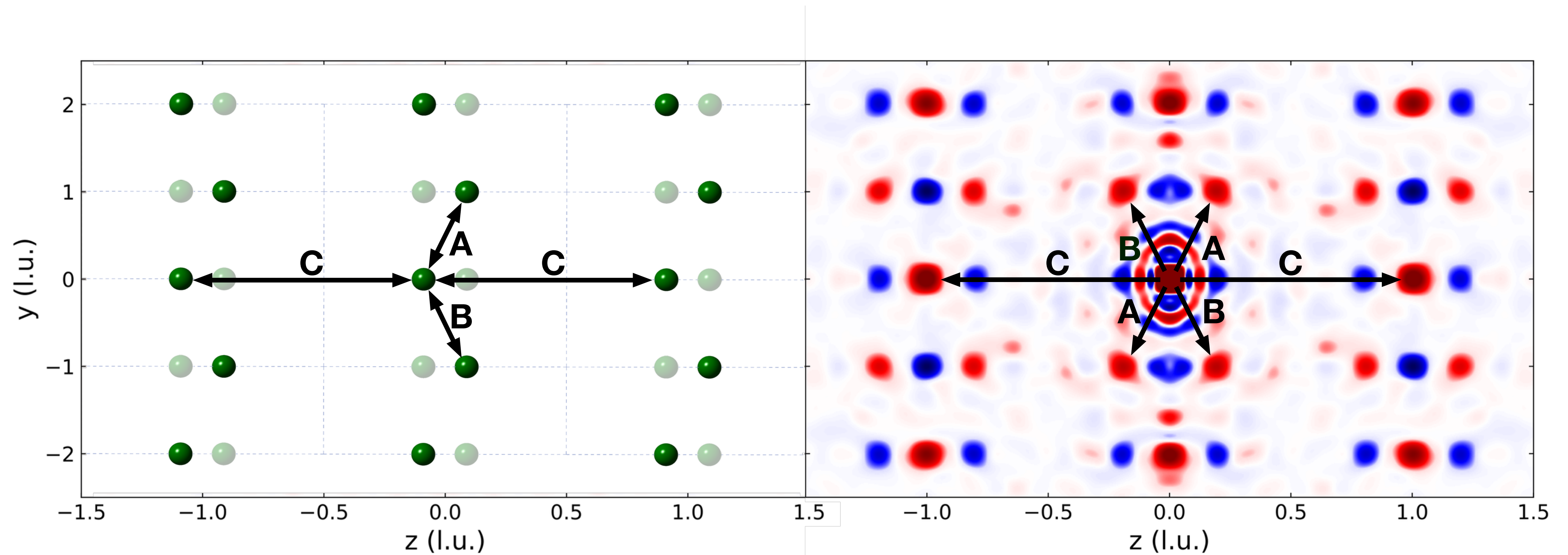


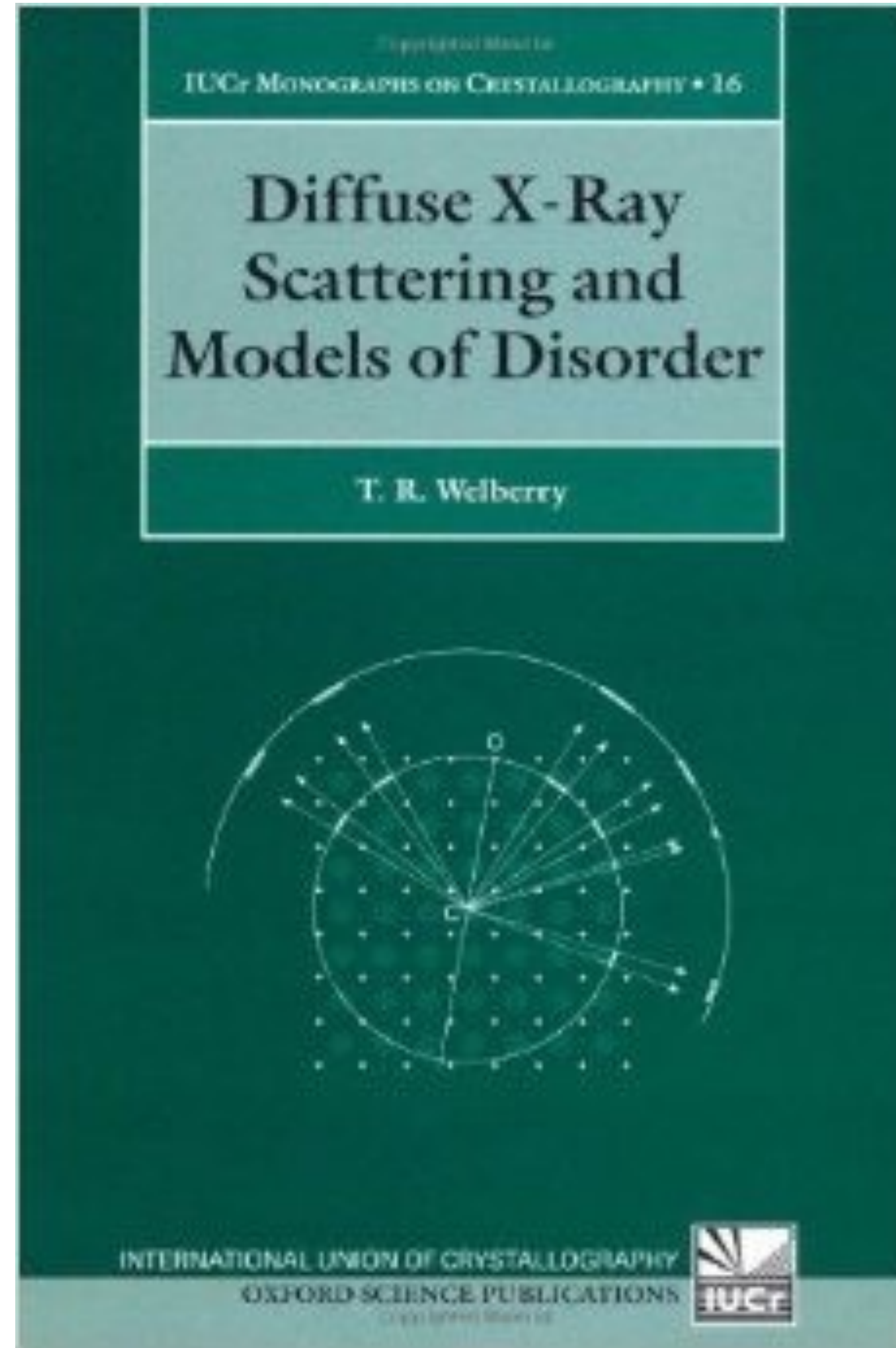
50K

200K

250K

REAL SPACE vs 3D- Δ PDF





24.3.3 *Ordering of Na within the two-leg ladders.*

Fig. 24.10(a) shows a small region near the origin of the $x = 0$ plane of the Δ PDF map obtained from the 50K X-ray data. The strong white origin peak indicates perfect positive correlation for an atom with itself. Other white peaks also indicate a positive correlation between an atom at the origin with another at a position given by the vectors A, B or C (and the reverse vectors -A, -B and -C). Conversely the dark peaks indicate strong negative correlations. It is quite straightforward to deduce from the observed pattern of white and dark peaks that the local arrangement of the Na ions must follow a pattern like that shown in Fig. 24.10(b), where the occupancy of the two Na sites on each rung of the two-leg ladders tends to alternate between $(Na\Box^\dagger)$ and $(\Box Na)$ producing a zig-zag chain of occupied sites. Neighbouring ladders at $z = \pm 1.0$ have the same occupancy pattern which is in phase with the ladder at $z = 0$.

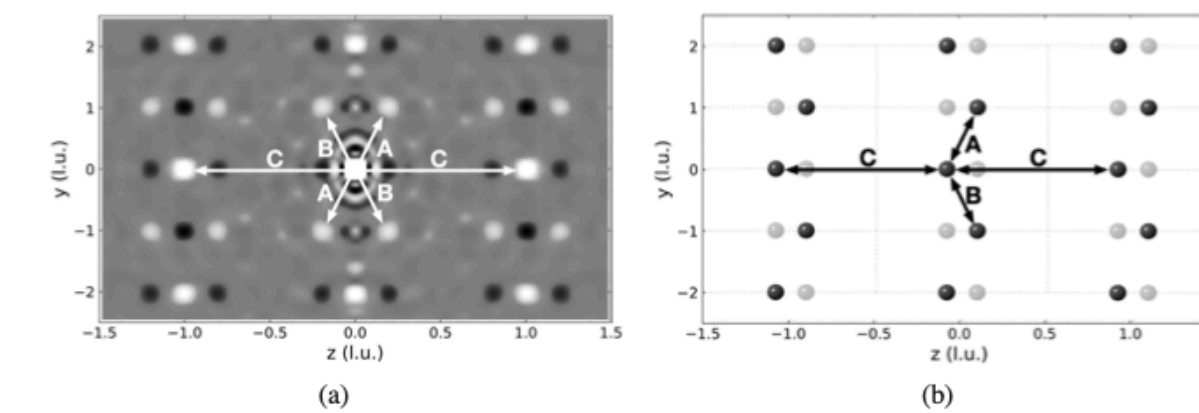


Fig. 24.10 A comparison of (a) the Δ PDF peak intensities at 50K in the $x = 0$ plane of $Na_{0.45}V_2O_5$ with (b) the derived real-space model of sodium ions. Data used in this figure are reproduced with kind permission of Dr Ray Osborn.

24.3.4 *Δ PDF peak intensities in the $z = 0$ plane.*

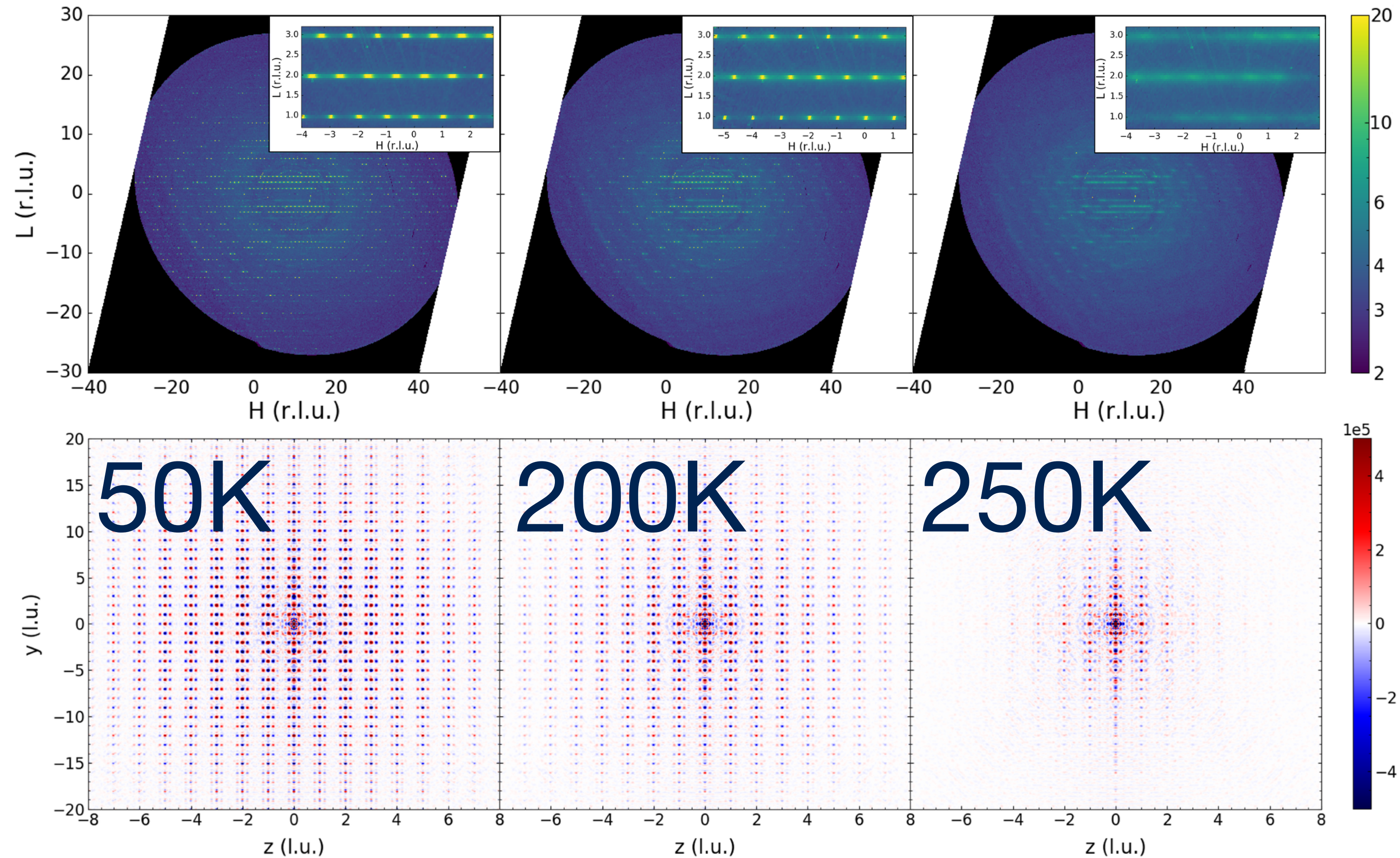
Fig. 24.12 shows the $z = 0$ plane of the Δ PDF map observed at three different temperatures. Fig. 24.11(b) shows an enlargement of part of Fig. 24.11(a) where white arrows (labelled A – F) have been used to identify different interatomic vectors. The same set of vectors is shown in Fig. 24.11(e) which is a plot of the $z = 0$ plane of the average structure. The maps are dominated by the same alternating correlations of Na occupancy along the ladder direction parallel to y . Similarly neighbouring chains at $x = \pm 1$ are in step with that at $x = 0$ for temperatures 50K and 150K but at 250K these correlations have been lost.

Although the maps are dominated by the correlations in the Na ladders there are numerous weaker peaks that correspond to correlations between the ladder Na_1 ions and the interstitial Na_2 ions. These correspond to vectors A, B, C and E in Fig. 24.11(e) and involve one Na_1 and one Na_2 ion. These peaks are clearly evident in the 50K map, somewhat less evident at 150K and even less evident at 250K. They are weak relative to those involving Na_1 ions alone simply because of the low occupancy of the Na_2 sites.

[†] here \Box is used to represent a vacant site

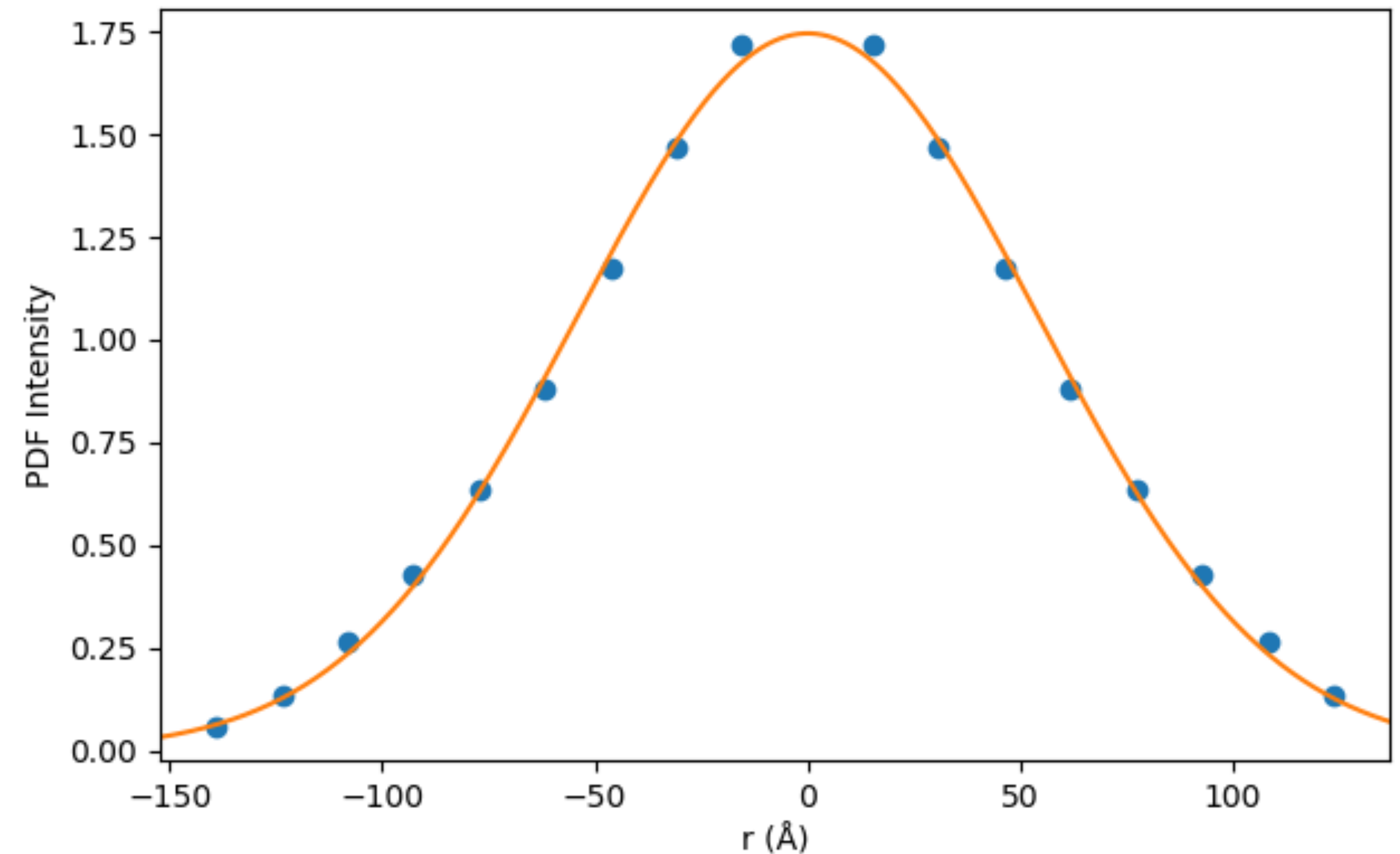
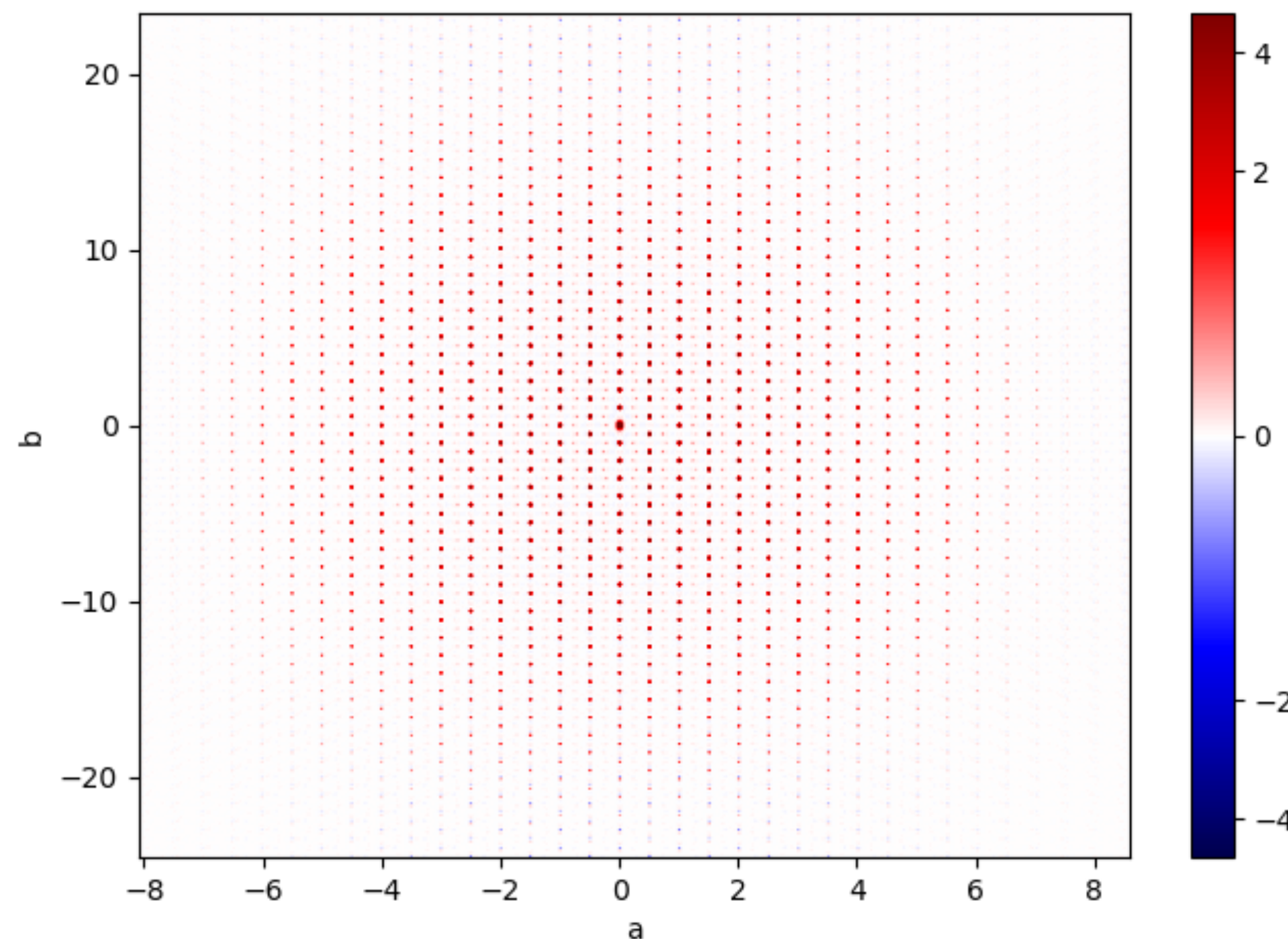
ORDER-DISORDER TRANSITION VIEWED IN REAL SPACE

$\text{Na}_{0.45}\text{V}_2\text{O}_5$

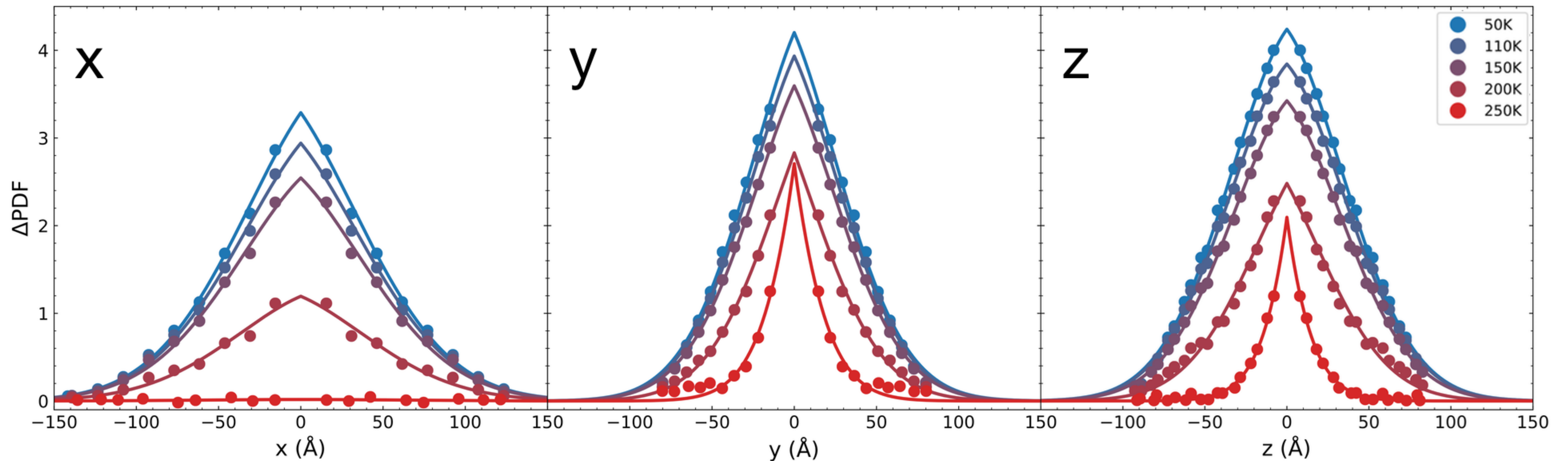


EFFECT OF Q-RESOLUTION

- Finite Q-resolution \Rightarrow Gaussian envelope in real space.
- The width can be determined from the total PDF
 - *i.e.*, the transform of the long-range crystal structure.

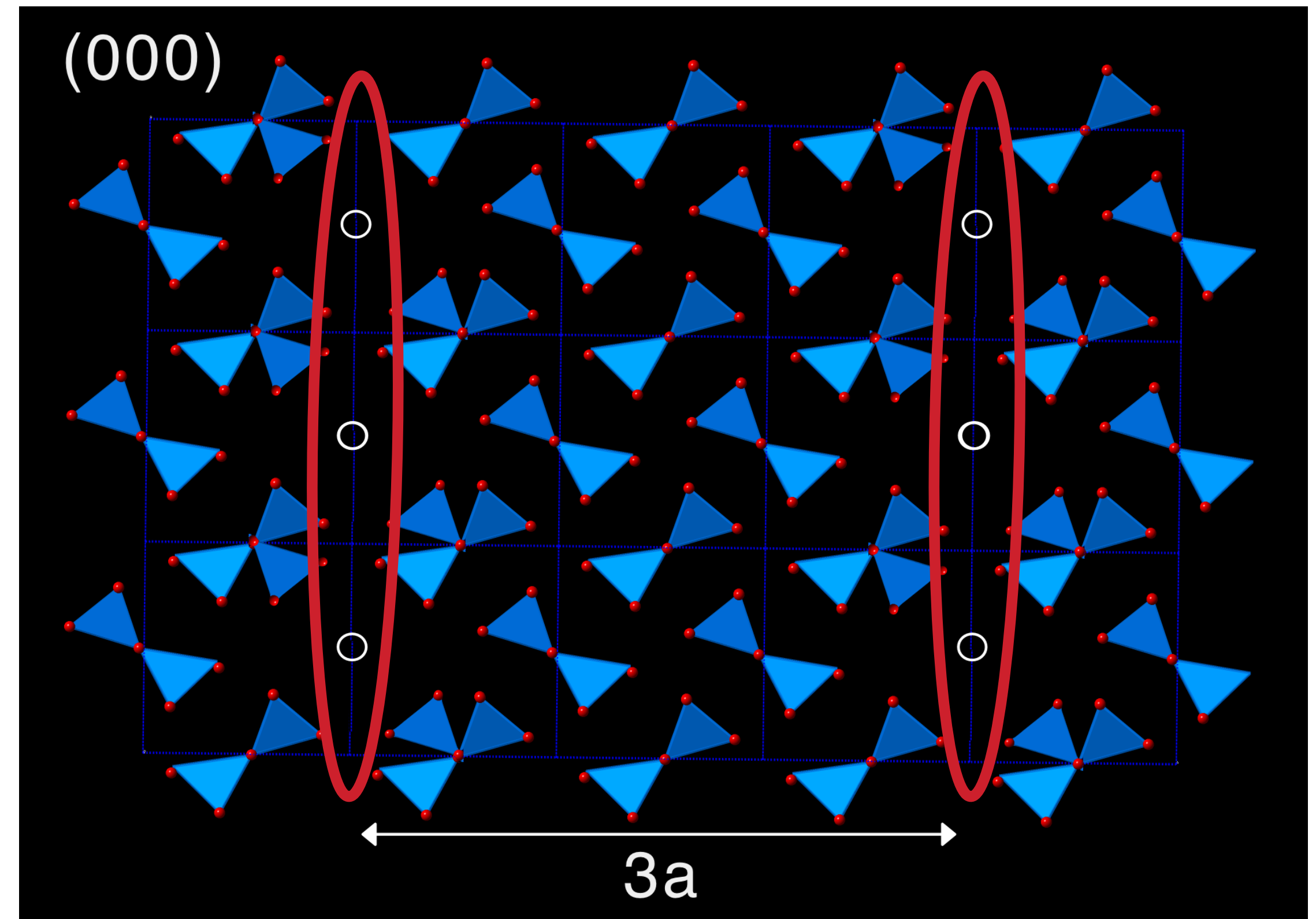
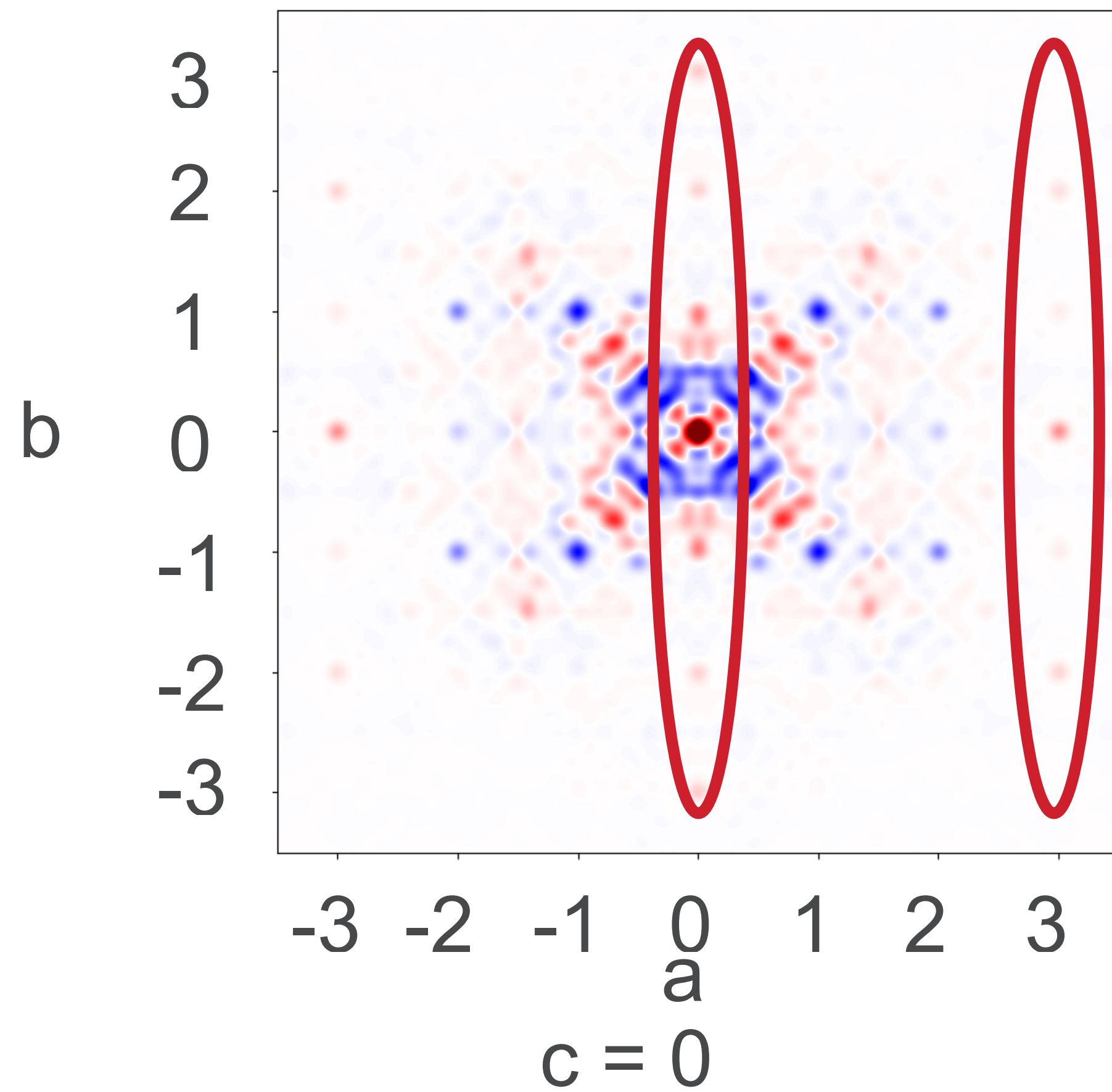


FITTING CORRELATION LENGTHS IN REAL SPACE



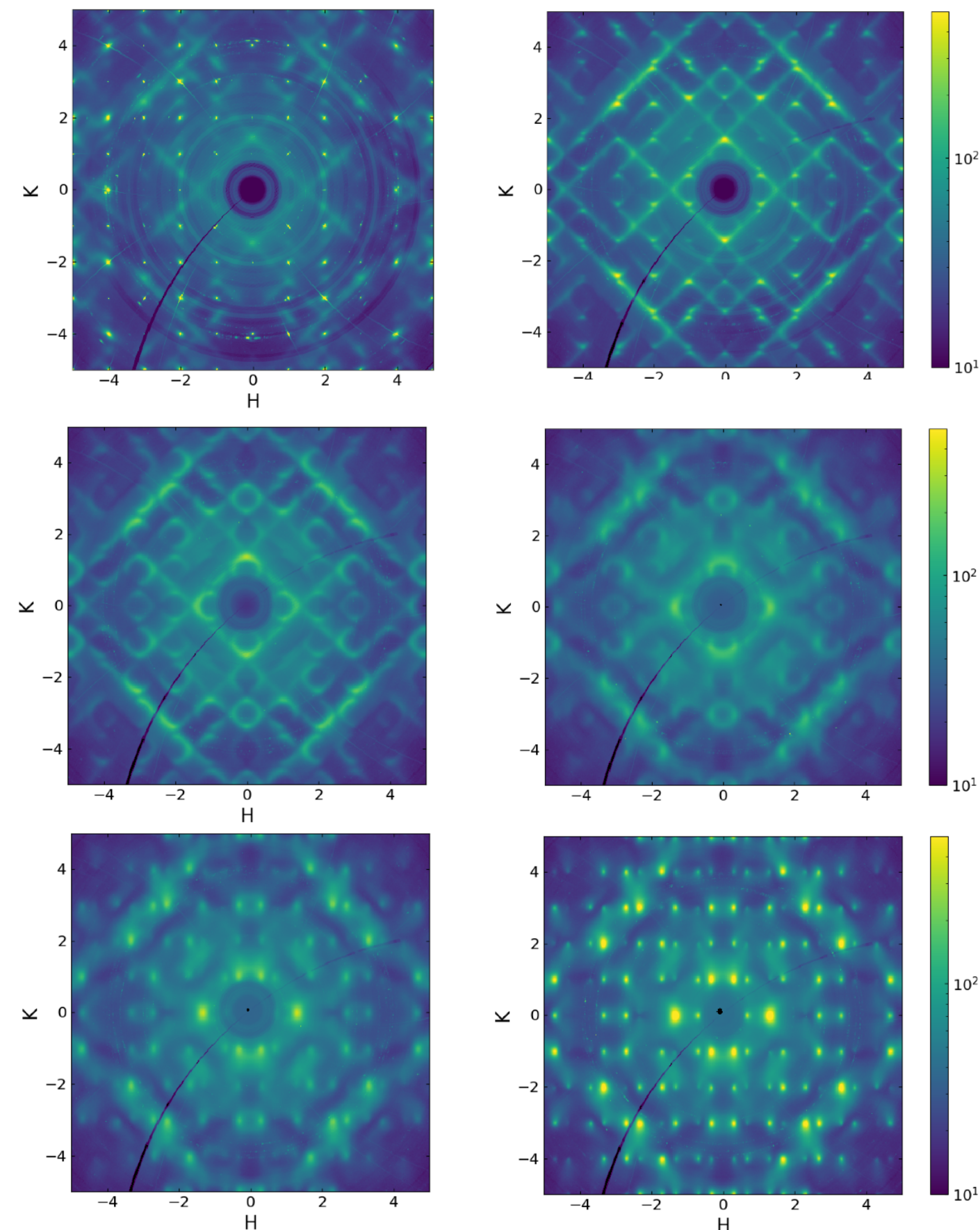
$$f(\mathbf{r}) = A \times G(\mathbf{r}) \times \exp(-|\mathbf{r}|/\xi)$$

BACK TO MULLITE



THE NATURE OF STRUCTURAL SOLUTIONS

B. D. Butler, T. R. Welberry, & R. L. Withers
 Phys Chem Minerals **20**, 323 (1993)



| Interatomic vector | α_{lmn} | Interatomic vector | α_{lmn} |
|--------------------------------------|----------------|--------------------------------------|----------------|
| $\frac{1}{2}\langle 1\ 1\ 0 \rangle$ | -0.24 | $\langle 0\ 2\ 0 \rangle$ | +0.13 |
| $[1\ 1\ 0]$ | -0.23 | $\frac{1}{2}\langle 3\ 1\ 0 \rangle$ | +0.22 |
| $[1\ -1\ 0]$ | -0.05 | $\frac{1}{2}\langle 1\ 3\ 0 \rangle$ | -0.01 |
| $\langle 1\ 0\ 0 \rangle$ | -0.06 | $\langle 1\ 0\ 1 \rangle$ | +0.07 |
| $\langle 0\ 1\ 0 \rangle$ | +0.22 | $\langle 0\ 1\ 1 \rangle$ | -0.12 |
| $\langle 0\ 0\ 1 \rangle$ | -0.03 | $\frac{1}{2}\langle 3\ 3\ 0 \rangle$ | +0.17 |
| $\frac{1}{2}[1\ -1\ 2]$ | +0.12 | $\langle 1\ 1\ 1 \rangle$ | -0.01 |
| $\frac{1}{2}[1\ 1\ 2]$ | +0.12 | $\frac{1}{2}\langle 3\ 1\ 2 \rangle$ | -0.11 |
| $\langle 2\ 0\ 0 \rangle$ | -0.12 | $\frac{1}{2}\langle 3\ 3\ 2 \rangle$ | -0.07 |

$$I_{diffuse} = N c_A c_B (b_B - b_A)^2 + \sum_{ij} \alpha_{ij} c_B c_A (b_B - b_A)^2 \exp(i\mathbf{Q} \cdot \mathbf{r}_{ij}); \quad \alpha_{ij} = \left(1 - \frac{P_{ij}}{c_j}\right)$$

“It is now possible to interpret the short-range order in the crystal structure without a detailed simulation of the disorder, which has in the past often required the optimization of a sometimes large number of model parameters fitted over a substantial volume of reciprocal space. In fact, the Δ PDF magnitudes directly determined from the reciprocal space data are simply related to the Warren-Cowley SRO parameters that have frequently been used to parametrize diffuse scattering models.” *Richard Welberry*

HOW DO I LOOK AT STATIC DISORDER?



U.S. DEPARTMENT OF
ENERGY

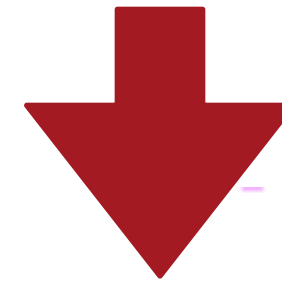
Argonne National Laboratory is a
U.S. Department of Energy laboratory
managed by UChicago Argonne, LLC.

Argonne 
NATIONAL LABORATORY

COMPARISON OF ELASTIC SCATTERING AND THE STATIC APPROXIMATION

$$G(\mathbf{r}, t) = \frac{1}{N} \left\langle \sum_{i=1}^N \sum_{j=1}^N \delta(\mathbf{r} - \mathbf{r}_i(t) + \mathbf{r}_j(0)) \right\rangle$$

$$S(\mathbf{Q}, \omega) = \frac{1}{N} \frac{1}{2\pi\hbar} \int_{-\infty}^{\infty} e^{-i\omega t} dt \int G(\mathbf{r}, t) e^{-i\mathbf{Q}\cdot\mathbf{r}} d\mathbf{r} \quad \hbar\delta(t) = \frac{1}{2\pi} \int_{-\infty}^{\infty} e^{i\omega t} d(\hbar\omega)$$



$$\left(\frac{d\sigma}{d\Omega} \right)_{coh}^{static} = b_{coh}^2 N \int G(\vec{r}, 0) e^{i\vec{Q}\cdot\vec{r}} d\vec{r}$$

$$\left(\frac{d\sigma}{d\Omega} \right)_{coh}^{elastic} = b_{coh}^2 N \int G(\vec{r}, \infty) e^{i\vec{Q}\cdot\vec{r}} d\vec{r}$$

CROSS CORRELATION CHOPPER

S. Rosenkranz and R. Osborn, PRAMANA- Journal of Physics, 71, 705 (2008).

TOF Laue Diffractometer

- highly efficient data collection
- wide dynamic range in Q

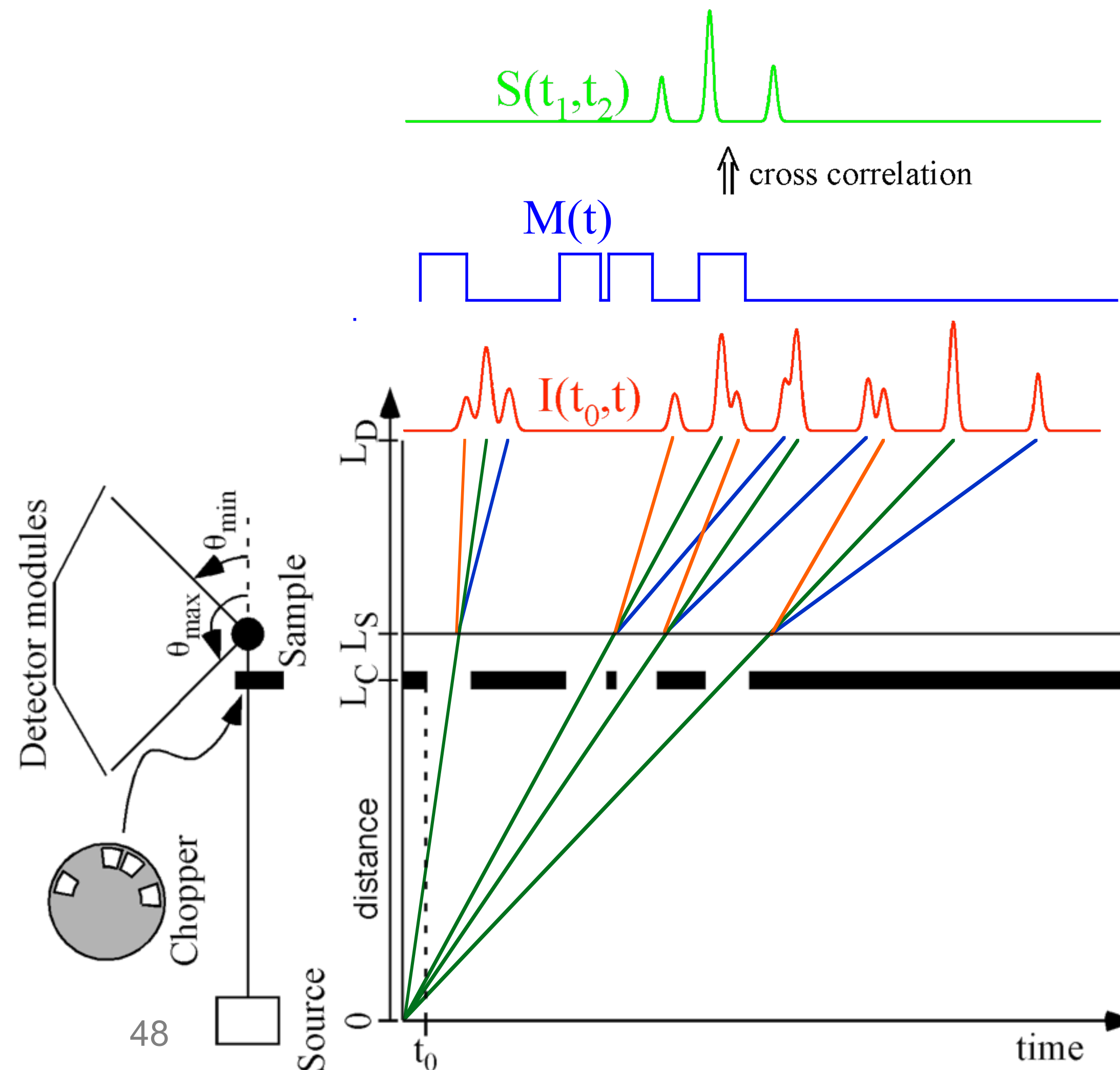
Statistical Chopper

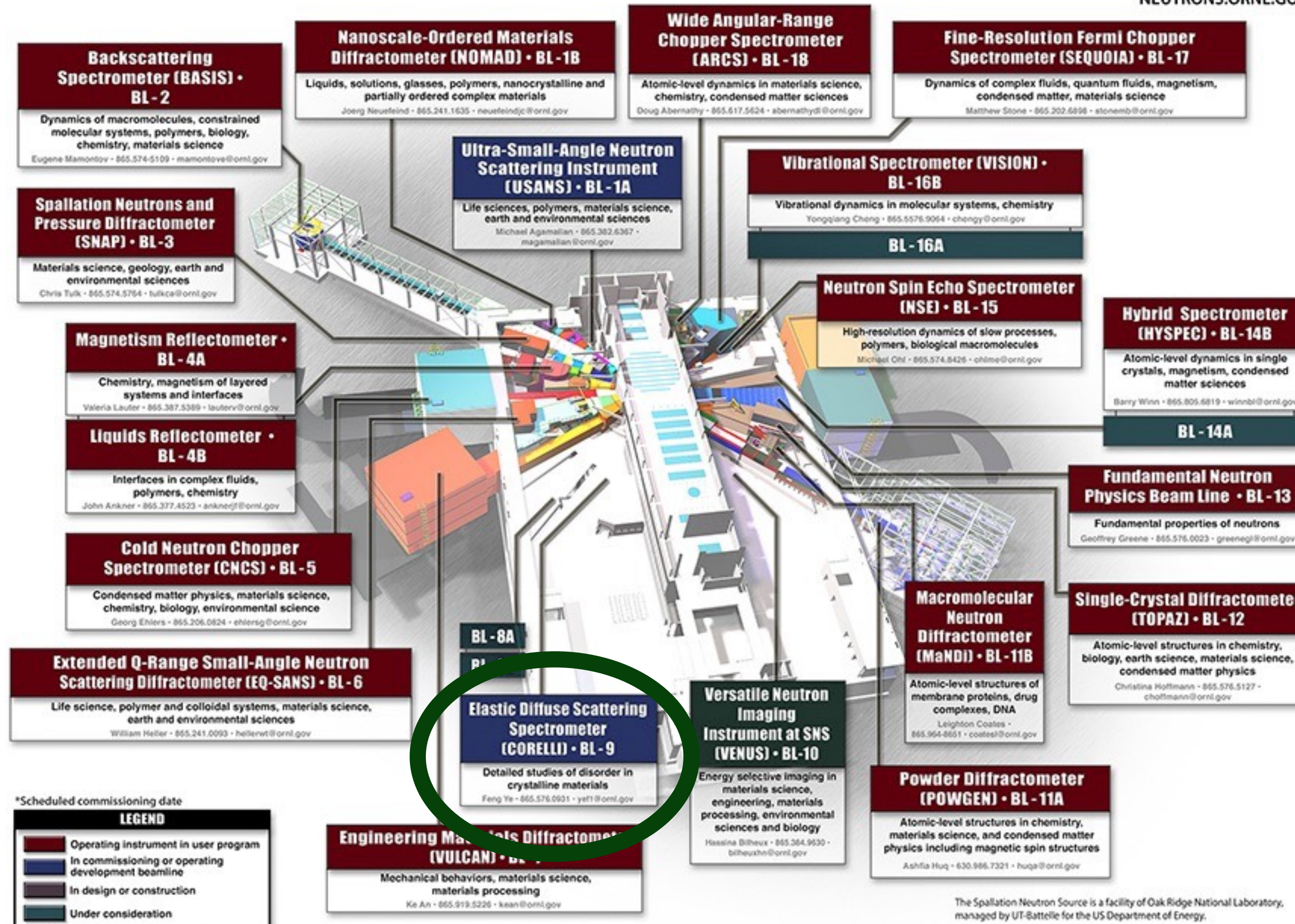
- elastic energy discrimination
- optimum use of white beam

Elastic scattering: $\hbar\omega = 0$

Inelastic scattering: $\hbar\omega = +E_0$

$\hbar\omega = -E_0$





14-G00875A/gim

Arcangelo Corelli (1653-1713)



Arcangelo Corelli was the greatest violinist of his age and an influential composer who became known as the "Father of the Concerto Grosso". This musical form contrasts music from a small ensemble of solo musicians with the full orchestra. Similarly, the properties of many materials are enriched by the interactions between both short and long-range ordering motifs that the *Corelli* instrument is designed to explore.

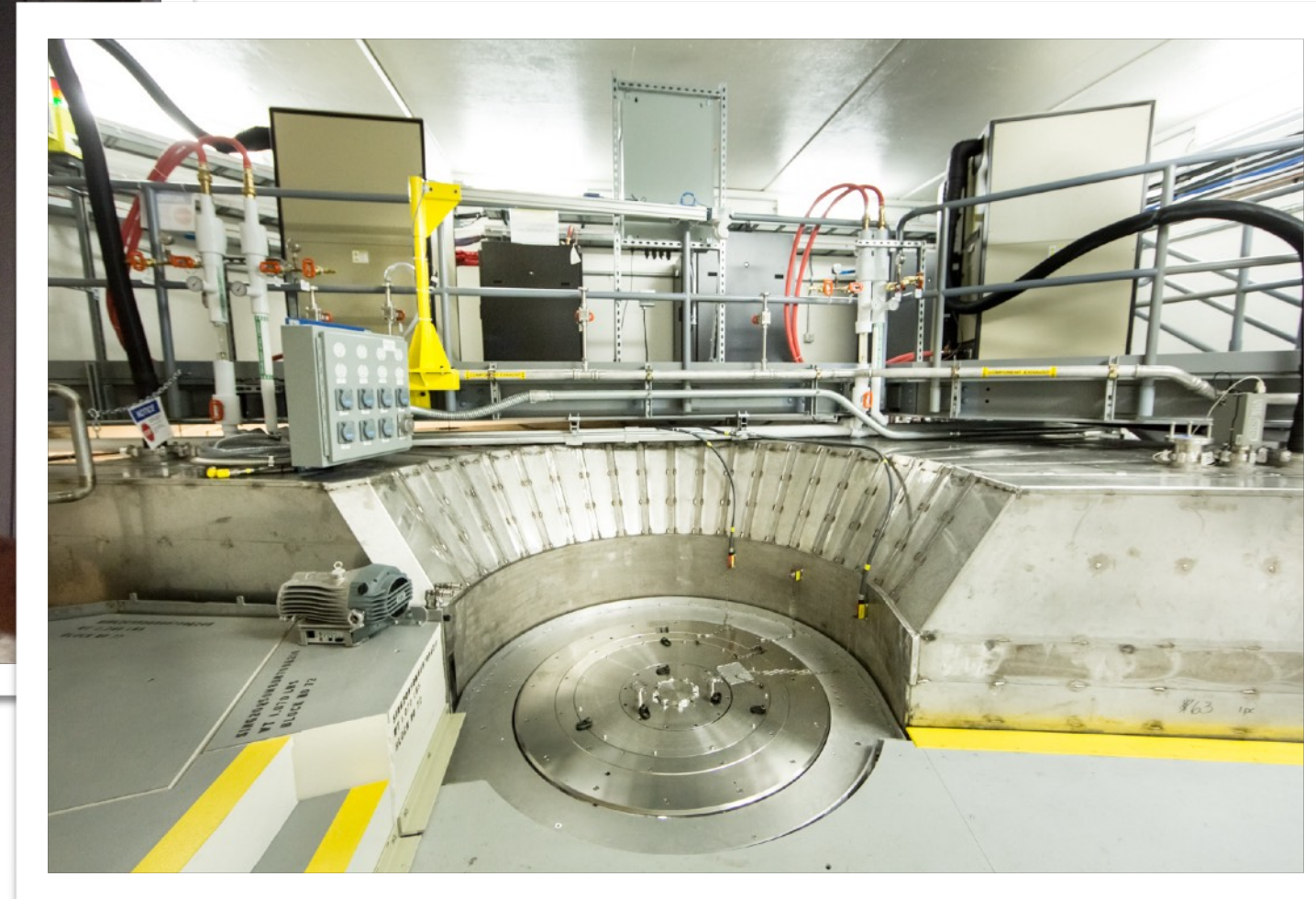
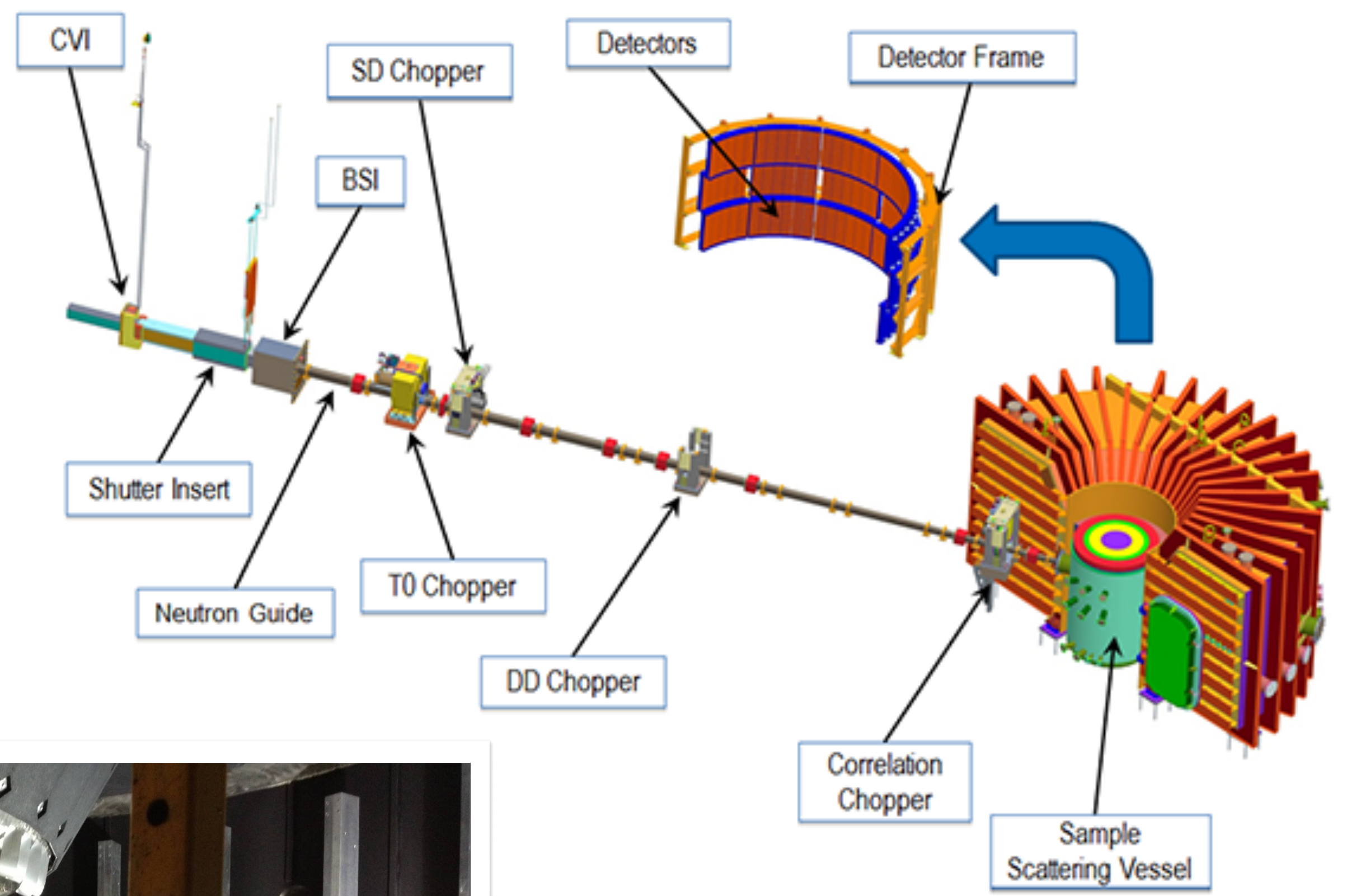


CORELLI

Instrument Scientists

Feng Ye

Arianna Minelli



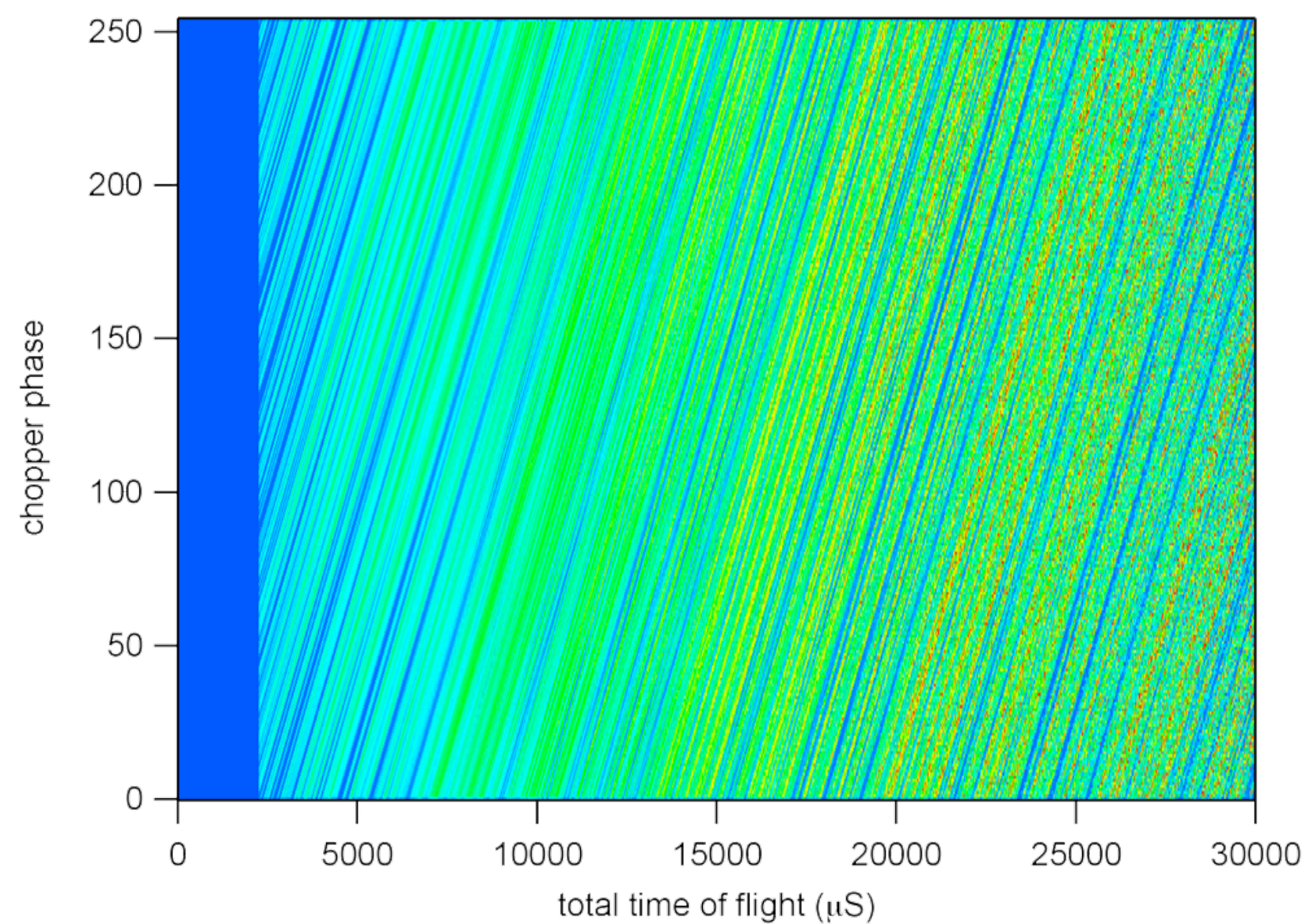
Instrument Proposers

Stephan Rosenkranz

Ray Osborn

CROSS CORRELATION IN ACTION

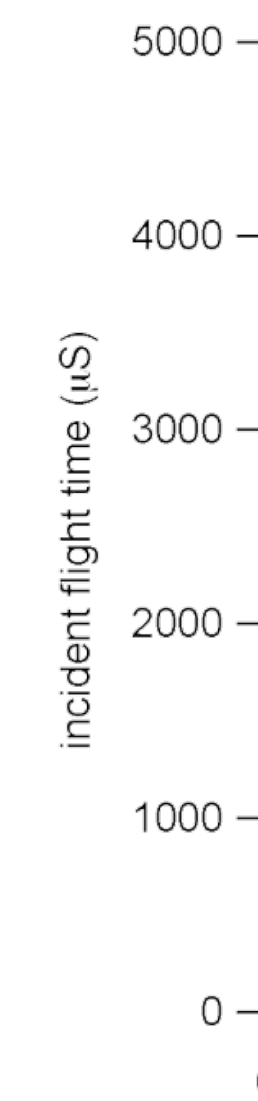
Raw Data



Cross Correlation



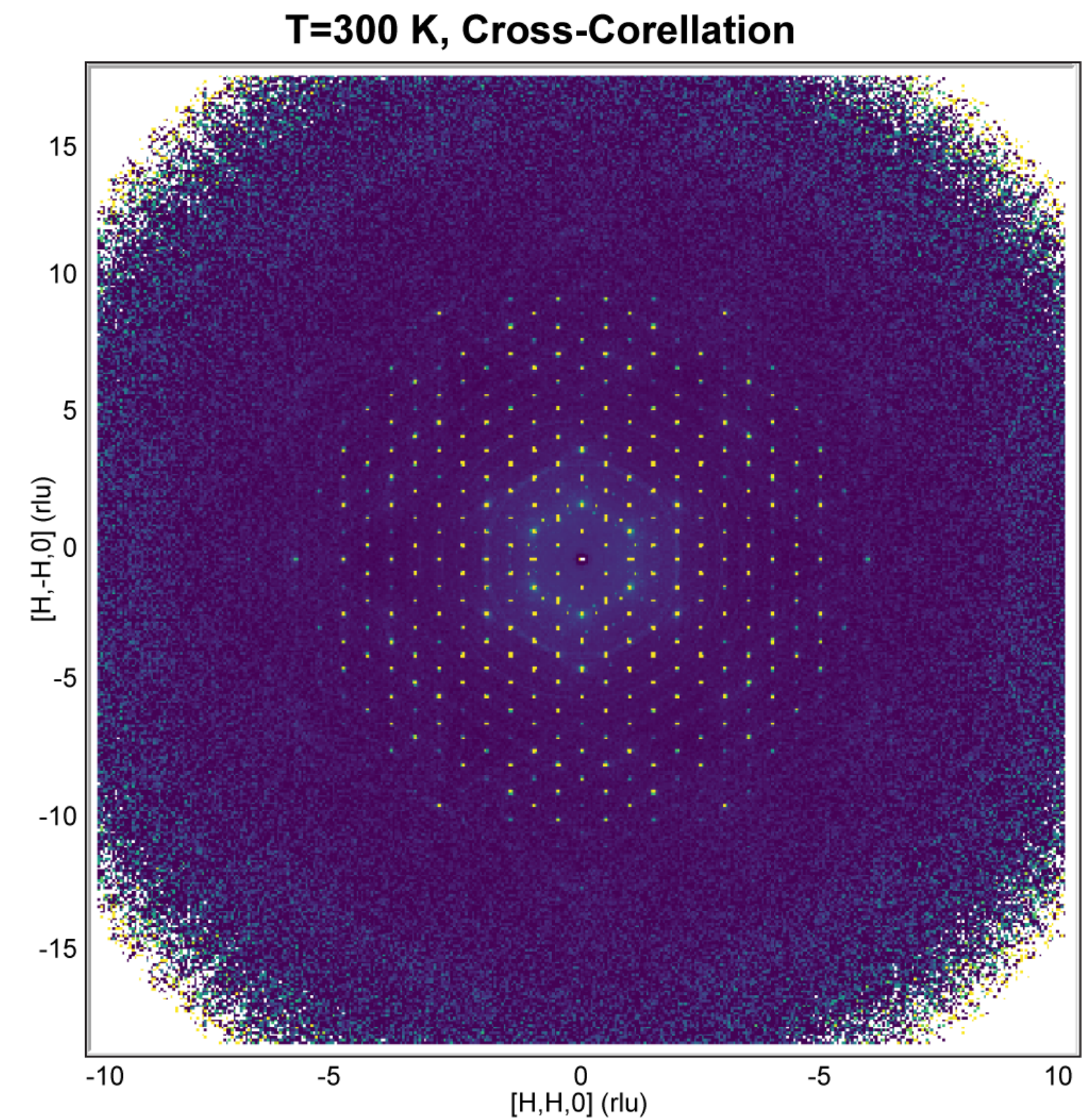
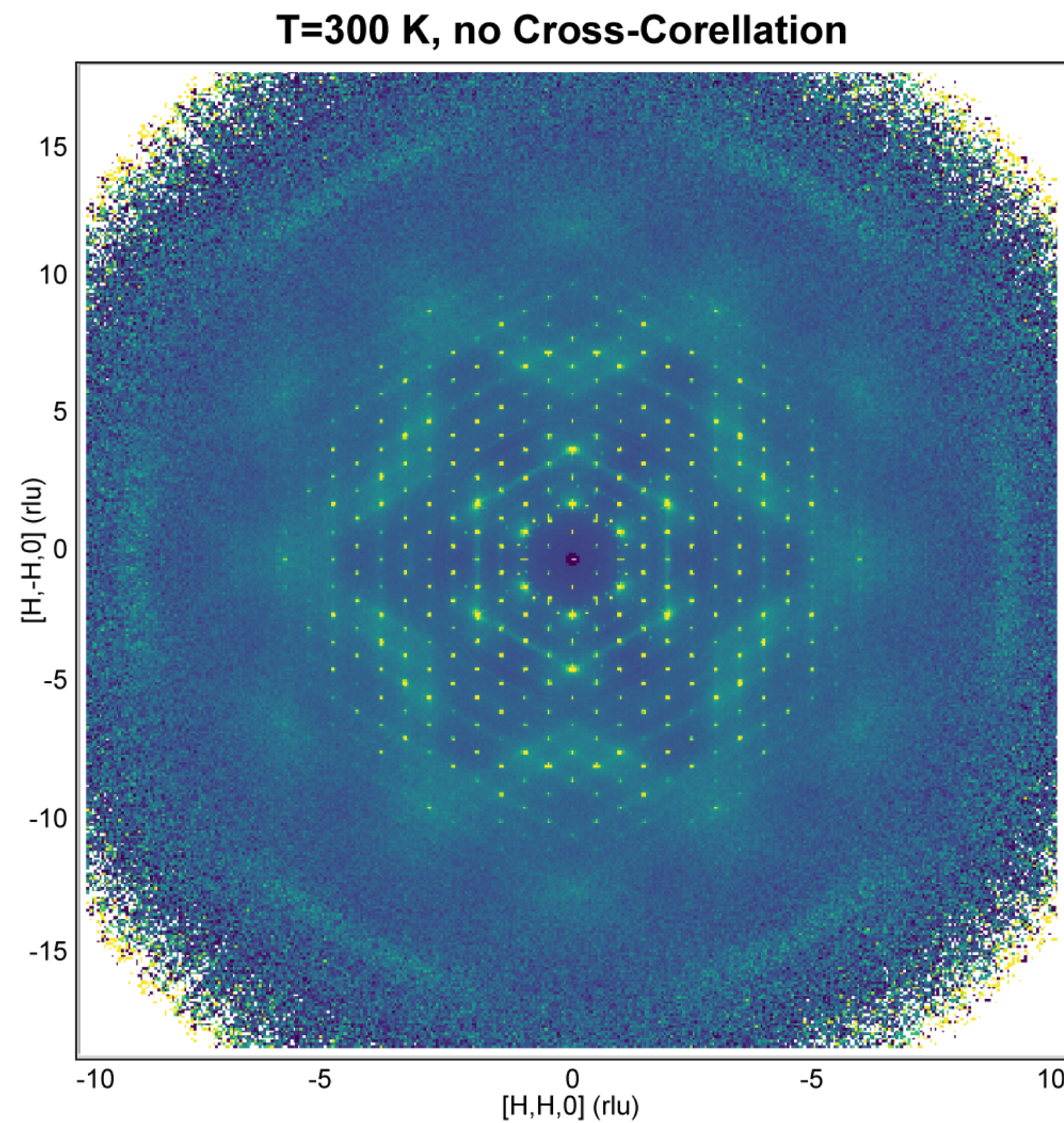
Reco



elastic inelastic

ELASTIC DISCRIMINATION WITH CROSS CORRELATION

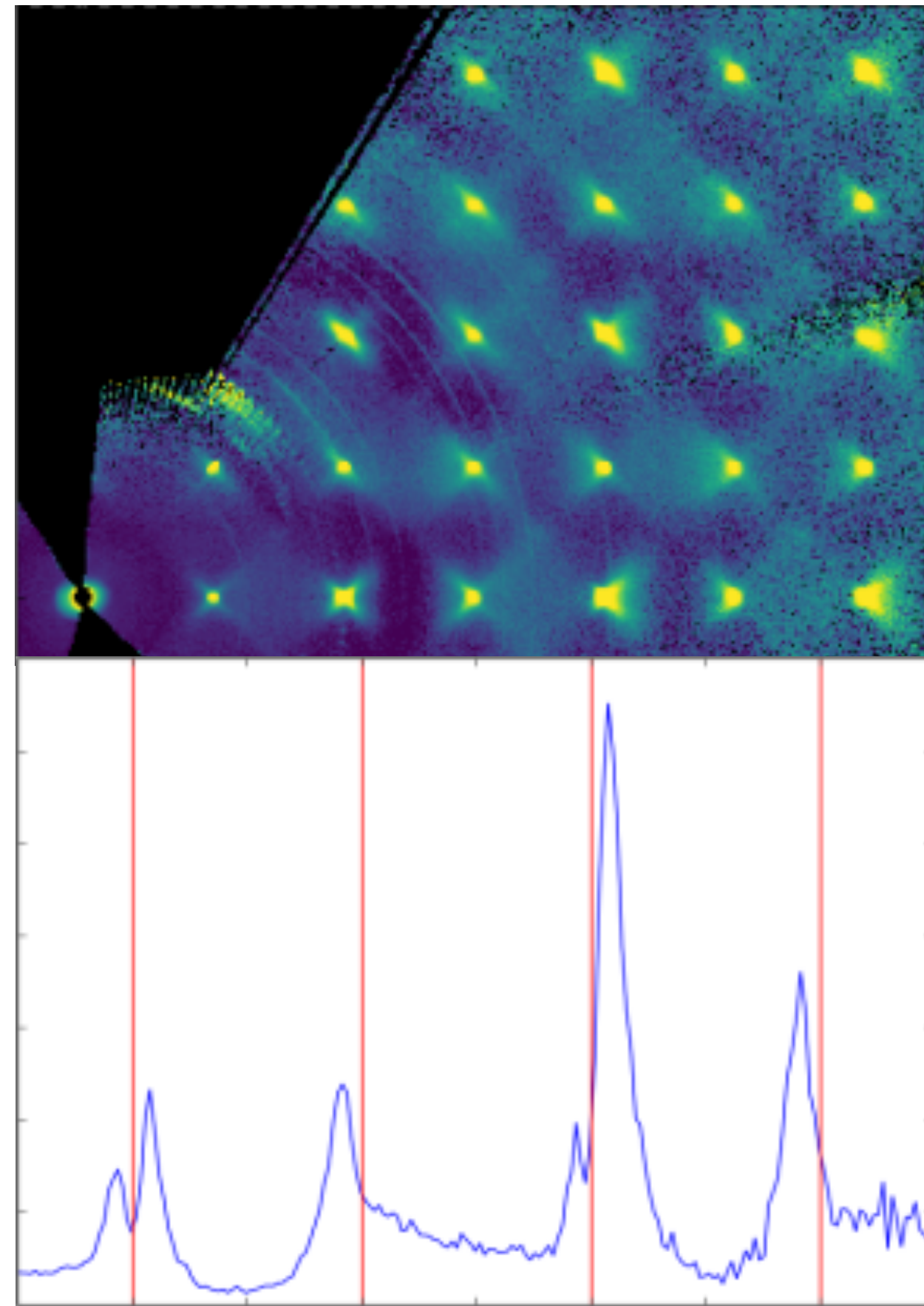
Benzil $C_{14}H_{10}O_2$



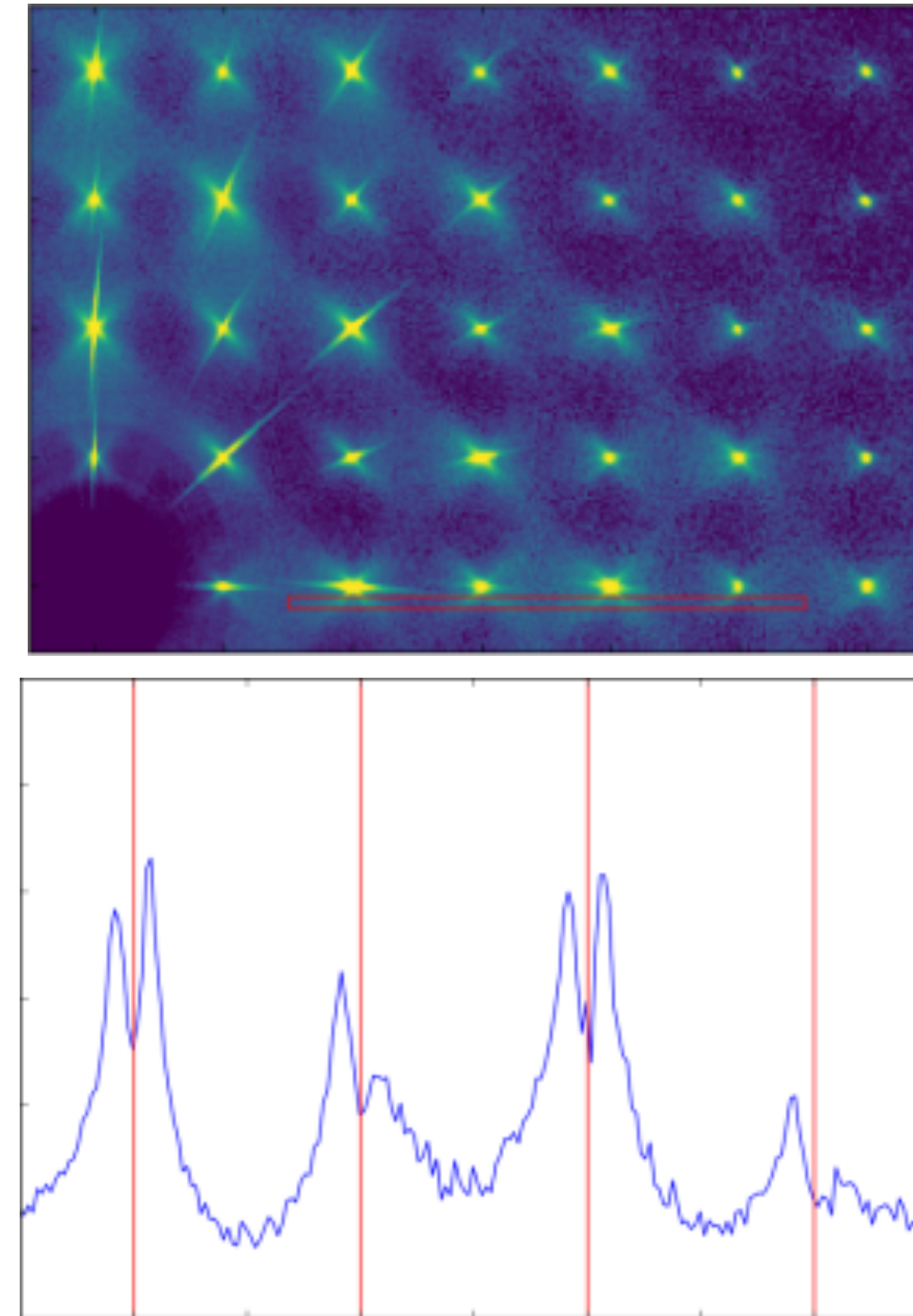
T. R. Welberry and R. Whitfield, *Quantum Beam Science* **2**, 2 (2018)

COMPLEMENTARITY OF NEUTRONS AND X-RAYS

$\text{Pb}(\text{Mg}_{1/3}\text{Nb}_{2/3})\text{O}_3$ -30% PbTiO_3 – M. J. Krogstad, *et al.*, *Nat Mater* 48, 1 (2018).



Corelli Neutrons



CHESX 55keV X-rays

SUBLATTICE MELTING IN SUPERIONIC $\text{Cu}_{1.8}\text{Se}$

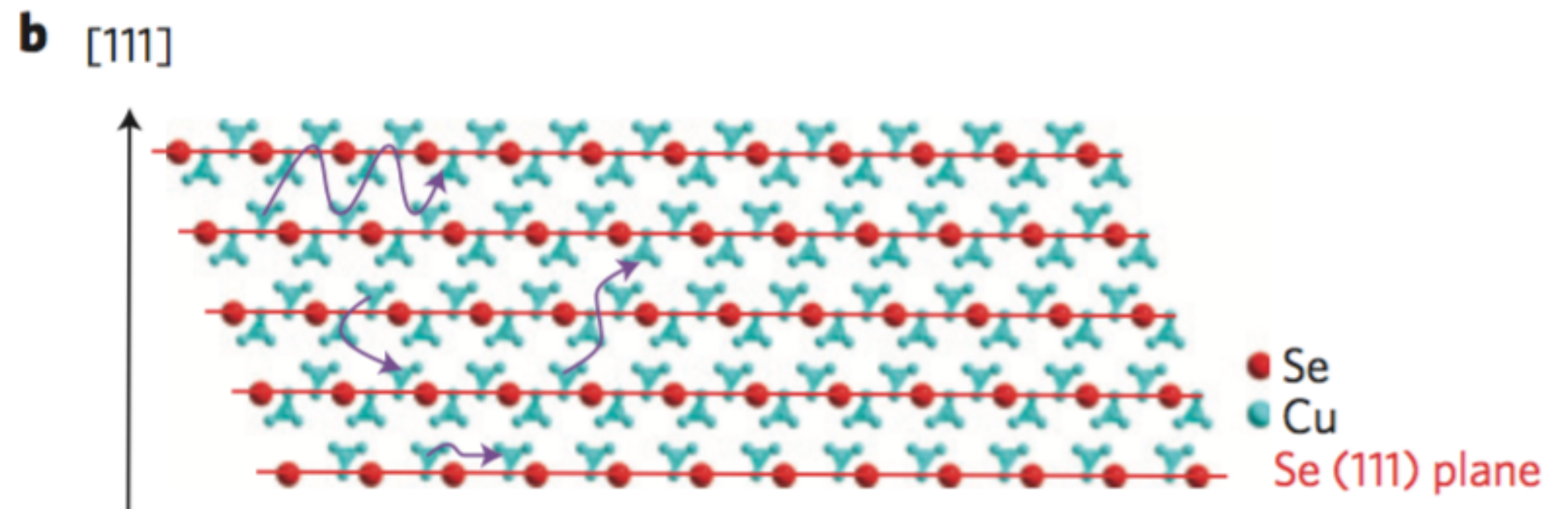
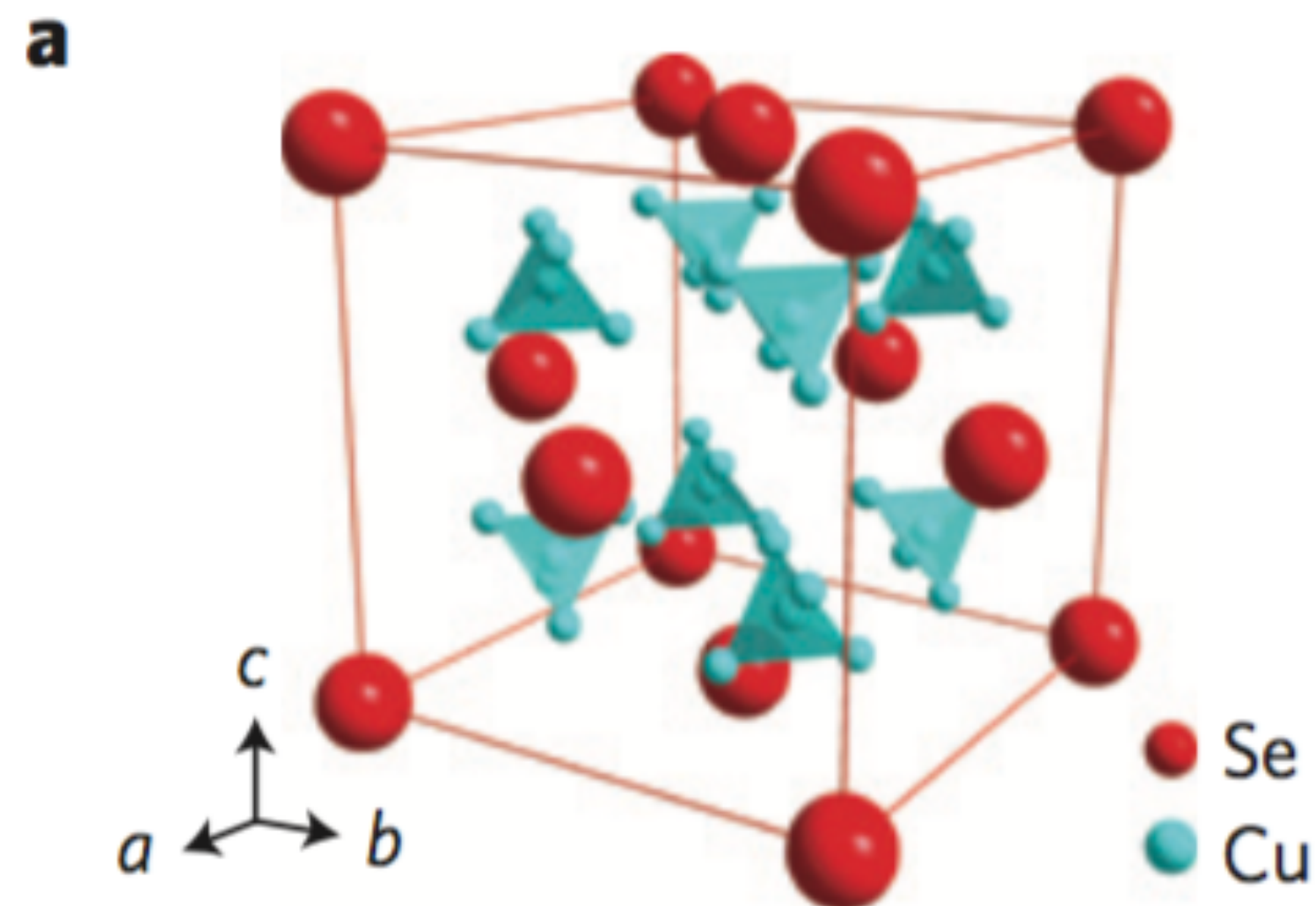
LETTERS

PUBLISHED ONLINE: 11 MARCH 2012 | DOI: 10.1038/NMAT3273

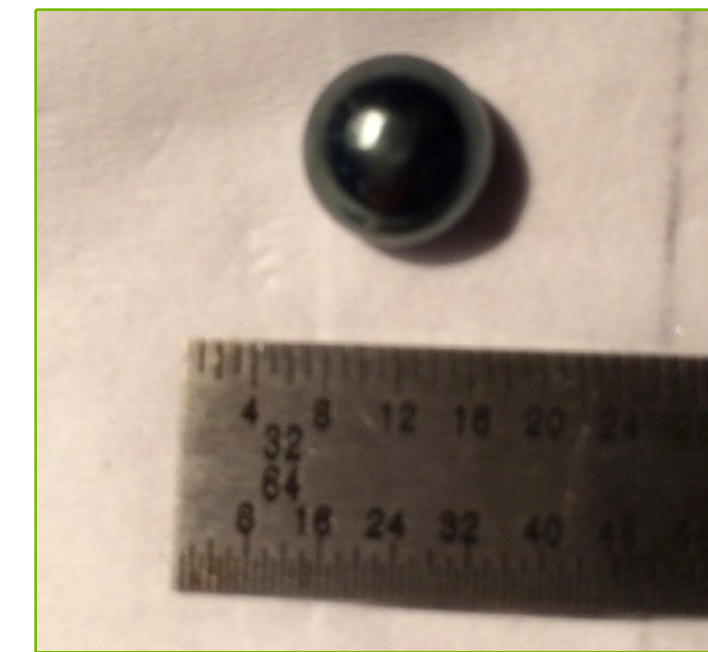
nature
materials

Copper ion liquid-like thermoelectrics

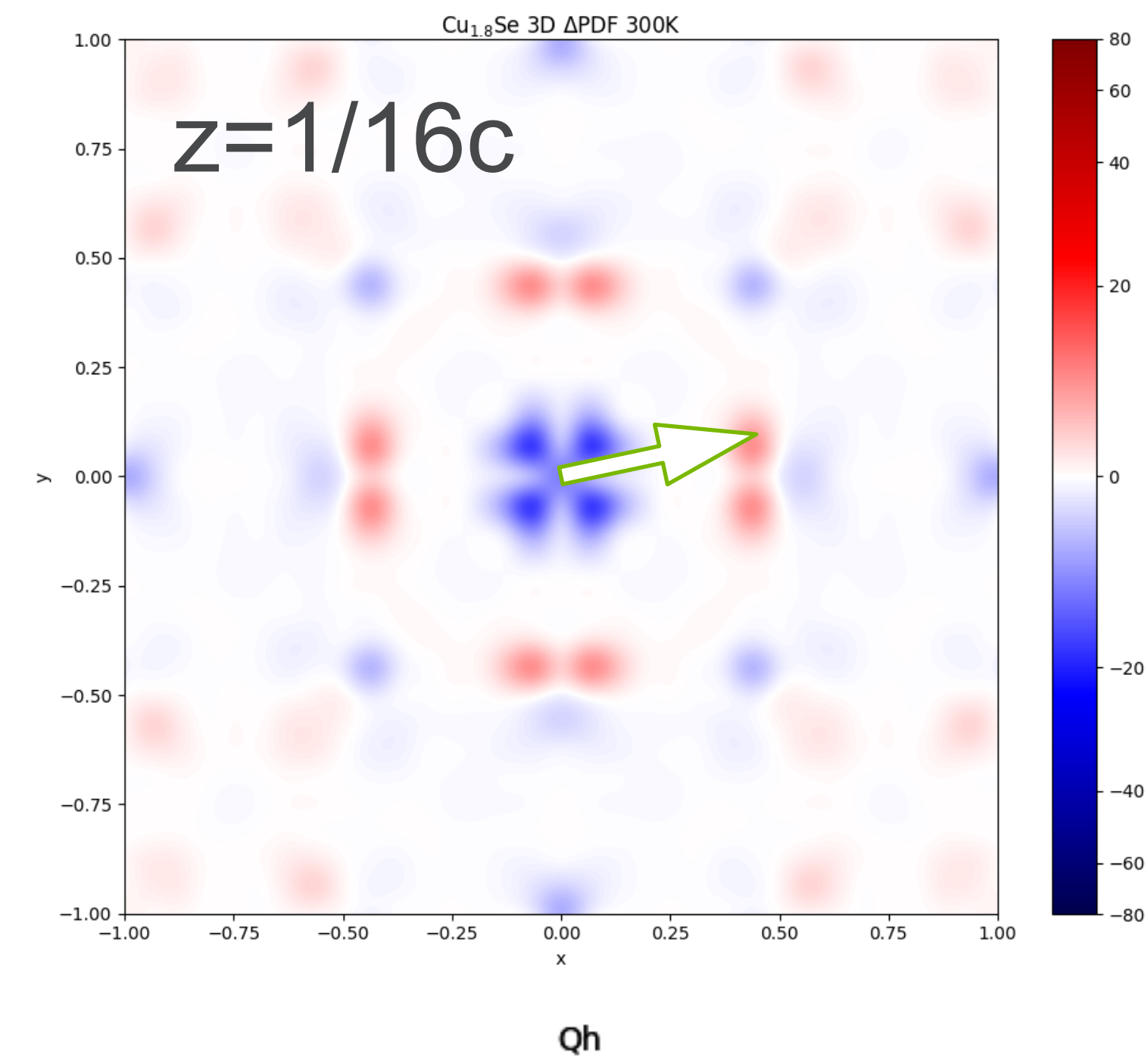
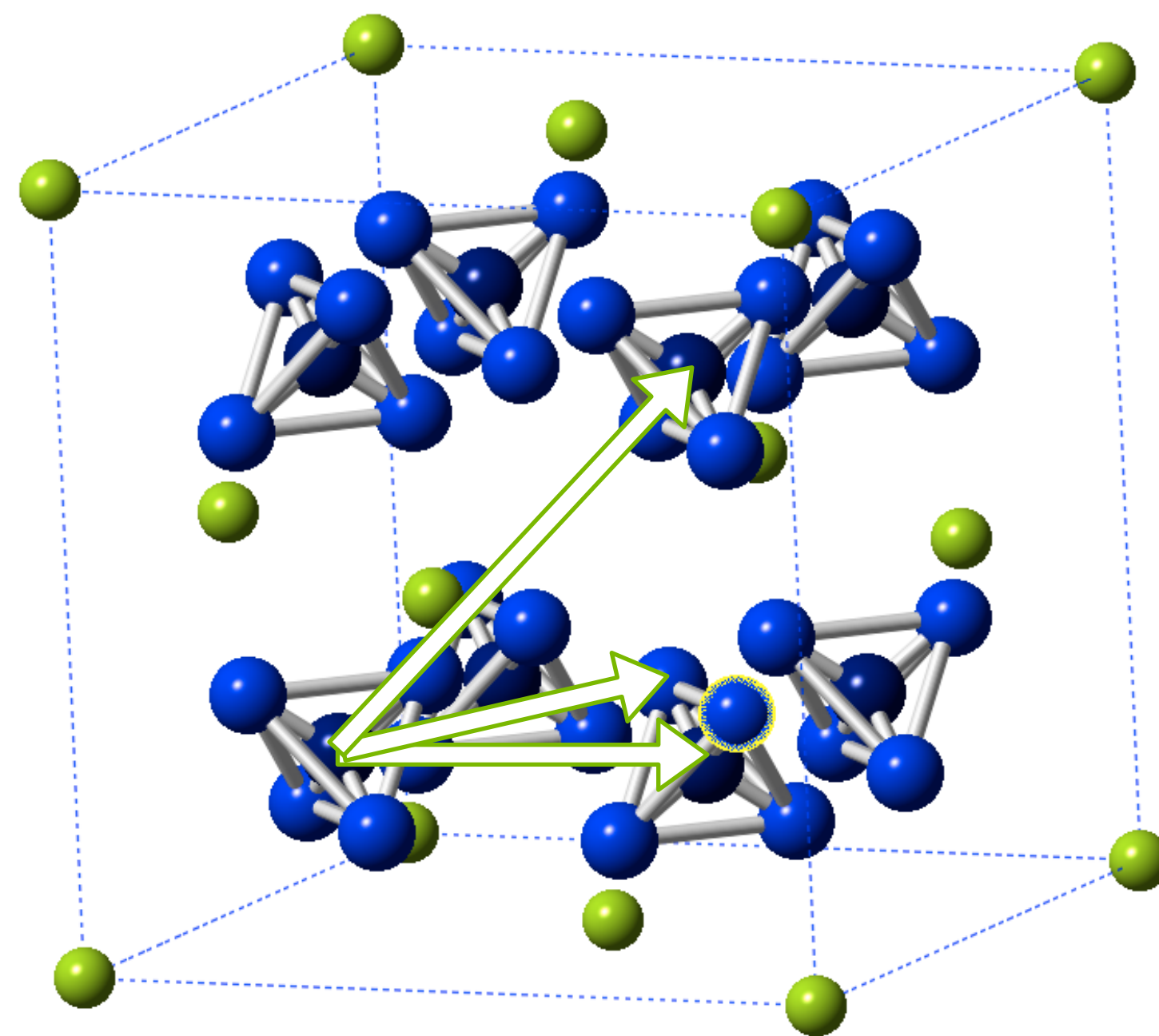
Huili Liu^{1,2}, Xun Shi^{1,3*}, Fangfang Xu³, Linlin Zhang³, Wenqing Zhang³, Lidong Chen^{1*}, Qiang Li⁴, Ctirad Uher⁵, Tristan Day⁶ and G. Jeffrey Snyder⁶



3D- Δ PDF ON CORELLI



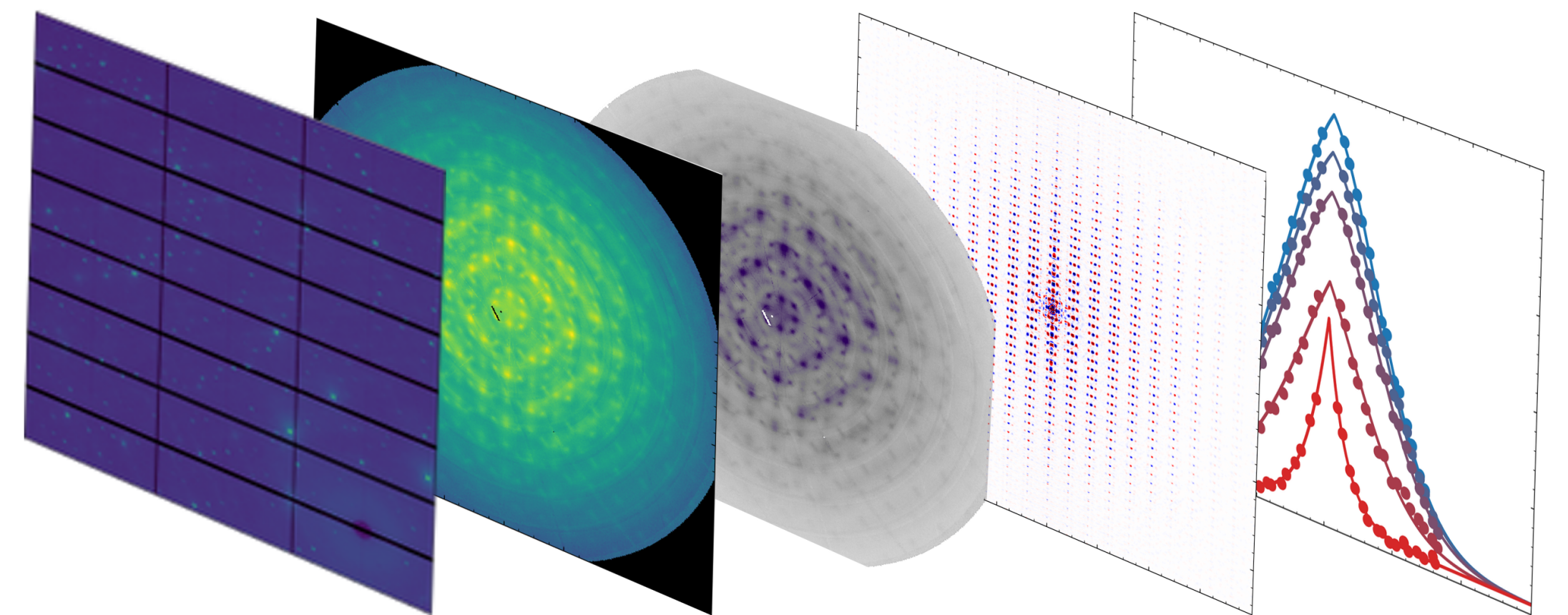
Alex Rettie



Symmetrized Corelli Data

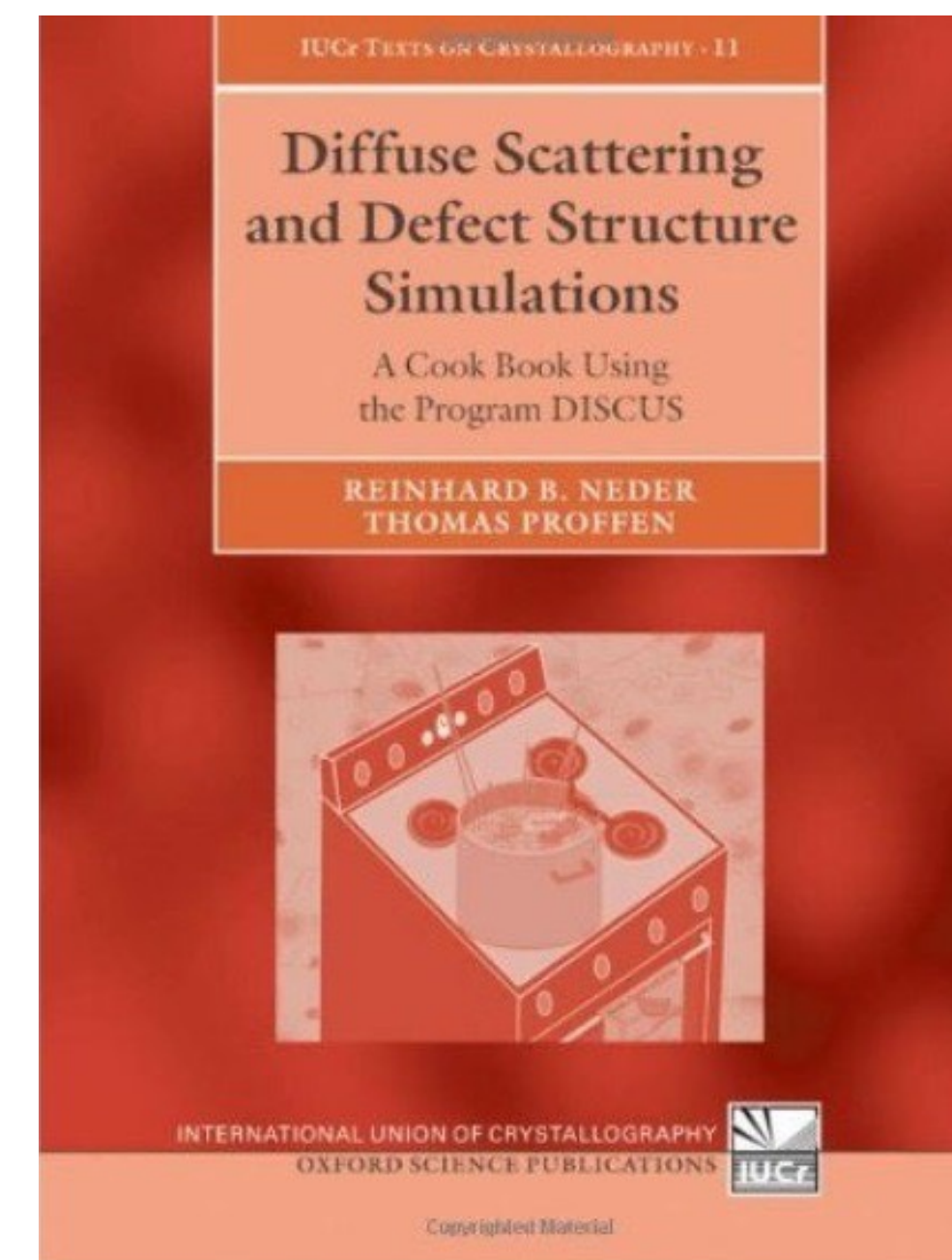
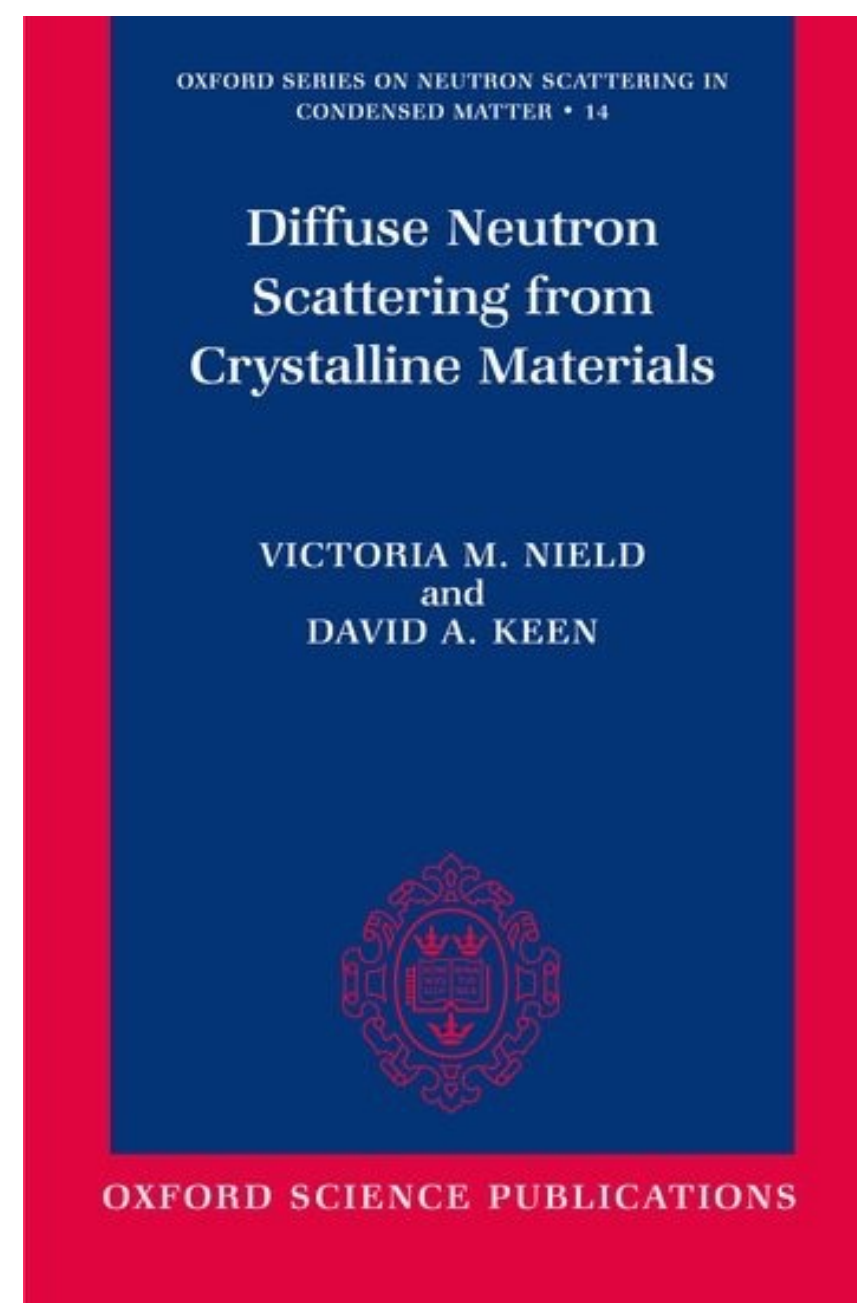
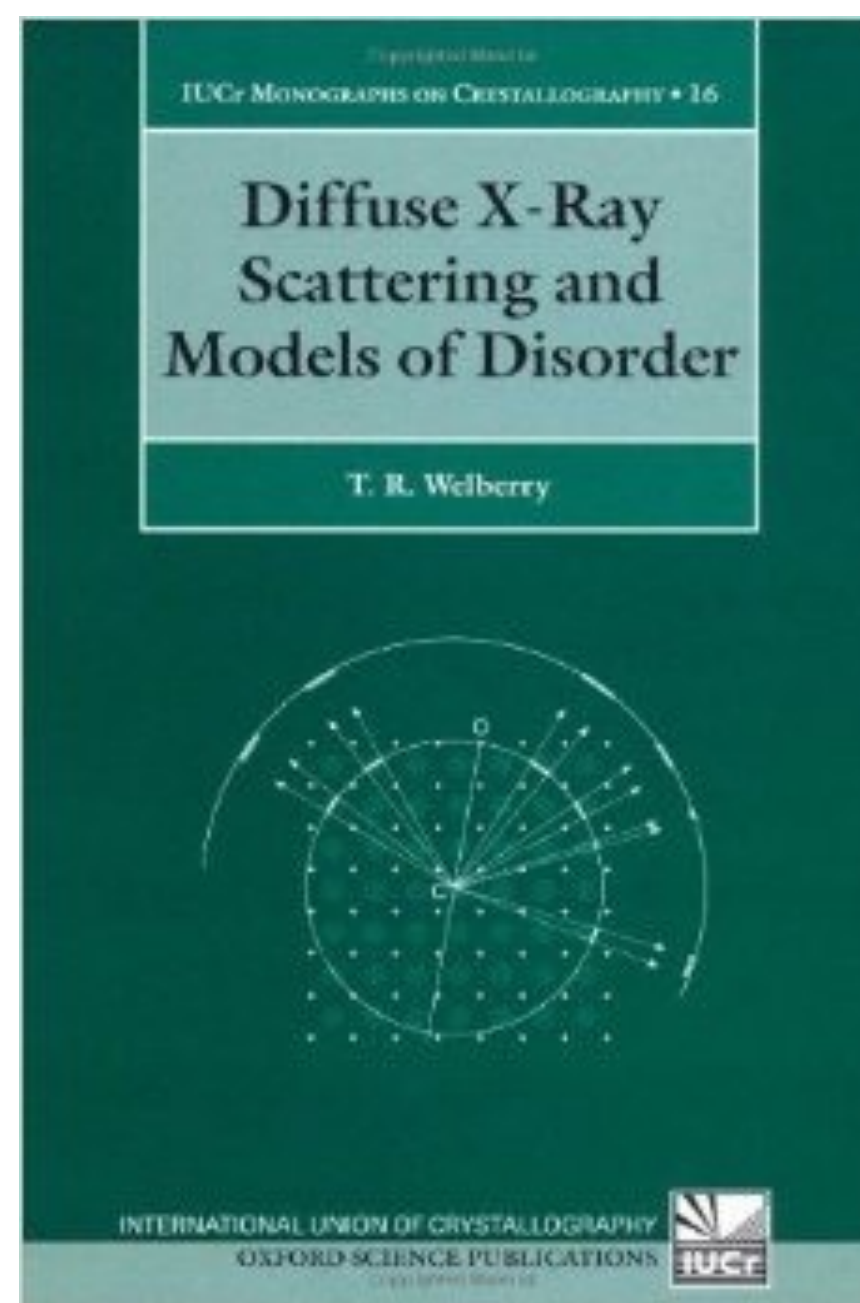
THE FUTURE

- Advances in instrumentation have transformed our ability to measure single crystal total scattering over large volumes of reciprocal space.
 - High-Energy X-rays
 - Time-of-Flight Neutrons
- This is enabling new ways of analyzing the data:
 1. Unsupervised machine learning
 2. *ab initio* computational modeling
 3. 3D- Δ PDF - real-space pair distributions
- The results give unique insight into disordered materials
 - Bridging the gap between diffraction and imaging



A FEW REFERENCES

- T. R. Welberry & B. Butler, Chem Rev **95**, 2369–2403 (1995).
- F. Frey, Acta Cryst B **51**, 592–603 (1995).
- T. R. Welberry & D. J. Goossens, Acta Cryst A **64**, 23–32 (2007).
- D. A. Keen & A. L. Goodwin, Nature News **521**, 303–309 (2015).



FEEDBACK

Single Crystal Diffuse Scattering - Raymond Osborn

- Lecture, Tuesday, August 6 - 11:10am to 12:10pm
- <https://forms.office.com/g/NRAfaeWR71>

